Quantum critical responses via holographic models and conformal perturbation theory

by

Todd Sierens

A thesis
presented to the University of Waterloo
in fulfillment of the
thesis requirement for the degree of
Doctor of Philosophy
in
Physics

Waterloo, Ontario, Canada, 2017

Examination committee members

The following members will serve on the examining committee for this thesis. The decision of the Examining Committee is by majority vote.

Role	Name	Title
Supervisor	Robert Myers	Adjunct Professor, Department of Physics and Astronomy, University of Waterloo Faculty Chair, Perimeter Institute for Theoretical Physics
Committee member	Roger Melko	Associate Professor, Department of Physics and Astronomy, University of Waterloo Associate Faculty, Perimeter Institute for Theoretical Physics
Committee member	Alex Buchel	Adjunct Professor, Department of Physics and Astronomy, University of Waterloo Professor, Department of Applied Mathematics and Department of Physics and Astronomy, University of Western Ontario Associate Faculty, Perimeter Institute for Theoretical Physics
Internal-external	Achim Kempf	Professor, Department of Applied Mathematics, University of Waterloo
External examiner	David Tong	Professor, University of Cambridge and Trinity College, Cambridge

I hereby declare that I am the sole author of this thesis. This is a true copy of the thesis, including any required final revisions, as accepted by my examiners.

I understand that my thesis may be made electronically available to the public.

Abstract

We investigate response functions near quantum critical points, allowing for finite temperature and a mild deformation by a relevant scalar. When the quantum critical point is described by a conformal field theory, we use conformal perturbation theory and holography to determine the two leading corrections to the scalar two-point function $\langle \mathcal{O}_0 \mathcal{O}_0 \rangle$ and to the conductivity σ. We build a bridge between the couplings fixed by conformal symmetry with the interaction couplings in the gravity theory. Knowledge of the high-frequency response allows us to derive non-perturbative sum rules. We construct a minimal holographic model that allows us to numerically obtain the response functions at all frequencies, independently confirming the corrections to the high-frequency response functions. In addition to probing the physics of the ultraviolet, the holographic model probes the physics of the infrared giving us qualitative insight into new physics scalings. We briefly investigate the hydrodynamic modes that occur in the field theory by observing the diffusive nature of the gauge field deep in the bulk using the membrane paradigm, allowing us to calculate the diffusion constant and DC conductivity.

Acknowledgments

I would like to take the opportunity to express my gratitude to those who have made the PhD experience an enjoyable one.

Firstly, I would like to start by thanking my supervisor, Rob Myers. Thank you for always finding the time to patiently answer all of my questions, and for providing me with stimulating projects to pour my time into.

I would also like to thank the members of my examination committee for agreeing to be on the defense committee and for reading my thesis.

I was fortunate to be a resident graduate student at the Perimeter Institute for Theoretical Physics. It is a unique environment with visiting physicists from all around the globe working on problems in all kinds of fields. The Black Hole Bistro kept me fed and the endless free coffee kept me awake.

During my time as a graduate student I have had many collaborators, including professors, postdoctoral fellows and other graduate students both at the Perimeter Institute and outside of Waterloo. I would like to thank the group of physicists who I worked with for the first publication of my physics career: Alexandre Belin, Janet Hung, Alexander Maloney, Shunji Matsuura and my supervisor, Rob Myers. I would also like to thank William Witczak-Krempa for collaborating with me on two subsequent projects, and Andrew Lucas for collaborating with me on our latest project.

I would like to thank the many friends who have supported me through my research as a PhD student both from Waterloo, and from away. Whether it is playing a board game, going on a trip, going camping or just sitting around a table at the Black Hole Bistro talking about physics, I treasure each memory.

I would like to thank my fellow fellows Julian, Tayler and Esmond for always being available to talk and to play games, it didn't matter if we talked about little problems or big problems, I always felt support from you. Generally our time together provided me with a much needed relief from the stress of graduate studies. We continue to prove that our friendship knows no distance. Catching up with Troy and Laura Gowan is always a highlight when I am visiting home.

To Trevor Rempel, my colleague, my rival, my friend. Our friendship over the past 12 years has truly been remarkable, nothing short of an adventure. I couldn't imagine going through any of my post-secondary studies without you. By the way, you still owe me a custom wake-up alarm recording. Our worldlines seem destined to cross, I look forward to that time (and place).

I am blessed to have such a loving and caring family. I would like to thank my mom and my dad for being the most supportive parents anybody could hope for. To my dad, Christopher, the glimmer that you get in your eye when you see something remarkable or when you figure out the inner mechanism of something that fascinates you sparked in me a similar curiosity for our world that has guided me to where I am today. To my mom, Brigitte, I would like to express my gratitude for everything you do for me. You truly care about my physical, emotional and mental well-being. No matter how old I get, I will always need my mom. I want to thank John and Cindy Hayward, my second set of parents, for always making me feel welcome when visiting your home. Of course, visits home are always highlighted by seeing the rest of my family. Thank you to Scott and Liane, to their kids, Tyson, Tessa, Sarah and Cole, to Brittany and Justin, to Joshua and to Tim for making holidays truly worth coming home for.

I was fortunate to have valuable and memorable relationships with all of my grandparents, three of whom I lost during my PhD studies. To Grandpa, you were truly an inspiring man and you are responsible for the character that I have today. You taught me the value of hard work and the value of working with my head, not with just my back. To Grandma, the nicest person I have ever met, you had a huge impact on my younger years and I will never forget spending summers in the garden, playing cards and drinking tea with you. To Pépère, thank you for feeding my interest in math, science and teaching, and for always giving me the sports section of the paper so I could update my statistics on the NHL. Finally, to Mémère, thank you for debating with me about science and physics and what use they are to the world. You challenge me to find a place in the world where I can make a difference.

Finally, I would like to thank my loving wife and best friend Lauren Elizabeth Hayward Sierens. Words can't express how much I care about you. I can confidently say that I would not have made it this far without you. You see through the hard times, and you fully enjoy the good times. You keep me sane. Every facet of my life that you have touched is brighter now. I am a better person because of you. Thank you for everything that you do.

Dedication

For Lauren
my wife
my partner
my best friend

Table of Contents

List of Tables

List of Figures

It's dangerous to go alone!

THE LEGEND OF ZELDA

Chapter 1

Introduction

A quantum critical point (QCP) is a second order phase transition between ground states at zero temperature. Quantum critical points are central to a wide range of physics including properties of magnets, non-Fermi liquids and efforts towards high-temperature superconductivity. Some of the best understood instances of QCPs are described by conformal field theories (CFT)s. In this thesis, we introduce the gauge/gravity duality, also known as holography, and demonstrate its power by comparing predictions created using conformal perturbation theory on conformal field theories with full dynamic numerical results found using holography. First, we give an overview for the gauge/gravity duality and then we show conformal perturbation techniques that allow us to calculate corrections to response functions in a CFT deformed by a relevant scalar operator. Finally, we use holography to not only confirm these corrections, but to build a bridge between couplings fixed by conformal symmetry, with coupling constants in the theory of gravity that tie the correspondence together. The holographic model that we present is able to access full-frequency responses to the scalar deformation numerically, providing an essential tool for understanding CFT response functions. In addition to these calculations we explore more complex theories of gravity such as the Reissner-Nordström black hole and confirm that the general holographic and conformal perturbation theory results hold there as well.

1.1 Quantum critical systems

A canonical example of a CFT is the quantum critical (QC) phase transition at zero temperature in the quantum Ising model in 1+1, 2+1 or 3+1 spacetime dimensions [1], which results from tuning the transverse magnetic field across a critical value. Some QC

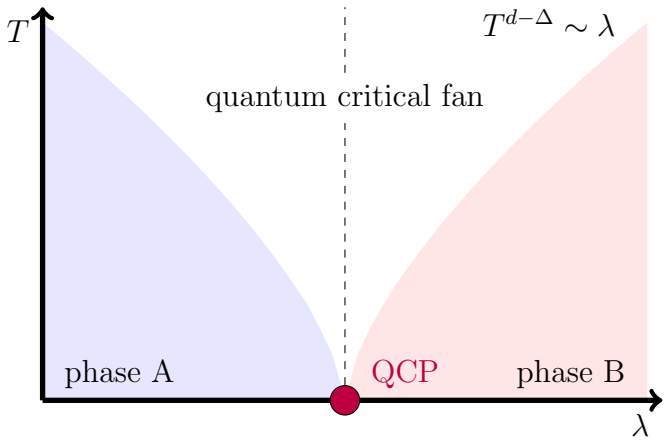

Figure 1.1: A phase diagram depicting a quantum critical point. The physics that we are probing lie inside of the *quantum critical fan*

phases exist without needing fine-tuning, such as the two-component Dirac fermion in 2+1 dimensions.

The action of the ϕ^4 QFT in $d = 2 + 1$ is

$$S = \int d^3x \left((\partial\phi)^2 + u(\phi \cdot \phi)^2 \right) + \lambda \int d^3x \phi \cdot \phi, \tag{1.1}$$

where $\phi_a(x)$ is a real N_s-component vector. For all N_s, the renormalization group (RG) fixed point at finite interaction u corresponds to a non-trivial CFT, often called the $O(N_s)$ Wilson-Fisher fixed point. For the case of a real scalar, $N_s = 1$, this critical point corresponds to the Ising model CFT. The relevant scalar $\mathcal{O} \sim \phi \cdot \phi$ is the mass operator, and λ the corresponding coupling that needs to be tuned to zero to reach the QCP. In general, $\mathcal{O}$ is an important operator in the spectrum, and it is not surprising that it plays a key role in determining the quantum dynamics for various observables. On the other hand the mass term $m^2\phi^2$ in scalar ϕ^4-theory describes a quantum critical Ising transition that is invariant under all symmetries of the theory and requires fine-tuning to reach the quantum phase transition. An important challenge in the study of CFTs is to understand their real-time dynamics [2], especially at finite temperature [3]. In the linear response regime, important examples are the conductivity σ and the scalar two-point function $\langle \mathcal{O}\mathcal{O} \rangle$. Monte Carlo simulations offer another window into these systems, however, as of now these simulations are able to make calculations for some Euclidean frequencies, but analytically continuing this data to the real time frequency domain is of course a challenge. These theories are typically strongly interacting, and as such, perturbative quantum field theory techniques

are of limited utility. In contrast, holography, which will be explained below, can yield real-time results for strongly interacting systems. Generally we are not able to to find an exact gravitational dual theory for every CFT of interest, so we content ourselves with matching properties between the theories and constructing models to observe universal qualitative behaviour.

Progress on applying holography and general CFT methods to study the hydrodynamic behaviour of quantum critical points has been made in [4–12]. For example, new sum rules for scalar observables, electrical conductivity and shear viscosity have been discovered using holography [12–14] which apply more broadly to a large class of CFTs including the Wilson-Fisher CFT. The authors of [15] recognized that the relevant scalar operator that is needed to tune to the QC phase transition in the $O(2)$ Wilson-Fisher theory plays an important role in the dynamics for the system. We find that quantum field theories deformed away from a QCP via a relevant scalar have a wide array of general properties that we can determine using techniques in conformal perturbation theory (chapter 3) and holography (chapters 4 and 5).

1.2 Holographic hydrodynamics

The work comprising this thesis began as a direct continuation of the work done in [15] where the authors track how deforming the critical theory by a relevant scalar operator affects the dynamics of transport properties. An overview is given in [15] where they introduce a scalar field into a gravitational theory that is a CFT on the boundary in order to probe the leading order corrections to the electrical conductivity, diffusion and DC conductivity of the CFT due to the scalar deformation. The initial goal of our endeavor was to make this effort more robust. For example the scalar field in [15] was introduced in an ad-hoc manner, with no dynamics governing the scalar field. It is just assumed that such a scalar field would exist in such a spacetime. Questions about existence and stability of such a scalar profile could be raised, but mostly, only the physics of the ultraviolet can be trusted as these fields are constructed purely on their near-boundary properties and are thus unaffected by bulk dynamics.

This thesis introduces a model in chapter 4 and in chapter 5 whose properties introduce a scalar field in the gravity theory and has the necessary properties in order to be the dual field for the scalar operator driving the deformation of the CFT. This thesis explores the effects that the scalar deformation to the CFT has at high temperatures, finite chemical potential and finite scalar deformation. Referring to figure 1.1, we are interested in the role

that the scalar deformation plays on the transport properties of the underlying quantum field theories that exist within the *quantum critical fan*.

This thesis is organized into chapters that begin with chapter 2 where we give a brief overview of the gauge/gravity duality and holographic hydrodynamics.

In chapter 3, we describe conformal perturbation theory and how we can use the operator product expansion (OPE) of two operators in order to understand the dynamics of various n-point functions, and in general, that up to some theory-dependent coefficients, we can obtain the leading two corrections that the relevant scalar deformation $\mathcal{O}$ has on the dynamics for various observables. In previous work produced by myself and collaborators, the results relating to the scalar-scalar two-point function can be found in [14] and the results relating to the conductivity can be found in [13] ($d = 3$) and in [14] (any d).

Chapter 4 starts to build a bridge between the methods of conformal perturbation theory and holography. By relating the partition functions for the quantum theory and gravitational theory via that AdS/CFT dictionary, we can calculate the same n-point functions holographically by understanding how scalar and gauge fields propagate in AdS space. The chapter builds a dictionary that relates the CFT coupling coefficients from chapter 3 to the coupling constants appearing in the gravitational theory. In previous work produced by myself and collaborators, the results presented in chapter 4 can be found in [14].

Chapter 5 is where it all comes together, and is the main chapter of this thesis. We move away from the QCP or equivalently the pure AdS regime and explore the correspondence in its full potential to describe a thermal dynamical system. We introduce a minimal model that has all of the ingredients needed to demonstrate the corrections to the scalar two-point function $\langle \mathcal{O}_0 \mathcal{O}_0 \rangle$ and to the conductivity $\sigma \sim \langle J_x J_x \rangle$ that are induced by the relevant scalar deformation $\mathcal{O}$ discussed in chapters 3 and 4. The model discussed in chapter 5 is able to confirm the exploratory predictions laid out in chapters 3 and 4 as well as provide a full-frequency analysis of the transport properties. We show that the system forms a dissipative fluid near the black hole horizon and that we can calculate the diffusion constant and the DC conductivity for the model. We also explore the implications of deforming the scalar field and adding a chemical potential to the system. In previous work produced by myself and collaborators, results presented in chapter 5 can be found in [14] and fine details about the conductivity in $d = 3$ can be found in [13].

Chapter 2

Gauge gravity duality and the AdS/CFT

In this thesis we use the Anti-de Sitter/Conformal Field Theory (AdS/CFT) correspondence [16–19] liberally in order to make elusive quantities in quantum field theories accessible. In this section we introduce an abridged description of the AdS/CFT correspondence, and gauge/gravity duality in general. The study of AdS/CFT is extremely vast and in this chapter we will be giving an overview to the salient aspects of the AdS/CFT correspondence that are heavily relied upon in this thesis. At its core, gauge/gravity duality demonstrates an equivalence between strongly-interacting conformal field theories and weakly-interacting gravitational theory in a negatively curved spacetime with a provocative twist: the number of spacetime dimensions for the gravity theory is one higher than the number of dimensions in the quantum field theory. In Chapter 4 we use a saddle point approximation[1] from AdS/CFT in order to evaluate correlation functions for the boundary quantum field theory using the equations of motion of gravity. In Chapter 5 we will be using the same prescription but for spacetimes that may have temperature and charge, and we show that the correspondence provides a tool for investigating these theories that are near to a quantum critical point.

[1] An approximation that allows us to use the classical gravitational action as the generating functional for the quantum observable $n-$point functions

2.1 $\mathcal{N} = 4$ Super Yang-Mills / type IIB superstring theory on $AdS_5 \times S^5$ correspondence

The AdS/CFT correspondence [17–23] is best known from its most prominent example, that $\mathcal{N} = 4$ Super Yang-Mills (SYM) theory with gauge group SU(N) and Yang-Mills coupling constant g_{YM} is dynamically equivalent to type IIB superstring theory with string length $l_s = \sqrt{\alpha'}$ and coupling constant g_s on $AdS_5 \times S^5$ with radius of curvature L and N units of $F_{(5)}$ units of flux on S^5. The free parameters on the field theory side, *i.e.,* g_{YM} and N, are mapped to the free parameters g_s and $L/\sqrt{\alpha'}$ on the string theory side by

$$\begin{aligned} g_{YM}^2 &= 2\pi g_s \\ 2g_Y^2 N^2 &= L^4/\alpha'^2 \,. \end{aligned} \tag{2.1}$$

The statement that these two theories are *dynamically equivalent* means that the two theories are exactly identical and describe the same physics from two different perspectives. Although this duality is very interesting in its own right, it is a very rigid equivalence. It is often useful to weaken the correspondence by taking the t'Hooft limit $N \to \infty$ and further taking the strong-coupling limit $\lambda \to \infty$ in order to open the doors to using this duality as a tool to probe strongly interacting quantum theories using the dynamics of classical gravity!

2.2 CFT algebra and AdS symmetries

Let us take some time to understand how a d-dimensional CFT_d can be related to the boundary of the anti de-Sitter space in $d+1$ dimensions AdS_{d+1}.

2.2.1 The conformal group

Conformal symmetry, in simple terms, is the symmetry that your point of view of the universe is not only invariant under translations and rotations but it is also invariant to *zooming* in and *zooming* out, *i.e.,* it is scale-invariant. There are $\frac{(d+1)(d+2)}{2}$ distinct continuous symmetries in the conformal group, they are translations, rotations, dilatations and special conformal transformations (SCT)s. Table 2.1 explains each of these generators and how many of them there are in a d-dimensional CFT. One finds that the conformal

Type	Generator	Transformation	Symmetry	no. of symmetries
translation	P_μ	$-i\partial_\mu$	$x^\mu \to x^\mu + a^\mu$	d
rotation/boost	$M_{\mu\nu}$	$i(x_\mu\partial_\nu - x_\nu\partial_\mu)$	$x^\mu \to M^\mu_\nu x^\nu$	$\frac{d(d-1)}{2}$
dilatation	D	$-ix^\mu\partial_\mu$	$x^\mu \to \lambda x^\mu$	1
SCT	K_μ	$i(2x_\mu x^\nu\partial_\nu - x^2\partial_\mu)$	$x^\mu \to \frac{x^\mu + a^\mu x^2}{1+2a^\nu x_\nu + a^2x^2}$	d

Table 2.1: A table summarizing the conformal generators

algebra is given by [23–25]

$$[M_{\mu\nu}, P_\rho] = i(g_{\nu\rho}P_\mu - g_{\mu\rho}P_\nu) \tag{2.2a}$$
$$[M_{\mu\nu}, M_{\rho\sigma}] = i(g_{\mu\sigma}M_{\nu\rho} + g_{\nu\rho}M_{\mu\sigma} - g_{\mu\rho}M_{\nu\sigma} - g_{\nu\sigma}M_{\mu\rho}) \tag{2.2b}$$
$$[M_{\mu\nu}, K_\rho] = i(g_{\nu\rho}K_\mu - g_{\mu\rho}K_\nu) \tag{2.2c}$$
$$[D, P_\mu] = iP_\mu \tag{2.2d}$$
$$[D, K_\mu] = -iK_\mu \tag{2.2e}$$
$$[P_\mu, K_\mu] = 2i(g_{\mu\nu}D + M_{\mu\nu}) \tag{2.2f}$$

which is a representation of the group SO(d,2).

2.2.2 Anti de-Sitter spacetime

Anti de-Sitter spacetime is usually introduced as being a hypersurface with negative curvature

$$(-X^0)^2 + \sum_{i=1}^{d+2}(X^i)^2 - (X^{d+2})^2 = -L^2 \tag{2.3}$$

where X^i are embedding coordinates and $d+1$ is the spacetime dimension for the AdS space. We can see that the isometry group of AdS spacetime is SO(d,2), which should come as no surprise, has $\frac{(d+1)(d+2)}{2}$ Killing generators.

A metric that covers a patch of AdS space is the Poincaré patch given by

$$ds^2 = \frac{L^2}{z^2}\left(-dt^2 + dz^2 + \eta_{ij}dx^i dx^j\right) \tag{2.4}$$

where L is the characteristic length scale of the AdS space. This metric solves the Einstein equation with cosmological constant $\Lambda = -\frac{(d(d-1))}{2L^2}$. The spacetime is conformally flat, in

fact, the continuous isometry group for Euclidean ($t = i\tau$) AdS$_{d+1}$ is $SO(d+1,1)$ [22]. The symmetry group involves $\frac{1}{2}d(d-1)$ rotations and d translations of the x_i and τ coordinates, 1 scale transformation $(\tau, z, x_i) \to \lambda(\tau, z, x_i)$, and d special conformal transformations. The corresponding Lorentzian continuous symmetry group is $SO(d,2)$.

2.3 Field-operator correspondence

Taking from the example for the duality between $\mathcal{N} = 4$ Super Yang-Mills theory and classical fields in type IIB supergravity on $AdS_5 \times S^5$ we will observe that there is an intimate relationship between gauge invariant field theory operators and dynamical classical fields in the gravitational theory [19, 20, 25]. In particular in order for the dynamical fields in the AdS spacetime to have the needed scaling dimensions near the boundary of AdS spacetime to represent the field theory operators properly the masses for the gravitational fields are fixed by the scaling dimensions for the CFT operators. The relationship is given in table 2.2. Given a spin-s operator $\mathcal{O}^{\alpha_i}$, conformal invariance of the two-point function requires [26]

$$\langle O_{\alpha_i}(x) O_{\alpha_j}(0)\rangle = c\frac{P_{ij}}{|x|^{2\Delta}} \tag{2.5}$$

where P_{ij} is the unique conformally invariant tensor and Δ is the scaling dimension for the operator $\mathcal{O}^{\alpha_i}$. The form for P_{ij} for spin 0, 1, and 2 operators is given by

$$P_{ij} \equiv \begin{cases} 1 & ; \quad \text{spin } 0 \\ I_{\mu\nu} = \delta_{\mu\nu} - 2\frac{x_\mu x_\nu}{x^2} & ; \quad \text{spin } 1 \\ \mathcal{I}_{\mu\nu;\sigma\rho} = \frac{1}{2}(I_{\mu\sigma}I_{\nu\rho} + I_{\mu\rho}I_{\nu\sigma}) - \frac{1}{d}\delta_{\mu\nu}\delta_{\sigma\rho} & ; \quad \text{spin } 2 \end{cases} \tag{2.6}$$

2.3.1 Scalar fields and scalar operators

Turning to an AdS scalar field with mass m as an example and requiring by the AdS/CFT dictionary (see *e.g.,* (2.18)) that the scalar field must have as a boundary condition that $\phi(z) \sim z^{\Delta}$, we can see from evaluating the Klein-Gordon equation near the AdS boundary

Type	CFT operator	AdS field	Mass/scaling dimension
scalar	$\mathcal{O}$	ϕ	$m^2L^2 = -\Delta(d-\Delta)$
massless spin-2	$T_{\mu\nu}$	$g_{\mu\nu}$	$m = 0$, $\Delta = d$
conserved 1-form	J_μ	A_μ	$m = 0$, $\Delta = d-1$
general p-form	$\boldsymbol{A}^{(p)}$	χ	$m^2L^2 = (\Delta-p)(d-\Delta-p)$
spin 1/2, 3/2	ψ	Ψ	$\lvert m\rvert L = \Delta - d/2$

Table 2.2: A table showing the duality between CFT operators and AdS fields with a column showing the relationship between the masses of AdS fields and the scaling dimensions for CFT operators.

$(z \to 0)$[2]

$$\begin{aligned} 0 =& (\nabla^2 - m^2)\phi \\ =& \frac{1}{\sqrt{-g}}\partial_z(\sqrt{-g}g^{zz}\partial_z\phi) - m^2\phi - g^{ij}\partial_i\phi\partial_j\phi \\ =& \frac{z^2}{L^2}\left(\partial_z^2\phi - \frac{d-1}{z}\partial_z\phi\right) - m^2\phi - \frac{z^2}{L^2}k^2\phi \\ \approx& \left(\frac{z^\Delta}{L^2}\right)\Big(\Delta(\Delta-1) - \Delta(d-1) - m^2L^2 + O(z^2)\Big) \\ =& \left(\frac{z^\Delta}{L^2}\right)\Big(\Delta(\Delta-d) - m^2L^2 + O(z^2)\Big) \end{aligned} \tag{2.7}$$

that the mass for the scalar field is fixed to $m^2L^2 = -\Delta(d-\Delta)$. Not only have we made a relationship between the mass of the gravitational scalar field and the scaling dimension for the CFT operator $\mathcal{O}$, but the relationship between m and Δ is such that for a given mass m there are two scaling dimensions that satisfy the relationship

$$\Delta_\pm = \frac{d}{2} \pm \sqrt{\frac{d^2}{4} + m^2L^2}\,. \tag{2.8}$$

Indeed, if we would solve the Klein-Gordon equation and evaluate the solution near the asymptotic boundary of AdS space we would get

$$\phi(z) = \phi_0 z^{\Delta_-} + \phi_1 z^{\Delta_+} + \cdots\,. \tag{2.9}$$

[2]We also utilized Lorentz invariance to express the non-radial directions in terms of their Fourier components $\phi = \int \frac{d^dk}{(2\pi)^d} e^{-i\boldsymbol{x}\cdot k}\phi(z)$, though this consideration does not affect the derivation.

These two independent modes are usually called the (z^{Δ_+}) normalizable and the (z^{Δ_-}) non-normalizable modes for the scalar field. We will denote the scaling dimension for the normalizable mode as $\Delta_+ = \Delta$ which leaves us with the dimension for the non-normalizable mode as $\Delta_- = d - \Delta$. On dimensional grounds, we can identify the mode ϕ_1 as the vacuum expectation value for the dual scalar field $\langle \mathcal{O} \rangle$, while the non-normalizable mode ϕ_0 as a source for the operator [20]. One final comment regarding the mass m of the scalar field, we can plainly see from table 2.2 that the mass squared will be negative when the scaling dimension for the CFT operator $\mathcal{O}$ is relevant *i.e.,* $\Delta < d$, and positive (massless) when the operator is irrelevant (marginal). The mass of the scalar field, however, is bounded from below $m^2 L^2 \geq -d^2/4$. The unitarity bound puts a restriction on the scaling dimension of the CFT operator [20] $\Delta \geq d/2 - 1$. The case when $\Delta < d/2$ is subtle since we identify Δ_- as the conformal dimension $\Delta = \Delta_-$. Thus, in the range of scaling dimensions $d/2 - 1 \leq \Delta \leq d/2$ the identification of the source λ and the vacuum expectation value $\langle \mathcal{O} \rangle$ are interchangeable, giving rise to an alternative quantization.

2.3.2 Electromagnetic gauge field and conserved currents

Similarly to the scalar field, the masses for all fields are determined by the scaling properties to their dual operators in the CFT. For a conserved CFT vector current dual to a massless AdS Maxwell field $J_\mu \leftrightarrow A_\mu$ we can show that the masslessness of the Maxwell field is necessary for the vector current to be conserved. A conserved vector current $\partial_\mu J^\mu = 0$ constrains the scaling dimension of J to $\Delta = d - 1$, this can seen by taking

$$0 = \partial_\mu \langle J^\mu J_\nu \rangle \,. \tag{2.10}$$

Consider now a massive gauge field in AdS space. The transverse equations of motion would be

$$\begin{aligned} 0 =& \nabla_\mu (F^{\mu x}) - m^2 A^x \\ =& \frac{z^2}{L^2} \left(\partial_z^2 A_x - \frac{d-3}{z} \partial_z A_x \right) - m^2 A_x. \end{aligned} \tag{2.11}$$

and if we would go through the same procedure as above, and assume that the near-asymptotic behaviour for the gauge field A_x as $z \to 0$ is $A_x \sim z^\alpha$, then we get

$$\alpha(\alpha - d + 2) = m^2 L^2. \tag{2.12}$$

From eq. (2.5) we expect $\alpha = \Delta - s$, thus we see that $\Delta = d - 1$ if and only if $m = 0$ which is precisely why massless gauge fields are dual to a conserved CFT vector currents.

2.3.3 Stress tensor and the graviton

The stress tensor is a symmetric, traceless tensor in a CFT. The scaling dimension for the stress tensor is fixed by setting $\Delta = d$ in order to satisfy

$$0 = \partial_\mu \langle T^{\mu\nu} T_{\sigma\rho} \rangle \,. \tag{2.13}$$

The CFT stress tensor is dual to the AdS metric since it is defined as the response of local QFT changes to the metric [25] $S_{\text{boundary}} \sim \int \gamma_{\mu\nu} T^{\mu\nu}$ where $\gamma_{\mu\nu}$ is the metric on the boundary. But, we can show generally that all symmetric conserved spin-2 operators are dual to massless fields in the bulk. The mass-scaling dimension relationship for a symmetric spin-2 operator is the same as for a scalar operator [20]

$$m^2 L^2 = \Delta(d - \Delta) \,, \tag{2.14}$$

therefore the dual to a conserved, symmetric, spin-2 CFT operator must be massless. A table summarizing a few cases of the field-operator mapping in AdS/CFT is given in table 2.2.

2.4 Calculating correlation functions

The relationship between quantum field theory operators and fields in AdS space is quite powerful. The exact prescription on how to relate between the observables of a CFT and the gravitational dynamics of the AdS space is to equate the partition function of the conformal field theory with the partition function computed by integrating over the AdS metric near the boundary [17].

$$Z_{\text{CFT}} = Z_{\text{AdS}} \tag{2.15}$$

Generally, the form of Z_{Ads} is not known, so what is commonly done is to perform the saddle point approximation of classical gravity, where we would make the approximation

$$Z_{\text{AdS}} \approx e^{-S_{\text{AdS}}} \tag{2.16}$$

where S_{AdS} is the action for the AdS gravity evaluated on shell. Given a deformation to the CFT action $S = S_{\text{CFT}} - \int d^d \phi_0 \mathcal{O}(x)$, using the prescription eq. (2.16) on how to relate observables in these two regimes we need to evaluate the gravitational action with the boundary condition that $\phi(z) \approx \phi_0 z^{d-\Delta}$. In this case, the partition function Z_{AdS} integrates over all possible field configurations for ϕ with the correct boundary condition

$$\left\langle \exp\left(\phi_0 \int d^d x \mathcal{O}\right) \right\rangle_{\text{CFT}} \approx e^{-S_{\text{AdS}}}\big|_{z\to 0, \phi \sim \phi_0 z^{d-\Delta}} \,. \tag{2.17}$$

Partition function in general can be calculated in this manner by treating the classical AdS action as a generating functional for correlation functions of the boundary CFT. An explicit expression for this claim is that an $n-$point function can be found by taking the variational derivative of the action

$$\langle \mathcal{O}(p_1)\mathcal{O}(p_2)\cdots\mathcal{O}(p_n)\rangle = -\frac{\delta^n S_{\text{gravity}}}{\delta\phi_0(p_1)\delta\phi_0(p_2)\cdots\delta\phi_0(p_n)}\delta(p_1+p_1+\cdots+p_n). \tag{2.18}$$

Throughout this thesis, we will sometimes elect to write the momentum conservation condition explicitly on the left hand side and suppress the indication for the delta function. If one is interested in converting this expression to position space, the correct approach is to Fourier transform the momentum-space version

$$\begin{aligned}\langle \mathcal{O}(x_1)\mathcal{O}(x_2)\cdots\mathcal{O}(x_n)\rangle = -\int \frac{d^d p_1 d^d p_2\cdots d^d p_n}{(2\pi)^{dn}} e^{-i(\boldsymbol{p}_1\cdot\boldsymbol{x}_1+\boldsymbol{p}_2\cdot\boldsymbol{x}_2+\cdots+\boldsymbol{p}_n\cdot\boldsymbol{x}_n)}\times \\ \frac{\delta^n S_{\text{gravity}}}{\delta\phi_0(p_1)\delta\phi_0(p_2)\cdots\delta\phi_0(p_n)}\delta(p_1+p_2+\cdots+p_n).\end{aligned} \tag{2.19}$$

This prescription can be extended to other operators in the CFT and if the gravity theory has interactions between the dynamical fields some n-point functions will become non-trivial in the boundary theory. The organization for these correlation function calculations are nearly identical to how Feynman diagrams are used to organize scattering amplitude calculations in Quantum Field Theory. We will use a similar method of graphical organization called Witten diagrams [17]. In order to make full use of these Witten diagrams, knowledge of the AdS propagators for the fields in question is useful. Chapter 4 of this thesis contains Witten diagram calculations in pure vacuum AdS space.

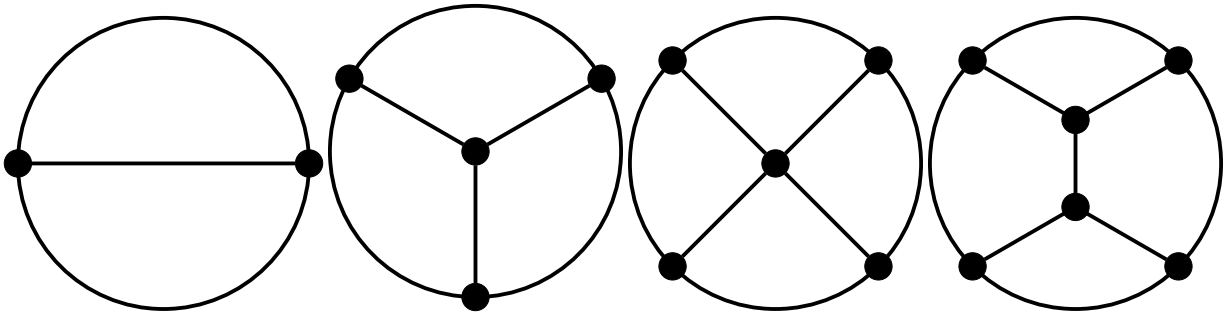

Figure 2.1: Examples of Witten Diagrams

2.5 Hydrodynamics

In this thesis, we showcase the power of AdS/CFT in the realm of hydrodynamics. Specifically, how we can use the AdS/CFT dictionary to calculate a linear response to small perturbations about an equilibrium system. In the gravitational sense, this means solving background gravitational equations of motion and then adding a small source field to the system and observe the effects that the source has on CFT observables. In particular we will be observing the effects that turning on a small relevant scalar field (controlled by temperature or charge) will have on the scalar two-point function $\langle \mathcal{O}_0 \mathcal{O}_0 \rangle$ and on the conductivity $\langle J_x J_x \rangle$ of the background theory.

2.5.1 Linear response theory

In the case of scalar fields, we have shown that a scalar field has a near-boundary solution to the equation of motion of the form

$$\phi(z,k) = \phi_0(k) z^{d-\Delta}(1 + O(z^2)) + \phi_1(k) z^{\Delta}(1 + O(z^2)) \tag{2.20}$$

The AdS/CFT dictionary guides us on how to find the one-point and two-point functions for the scalar field. There is some subtlety involved, however, due to UV divergences appearing in boundary contributions to the action. Appendix A explains how to navigate these subtleties and extract the correct forms for the one-point and two-point functions of a scalar field

$$\langle \mathcal{O}(k) \rangle = \left(\frac{L}{\ell_p} \right)^{d-1} (2\Delta - d)\phi_1(k)\,. \tag{2.21}$$

This formula for the one-point function provides a very useful insight on how the gravitational fields are related to CFT information: we have already identified the leading order behaviour for the scalar field $\phi_0 z^{d-\Delta}$ provides the source for the for the perturbation in the CFT action, but eq. (2.21) explains that the complimentary asymptotic behaviour of the scalar field $\phi_1 z^{\Delta}$ encodes the response of the CFT as a result of the perturbation. The two-point function is similarly found to be

$$\begin{aligned} \langle \mathcal{O}(-k)\mathcal{O}(k) \rangle =& \frac{\delta \langle \mathcal{O} \rangle}{\delta \phi_0} \\ =& \left(\frac{L}{\ell_p} \right)^{d-1} (2\Delta - d) \frac{\phi_1(k)}{\phi_0(k)}. \end{aligned} \tag{2.22}$$

The case $2\Delta = d$ requires an alternative renormalization procedure which we discuss for $d = 3$ in appendix D.3. It may seem strange to see the source appear in eq. (2.22), but the quotient ϕ_1/ϕ_0 is well defined as explained in Appendix A.

The conductivity is similarly defined with respect to the retarded propagator

$$\sigma^{ij}(\omega) \equiv \frac{G_R^{ij}(\omega)}{i\omega}\,, \tag{2.23}$$

where $G_R^{ij}(\omega)$ is the retarded propagator for the Maxwell field in momentum space with the spatial component to the momentum set to zero $k = (\omega, \mathbf{0})$. The retarded propagator is best described as the kernel for the action connecting two gauge fields

$$S_{\text{Maxwell}} = -\frac{1}{4g_4^2}\int \frac{d^dk}{(2\pi)^d}\frac{1}{2}A_x(-\boldsymbol{k})G_R^{xx}(\boldsymbol{k})A_x(\boldsymbol{k})\Big|_{z\to 0}\,. \tag{2.24}$$

Writing the retarded propagator in this manner we can identify its near boundary limit with the vector two-point function

$$G_R^{xx}|_{z\to 0} = \langle J_x(-k)J_x(k)\rangle \tag{2.25}$$

And as we will be often using Euclidean-time frequency $\Omega = -i\omega$ it is useful to write down the formula for the conductivity in Euclidean-time frequency

$$\sigma(\Omega) = -\frac{\langle J_x(i\Omega)J_x(-i\Omega)\rangle}{\Omega}\,. \tag{2.26}$$

2.5.2 The membrane paradigm

Another useful probe for understanding hydrodynamic modes in a thermal field theory is by investigating poles of the retarded correlators from holography in spacetimes with black hole horizons [4, 27, 28]. These poles are a direct counterpart to hydrodynamic modes. Using holography, we can probe the infrared correlation functions for the dual thermal field theory. That is, there is a black hole solution to the Einstein-Maxwell equations, and a Maxwell field that satisfies the equation of motion [3]

$$0 = \nabla_a\left(XF^{a\mu}\right)\,, \tag{2.27}$$

[3] We will investigate this situation in depth in chapter 5

where $X = X(z)$ is some scalar field with only radial dependence. If we constrain our attention to surfaces of constant z then eq. (2.27) implies a conservation law $\partial_\mu j^\mu = 0$ for

$$j^\mu = \sqrt{-g} X \, F^{\mu z})\Big|_{z_m} \tag{2.28}$$

where $z_m = z_h + \epsilon$ is a hypersurface that is very near to the black hole horizon ($z_m - z_h \ll z_h$) [4, 7, 27]. In appendix B, you can see a detailed derivation for how the Maxwell field near the black hole horizon is dispersive and obeys Fick's law

$$j^i = -D \, \partial_i j^t \,, \tag{2.29}$$

where the diffusivity is found to be

$$D = \sqrt{-g}\sqrt{-g^{xx} g^{xx} g^{tt} g^{uu}} X \Big|_{z=z_h} \int_0^{z_h} \frac{dz g_{tt} g_{zz}}{\sqrt{-g} X}. \tag{2.30}$$

Furthermore, applying Ohm's law $j^x = \sigma E^x$ near the horizon gives us the DC conductivity

$$\sigma(\omega = 0) = \frac{\sqrt{-g}\sqrt{-g^{xx} g^{xx} g^{tt} g^{zz}} X}{g_d^2} \,. \tag{2.31}$$

Chapter 3

Conformal perturbation theory

3.1 Correlators

Correlation functions and quantum field theory go hand-in-hand, it is hard to imagine doing quantum field theory without discussing correlators or propagators. Quantum Field Theory traditionally deals with scattering amplitudes and in practice these amplitudes are given in the form of correlation functions [24]. Correlation functions may have an even more intimate relationship with CFTs. Conformal symmetry completely restricts the form that two-point and three-point functions can take. For example, the scalar two-point function is fixed up to some theory dependent constant

$$\langle \mathcal{O}(x)\mathcal{O}(0)\rangle = \frac{C_{\mathcal{O}\mathcal{O}}}{|x|^{2\Delta}} \tag{3.1}$$

where Δ is the scaling dimension for the operator $\mathcal{O}(\lambda x) = \lambda^{-\Delta}\mathcal{O}(x)$. In this section, we use conformal perturbation theory and operator product expansions as tools to understand how introducing a relevant scalar operator affects other dynamical observables such as the conductivity. As with many aspects of quantum field theory, we will primarily be taking expectation values in momentum space. To find the position-space correlation functions we can apply eq. (2.19) once we know the momentum-space correlation function. One notational shortcut that we often employ when quoting momentum space correlation functions is that there is momentum conservation, *i.e.,* the momentum-space two-point function is given by

$$\langle \mathcal{O}(p_1)\mathcal{O}(p_2)\rangle = \mathcal{C}_{\mathcal{O}\mathcal{O}}\, p_1^{2\Delta-d}\, \delta^d(p_1+p_1), \tag{3.2}$$

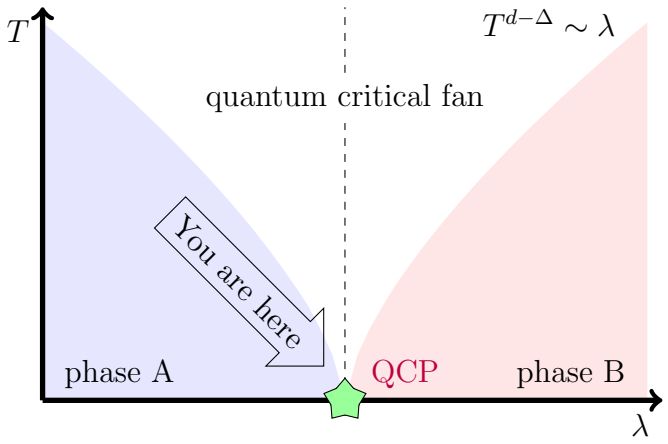

Figure 3.1: In this chapter we probe the quantum critical point

but throughout the remainder of this thesis, and as is standard in the literature, we will ignore writing these delta functions explicitly and absorb the momentum conservation implication by ensuring that the momenta of the operators in the correlation function add to zero

$$\langle \mathcal{O}(-k)\mathcal{O}(k)\rangle = \mathcal{C}_{\mathcal{O}\mathcal{O}} k^{2\Delta-d}\,. \tag{3.3}$$

Figure 3.1 is a reminder that in chapters 3 and 4 we are looking at a QCP, which means the temperature and the scalar deformation are set to zero and we have a legitimate conformal field theory dual to pure and free AdS space.

3.1.1 Two-point functions

The scalar two-point function

As was briefly mentioned in the previous section as the canonical example, the scalar two-point function for a CFT scalar operator $\mathcal{O}_0$ with scaling dimension Δ_0 is fixed by conformal symmetry up to an over constant [24, 26, 29]

$$\langle \mathcal{O}_0(x)\mathcal{O}_0(0)\rangle = \frac{C_{\mathcal{O}_0\mathcal{O}_0}}{|x|^{2\Delta}}. \tag{3.4}$$

We will be working through this thesis in momentum space. We can find the momentum space scalar two-point function via a Fourier transform

$$\langle \mathcal{O}_0(-k)\mathcal{O}_0(k)\rangle = \mathcal{C}_{\mathcal{O}_0\mathcal{O}_0} k^{2\Delta-d} \tag{3.5}$$

where we explicitly are absorbing the momentum space delta function in the definition of the momentum space two-point function as described above. If $\Delta - d/2$ is an integer we find an extra factor of $\log k$. We will ignore this minutia as it will become obvious that the transport functions are well behaved with respect to the scaling dimension Δ and so we can extract these special cases from the limiting behaviour of the scaling dimension.

Conductivity

For the conserved vector current J_μ, we note that the operator dimension is fixed to $\Delta_J = d - 1$. In a pure CFT we find that the vector two-point function is

$$\langle J_\mu(x) J_\nu(0)\rangle = \frac{C_{JJ}}{|x|^{2d-2}} I_{\mu\nu}(x) \tag{3.6}$$

where $I_{\mu\nu}(x) = \delta_{\mu\nu} - 2\frac{x_\mu x_\nu}{x^2}$ is the familiar unique conformally invariant tensor. The dimension is fixed by the Ward identity $\partial^\mu \langle J_\mu(x) J_\nu(0)\rangle = 0$. Once again, we are interested in the conductivity in momentum space. Conformal invariance ensures that the vector two-point function in momentum space is given by

$$\langle J_\mu(-k) J_\nu(k)\rangle = -\mathcal{C}_{JJ} k^{d-2} I_{\mu\nu}(k) \tag{3.7}$$

where $I_{\mu\nu}(k) = \delta_{\mu\nu} - \frac{k_\mu k_\nu}{k^2}$. Note that we are using a relaxed notation in reusing the tensor I. The tensor $I_{\mu\nu}(k)$ still represents the most general tensor that satisfies the conformal invariance, but also the Ward identity becomes almost trivial to see, now realized by $k^\mu I_{\mu\nu} = 0$. So, to recap, in a pure CFT any two-point function will be fixed up to some constant $\mathcal{C}_{\mathcal{O}_0\mathcal{O}_0}$ for the scalar propagator for $\mathcal{O}_0$ and $\mathcal{C}_{JJ}$ for the conductivity from the vector current J_μ.

Stress two-point function

The stress two-point function is similarly constrained, the stress scaling dimension is fixed to be $\Delta = d$ by conservation of energy, and the two-point function is fixed up to an overall constant

$$\langle T_{\mu\nu}(x) T_{\rho\sigma}(0)\rangle = \frac{C_{TT}}{|x|^{2d}} \mathcal{I}_{\mu\nu;\rho\sigma}(x) \tag{3.8}$$

where C_{TT} is the central charge of the CFT and $\mathcal{I}$ is given in eq. (2.6). Similarly, we can write the stress two-point function in momentum space

$$\langle T_{\mu\nu}(-k) T_{\rho\sigma}(k)\rangle = \mathcal{C}_{TT} |k|^d \mathcal{I}_{\mu\nu;\rho\sigma}(k) \tag{3.9}$$

where we introduce the momentum space version of $\mathcal{I}$ which is the unique conformally invariant tensor form that is symmetric in $\mu \leftrightarrow \nu$ and $\rho \leftrightarrow \sigma$

$$\mathcal{I}_{\mu\nu;\rho\sigma}(k) = \frac{1}{2}\left(I_{\mu\rho}(k)I_{\nu\sigma}(k) + I_{\mu\sigma}(k)I_{\nu\rho}(k)\right) - \frac{I_{\mu\nu}(k)I_{\rho\sigma}(k)}{d-1}\,. \tag{3.10}$$

3.1.2 Three-point functions

Three-point functions have more complicated structure, yet each three-point function is, like two-point functions, fixed up to some overall constant by conformal symmetries [30,31].

$\mathcal{C}_{\mathcal{O}_0\mathcal{O}_0\mathcal{O}}$

We are interested in the three-point function $\langle\mathcal{O}_0(p_1)\mathcal{O}_0(p_2)\mathcal{O}(p_3)\rangle$, which is the correlation function involving a scalar operator evaluated at two points $\mathcal{O}_0$ and a scalar operator $\mathcal{O}$ evaluated at one point. The reason why this type of correlation function is of interest is the role that it plays in evaluating the scalar propagator $\langle\mathcal{O}_0\mathcal{O}_0\rangle$. The momentum space three-point function for $\langle\mathcal{O}_0(p_1)\mathcal{O}_0(p_2)\mathcal{O}(p_3)\rangle$ is fixed up to an overall constant [29]

$$\langle\mathcal{O}_0(p_1)\mathcal{O}_0(p_2)\mathcal{O}(p_3)\rangle = \mathcal{C}_{\mathcal{O}_0\mathcal{O}_0\mathcal{O}}\, I\left(d/2-1, \Delta_0 - d/2, \Delta_0 - d/2, \Delta - d/2\right) \tag{3.11}$$

where the integral I is sometimes called a triple Bessel integral [30] and it is defined as

$$I(a,b,c,d) \equiv \int_0^\infty dx\, x^a p_1^b p_2^c p_3^d K_b(p_1x)K_c(p_2x)K_d(p_3x). \tag{3.12}$$

The function $K_\nu(x)$ is the modified Bessel function which exponentially decays as $x \to \infty$. We will see in chapter 4 that the Bessel functions play a central role for propagators in AdS space. At this point we would like to note that the d appearing in the above equation is a variable, and is not the dimension for the conformal space. With the purpose of using the $\mathcal{O}_0\mathcal{O}_0$ OPE in order to calculate the high-frequency behaviour of general scalar propagator, we want to probe the local behaviour of for the scalar two-point function and hence we will enforce $p_{1,2} \gg p_3$. In order to more easily compare with the remainder of the thesis, we will assumed that each p_i is purely along the time-direction, and we let $p_3 = p \ll \Omega$ will take $p_1 = -\Omega$ and $p_2 = \Omega - p$. Since we are working in momenta in which p is small, we will employ the following expansion to the Bessel function involving p

$$K_d(px) \approx \frac{\Gamma(d)2^{d-1}}{(px)^d} + \frac{\Gamma(-d)(px)^d}{2^{d+1}} + O(p^{2-d}) \tag{3.13}$$

With these approximations in mind the three-point is approximately

$$\begin{aligned}\langle \mathcal{O}_0(-\Omega)\mathcal{O}_O(\Omega-p)\mathcal{O}(p)\rangle =& \mathcal{C}_{\mathcal{O}_0\mathcal{O}_0\mathcal{O}}\, 2^{\Delta-d/2-1}\Gamma(\Delta-d/2)\Psi(d,d-\Delta,\Delta_0)\Omega^{2\Delta_0+\Delta-2d} \\ &+\mathcal{C}_{\mathcal{O}_0\mathcal{O}_0\mathcal{O}}\, 2^{d/2-\Delta-1}\Gamma(d/2-\Delta)\Psi(d,\Delta,\Delta_0)p^{2\Delta-d}\Omega^{2\Delta_0-\Delta-d}\,,\end{aligned} \tag{3.14}$$

where

$$\Psi(d,\Delta,\Delta_0)\equiv\int_0^\infty dx x^{\Delta-1}K_{\Delta_0-d/2}(x)^2=\frac{\sqrt{\pi}\Gamma\left(\frac{\Delta}{2}\right)\,\Gamma\left(\frac{\Delta+d-2\Delta_0}{2}\right)\,\Gamma\left(\frac{\Delta+2\Delta_0-d}{2}\right)}{4\,\Gamma\left(\frac{\Delta+1}{2}\right)}. \tag{3.15}$$

This integral of a power function multiplied by the square of a Bessel functions will occur frequently in the subsequent sections.

$\mathcal{C}_{JJ\mathcal{O}}$

Conformal invariance also fixes the form for the three-point function $\langle J_\mu(p_1)J_\nu(p_2)\mathcal{O}(p_3)\rangle$ up to an overall constant. Slightly more complicated than the scalar-scalar-scalar version is

$$\begin{aligned}\langle J_x(p_1)J_x(p_2)\mathcal{O}(p_3)\rangle = \mathcal{C}_{JJ\mathcal{O}}\Big[&I(d/2,d/2-1,d/2-1,\Delta-d/2+1) \\ &+\frac{\Delta}{2}(d-2-\Delta)I(d/2-1,d/2-1,d/2-1,\Delta-d/2)\Big]\,.\end{aligned} \tag{3.16}$$

Eq. (3.16) holds as long as the momenta are transverse to the x-direction, but we will only require the transverse form of this expression in order to study the conductivity. If we similarly restrict our attention to the same limits as the previous section ($p_1=-\Omega$, $p_2=\Omega-p$ and $p_3=p$ with $|p|\ll|\Omega|$) and use the Bessel function approximation eq. (3.13) then we can break down eq. (3.16) in order to break down how each part might contribute

to the conductivity

$$\begin{aligned}\langle J_x(-\Omega)J_x(\Omega-p)\mathcal{O}(p)\rangle = \\ \mathcal{C}_{JJ\mathcal{O}}\Big[\quad & \Gamma(\Delta-d/2+1)2^{\Delta-d/2}\,\Psi(d,d-\Delta,d-1)\Omega^{\Delta-2} \\ & +\Gamma(1-d/2-\Delta)2^{2-\Delta+d/2}\,\Psi(d,\Delta-2,d-1)p^{2\Delta-d+2}\,\Omega^{d-\Delta-4} \\ & +\Delta(d-2-\Delta)2^{\Delta-d/2-2}\,\Gamma(\Delta-d/2)\Psi(d,d-\Delta,d-1)\Omega^{\Delta-2} \\ & +\Delta(d-2-\Delta)2^{d/2-\Delta-2}\,\Gamma(d/2-\Delta)\Psi(d,\Delta,d-1)p^{2\Delta-d}\,\Omega^{d-2-\Delta}\Big]\end{aligned} \tag{3.17}$$

3.2 Conformal perturbation theory

A recurring theme in this thesis is the claim that if a conformal field theory is being deformed by a relevant scalar operator

$$S = S_{\text{CFT}} + \lambda \int d^d x\, \mathcal{O}(x) \tag{3.18}$$

with scaling dimension Δ, then the propagator for some generic operator $\mathcal{Y}$ will have a characteristic high-frequency expansion.

$$\langle \mathcal{Y}(-\Omega)\mathcal{Y}(\Omega)\rangle_{\lambda,T} = \Omega^{2\Delta_{\mathcal{Y}}-d}\left(\mathcal{C}_{\mathcal{Y}\mathcal{Y}} + b\frac{\lambda}{\Omega^{d-\Delta}} + a\frac{\langle\mathcal{O}\rangle}{\Omega^{\Delta}} + O(\Omega^{-d})\right) \tag{3.19}$$

We will use conformal perturbation theory in order to determine the coefficients a and b for various propagators and then we will use holography to confirm these results. Holography will also provide powerful models in order to probe the full frequency dynamics of such transport functions.

3.2.1 Relevant deformation

In order to understand why the two correction terms in eq. (3.19) would appear, let us consider the CFT expectation value as a path integral taken near to the quantum critical

point:

$$\begin{aligned}\langle \mathcal{Y}(-\Omega)\mathcal{Y}(\Omega)\rangle_\lambda =& \frac{1}{\mathcal{Z}[h]}\int D\Phi_{\text{CFT}}\, e^{-S_{\text{CFT}}+\lambda\mathcal{O}(0)}\mathcal{Y}(-\Omega)\mathcal{Y}(\Omega)\\ =& \frac{\mathcal{Z}[0]}{\mathcal{Z}[h]}\langle \mathcal{Y}(-\Omega)\mathcal{Y}(\Omega)e^{\lambda\mathcal{O}(0)}\rangle_{\text{CFT}}\\ =& \langle \mathcal{Y}(-\Omega)\mathcal{Y}(\Omega)(1+\lambda\mathcal{O}(0)+\cdots\rangle_{\text{CFT}}\\ =& \Omega^{2\Delta_{\mathcal{Y}}-d}\left(\mathcal{C}_{\mathcal{Y}\mathcal{Y}}+b\frac{\lambda}{\Omega^{d-\Delta}}+\cdots\right)\end{aligned} \tag{3.20}$$

Where $\mathcal{O}(0)$ is the zero momentum mode for the scalar operator $\mathcal{O}$ and the power of Ω follows from dimensional analysis. There would of course be a cascade of corrections to the propagator analytic in λ.

3.2.2 Operator product expansion

It will also often be the case that the pure CFT momentum-space OPE will take the form

$$\mathcal{Y}(-\Omega)\mathcal{Y}(\Omega+p) = \Omega^{2\Delta_{\mathcal{Y}}-d}\left(\mathcal{C}_{\mathcal{Y}\mathcal{Y}}+a\frac{\mathcal{O}(p)}{\Omega^{\Delta}}+\cdots\right). \tag{3.21}$$

Normally in a conformal field theory the expectation value $\langle\mathcal{O}\rangle = 0$. But, in general we would like to find the expectation values for quantum field theories near the QCP but with finite temperature T and scalar deformation λ[1]. The scalar deformation will be valid when the frequencies are large $\Omega^{d-\Delta} \gg \lambda$ and we can extend this analysis such that the temperatures we consider are always much larger than the scalar deformation parameter $\lambda \ll T^{d-\Delta}$. With this in mind eq. (3.21) can be evaluated at zero momentum and at finite temperatures

$$\langle \mathcal{Y}(-\Omega)\mathcal{Y}(\Omega)\rangle_T = \Omega^{2\Delta_{\mathcal{Y}}-d}\left(\mathcal{C}_{\mathcal{Y}\mathcal{Y}}+a\frac{\langle\mathcal{O}\rangle_T}{\Omega^{\Delta}}+\cdots\right). \tag{3.22}$$

If we combine the result of eq. (3.22) with that explained in eq. (3.20) we have a prediction for the first few corrective terms of a propagator near the QCP at finite temperature and scalar deformation

$$\langle \mathcal{Y}(-\Omega)\mathcal{Y}(\Omega)\rangle_{\lambda,T} = \Omega^{2\Delta_{\mathcal{Y}}-d}\left(\mathcal{C}_{\mathcal{Y}\mathcal{Y}}+b\frac{\lambda}{\Omega^{d-\Delta}}+a\frac{\langle\mathcal{O}\rangle_T}{\Omega^{\Delta}}+\cdots\right). \tag{3.23}$$

[1]See figure 1.1 for an example phase diagram, we are considering quantum field theories that lie somewhere inside of the *critical fan*

By doing a variety of manipulations one can set the coefficients a and b in terms of the CFT data *e.g.*, $\mathcal{C}_{\mathcal{O}\mathcal{O}}$, $\mathcal{C}_{\mathcal{Y}\mathcal{Y}\mathcal{O}}$, Δ and Δ_0. We will show explicitly demonstrate how to find these coefficients for $\langle \mathcal{O}_0 \mathcal{O}_0 \rangle$ and $\langle J_x J_x \rangle$ below and again holographically in chapter 5.

3.2.3 Scalar correlators

We will now fix the high-frequency expansion for propagators in the deformed CFTs in terms of the CFT parameters. The CFTs which we are interested in will contain a scalar operator $\mathcal{O}_0$ and a conserved vector current J_μ. We wish to find a high-frequency expansion for the scalar propagator $\langle \mathcal{O}_0 \mathcal{O}_0 \rangle$ and the electric conductivity $\langle J_x J_x \rangle$ in such a theory that is deformed away from criticality by a relevant scalar operator $\mathcal{O}$. The goal of this section is to show how we can use conformal perturbation theory in order to exactly specify the coefficients in terms of CFT data. The expected expansion for the CFT propagator is given by eq. (3.23), and explicitly for a scalar operator $\mathcal{O}_0$ is

$$\langle \mathcal{O}_0(-\Omega)\mathcal{O}_0(\Omega)\rangle_{\lambda,T} = \Omega^{2\Delta_0-d}\left(\mathcal{C}_{\mathcal{O}_0\mathcal{O}_0} + b\frac{\lambda}{\Omega^{d-\Delta}} + a\frac{\langle\mathcal{O}\rangle_T}{\Omega^{\Delta}} + \cdots\right). \tag{3.24}$$

The coefficients a and b are only temporary placeholders, as each two-point function will have different values for the coefficients in terms of CFT data. We can identify the first term in eq. (3.14) with the second term in eq. (3.20). We can therefore connect the two equivalent approaches

$$b = \mathcal{C}_{\mathcal{O}_0\mathcal{O}_0\mathcal{O}}\, 2^{\Delta-d/2-1}\Gamma(\Delta-d/2)\Psi(d,d-\Delta,\Delta_0)\Omega^{2\Delta_0+\Delta-2d}\,. \tag{3.25}$$

Let us now examine the OPE for two scalar fields

$$\mathcal{O}_0(-\Omega)\mathcal{O}_0(\Omega+p) = \Omega^{2\Delta_0-d}\left(\mathcal{C}_{\mathcal{O}_0\mathcal{O}_0} + a\frac{\mathcal{O}(p)}{\Omega^{\Delta}} + \cdots\right). \tag{3.26}$$

We can apply $\langle \cdots \mathcal{O}(-p)\rangle_{T=0,\lambda=0}$ to both sides of this equation and arrive at

$$\begin{aligned}\langle \mathcal{O}_0(-\Omega)\mathcal{O}_0(\Omega-p)\mathcal{O}(p)\rangle_0 &= \Omega^{2\Delta_0-d}\left(\mathcal{C}_{\mathcal{O}_0\mathcal{O}_0}\cancel{\langle\mathcal{O}(-p)\rangle_0} + a\frac{\langle\mathcal{O}(p)\mathcal{O}(-p)\rangle_0}{\Omega^{\Delta}} + \cdots\right)\\ &= a\Omega^{2\Delta_0-d}\frac{\mathcal{C}_{\mathcal{O}\mathcal{O}}p^{2\Delta-d}}{\Omega^{\Delta}} + \cdots\,.\end{aligned} \tag{3.27}$$

As we can see the evaluation of the vacuum expectation value of the scalar operator is null. We can now compare eq. (3.27) with the second term in eq. (3.14) to make the association

$$a\mathcal{C}_{\mathcal{O}\mathcal{O}} = \mathcal{C}_{\mathcal{O}_0\mathcal{O}_0\mathcal{O}}\, 2^{d/2-\Delta-1}\Gamma(d/2-\Delta)\Psi(d,\Delta,\Delta_0). \tag{3.28}$$

Substituting eqs. (3.28) and (3.25) into eq. (3.24) we arrive at

$$\begin{aligned}\langle \mathcal{O}_0(-\Omega)\mathcal{O}_0(\Omega)\rangle = \Omega^{2\Delta_0-d}\Bigg(& \quad \mathcal{C}_{\mathcal{O}_0\mathcal{O}_0} \\ & + \frac{\lambda \mathcal{C}_{\mathcal{O}_0\mathcal{O}_0\mathcal{O}}\, 2^{\Delta-d/2-1}\Gamma(\Delta-d/2)\Psi(d,d-\Delta,\Delta_0)}{\Omega^{d-\Delta}} \\ & + \frac{\langle\mathcal{O}\rangle \mathcal{C}_{\mathcal{O}_0\mathcal{O}_0\mathcal{O}}\, 2^{d/2-\Delta-1}\Gamma(d/2-\Delta)\Psi(d,\Delta,\Delta_0)}{\mathcal{C}_{\mathcal{O}\mathcal{O}}\Omega^{\Delta}}\Bigg).\end{aligned} \tag{3.29}$$

As a reminder, the expectation values taken in eq. (3.29) are evaluated in the quantum field theory anywhere inside of the critical fan, *i.e.,* at finite temperature and scalar deformation.[2]

Eq. (3.29) shows how conformal perturbation theory has provided us with the analytic high-frequency corrections to the scalar propagator purely in terms of CFT data.

3.2.4 Conductivity

A similar analysis can be done for the electrical conductivity. From dimensional analysis and eq. (3.17), we can see that terms from both of the triple Bessel integrals contribute to the deformation by the scalar operator (the first and third terms) and the fourth term contributes to the scalar one-point function. Recall that the conductivity is related to the propagator by eq. (2.23), in terms of the vector two-point function, the Euclidean conductivity is

$$\sigma(\Omega) = -\frac{\langle J_x(-\Omega)J_x(\Omega)\rangle}{\Omega}. \tag{3.30}$$

The expected decomposition of the vector two-point function is

$$\langle J_x(-\Omega)J_x(\Omega)\rangle_{\lambda,T} = \Omega^{d-2}\left(\mathcal{C}_{JJ} + b\frac{\lambda}{\Omega^{d-\Delta}} + a\frac{\langle\mathcal{O}\rangle_T}{\Omega^{\Delta}} + \cdots\right). \tag{3.31}$$

Using dimensional analysis, we can relate the second term of eq. (3.31) with the first and third terms in eq. (3.17) giving

$$b = \mathcal{C}_{JJ\mathcal{O}}(\Delta-2)(d-\Delta)2^{\Delta-d/2-2}\,\Gamma(\Delta-d/2)\Psi(d,d-\Delta,d-1). \tag{3.32}$$

[2]In fact, when we write expectation values we will assume that they are being performed in the general theory, only when we are taking a vacuum expectation value will we denote it as such.

In order to fix a in eq. (3.31) we will need to look at the OPE between two transverse vector currents.

$$J_x(-\Omega)J_x(\Omega+p) = \Omega^{d-2}\left(\mathcal{C}_{JJ} + a\frac{\mathcal{O}(p)}{\Omega^{\Delta}} + \cdots\right). \tag{3.33}$$

Following the methods of the previous section we can apply $\langle \cdots \mathcal{O}(-p)\rangle_{T=0,\lambda=0}$ to both sides of the equation to get

$$\begin{aligned}\langle J_x(-\Omega)J_x(\Omega-p)\mathcal{O}(p)\rangle_0 &= \Omega^{d-2}\left(\mathcal{C}_{JJ}\cancel{\langle\mathcal{O}(-p)\rangle_0} + a\frac{\langle\mathcal{O}(p)\mathcal{O}(-p)\rangle_0}{\Omega^{\Delta}} + \cdots\right). \\ &= a\Omega^{d-2}\,\frac{\mathcal{C}_{\mathcal{O}\mathcal{O}}p^{2\Delta-d}}{\Omega^{\Delta}} + \cdots\end{aligned} \tag{3.34}$$

We can now compare equation (3.34) with the fourth term in eq. (3.17) to make the association

$$a\mathcal{C}_{\mathcal{O}\mathcal{O}} = \mathcal{C}_{JJ\mathcal{O}}\,\Delta(d-2-\Delta)2^{d/2-\Delta-2}\Gamma(d/2-\Delta)\Psi(d,\Delta,\Delta_0). \tag{3.35}$$

We now have a conformal perturbation theory prediction for how the conductivity is affected by a relevant scalar deformation near the quantum critical point

$$\begin{aligned}\sigma(\Omega) = -\Omega^{d-3}\Bigg(&\quad \mathcal{C}_{JJ} \\ &+ \frac{\lambda\mathcal{C}_{JJ\mathcal{O}}(\Delta-2)(d-\Delta)2^{\Delta-d/2-2}\,\Gamma(\Delta-d/2)\Psi(d,d-\Delta,d-1)}{\Omega^{d-\Delta}} \\ &+ \frac{\langle\mathcal{O}\rangle\mathcal{C}_{JJ\mathcal{O}}\,\Delta(d-2-\Delta)2^{d/2-\Delta-2}\Gamma(d/2-\Delta)\Psi(d,\Delta,\Delta_0)}{\mathcal{C}_{\mathcal{O}\mathcal{O}}\Omega^{\Delta}}\Bigg).\end{aligned} \tag{3.36}$$

Chapter 4

AdS/CFT: The bridge between CFT data and AdS dynamics

In this chapter, we will using the AdS/CFT correspondence in order to derive the forms of the CFT scalar propagator and the electrical conductivity in the presence of a relevant operator which is deforming the system. The calculations in this chapter will be using the gravitational theory, and we will form the bridge between the gravitational couplings and the CFT data presented in the previous chapter. A simple and useful form of the metric describing AdS space is the Poincaré patch

$$ds^2 = \frac{L^2}{z^2}(-dt^2 + dz^2 + \eta_{ij}dx^i dx^j) \tag{4.1}$$

where L is the curvature scale of the anti de-Sitter spacetime. This spacetime is negatively curved with a cosmological constant $\Lambda = -\frac{d(d-1)}{2L^2}$. We will go into detail on how to calculate CFT correlators using AdS space and how we can use this powerful technique in order to get full-frequency responses for the CFT scalar propagator and AC conductivity. We also confirm the perturbative results outlined in chapter 3. In chapter 5, we investigate spacetimes that are asymptotically AdS but which enable us to incorporate temperature and scalar deformation into the quantum system, but for now we will be relating pure AdS properties with purely CFT properties.

4.1 A minimal bulk action

In this section we will construct an explicit minimal holographic model that incorporates a relevant scalar operator that is tuning the critical point.

The ingredients needed to investigate the effects that a scalar deformation of a CFT away from a QCP are given in table 4.1. Primarily, we need to measure the source and response of a scalar field ψ, as well as an electromagnetic gauge field A_a. The scalar deformation is represented in the gravitational theory as a scalar field ϕ. As seen from eqs. (3.29) and (3.36), in order for the scalar deformation to affect the propagators of the scalar field ψ and of the gauge field A_a, we require for there to be couplings ϕF^2 and $\phi\psi^2$. About the background gravitational theory, the scalar field ϕ has no sources, therefore the equations of motion for all of the dynamical fields in this model are trivial. A novel addition to the model to rectify this issue is a mechanism to self-consistently provide a source for the scalar deformation. This is engineered by introducing a coupling between the scalar field ϕ and gravity via $\phi\, C^2$ where $C_{\mu\nu\rho\sigma}$ is the Weyl curvature for the gravitational theory. The Weyl curvature provides the scalar operator with a vacuum expectation $\langle\mathcal{O}\rangle \sim T^{\Delta}$. The choice of Weyl tensor is natural since it represents a measure of the magnitude of non-conformality in the spacetime. Zero temperature corresponds to pure AdS space which is conformally flat, hence the Weyl tensor is null, so the vacuum expectation for the scalar will be zero. An action for such a theory that includes all necessary ingredients is given by

$$S = S_0 + S_\phi + S_\psi + S_A \tag{4.2}$$

where

$$S_0 = \frac{1}{2\ell_p^{d-1}} \int d^{d+1}x\sqrt{-g}\left(R + \frac{d(d-1)}{L^2}\right), \tag{4.3}$$

$$S_\phi = -\frac{1}{2\ell_p^{d-1}} \int d^{d+1}x\sqrt{-g}\left[(\nabla_a\phi)^2 + m^2\phi^2 - 2\alpha_C L^2 \phi\, C_{abcd}C^{abcd}\right], \tag{4.4}$$

$$S_\psi = -\frac{1}{2\ell_p^{d-1}} \int d^{d+1}x\sqrt{-g}\left[(\nabla_a\psi)^2 + (m_0^2 - \alpha_\psi\phi)\psi^2\right], \tag{4.5}$$

$$S_A = -\frac{1}{4g_d^2} \int d^{d+1}x\sqrt{-g}\left(1 + \alpha_F\phi\right) F_{ab}F^{ab}. \tag{4.6}$$

F_{ab} is the field strength of A_a, and C_{abcd} is the Weyl curvature tensor. The scalar action is normalized with a factor of $1/\ell_p^{d-1}$ to ensure that the scalar field ϕ is dimensionless, which will be convenient in the following calculations. The gauge field A_a has the usual dimension of inverse length and so the Maxwell coupling g_d is dimensionless. The scaling

Bulk coupling	Bulk operator	CFT correlator ($T=0$)	Observable
L^{d-1}/ℓ_p^{d-1}	R	$\langle T_{\mu\nu}\, T_{\rho\delta}\rangle$	C_T
$1/g_d^2$	$F_{ab}F^{ab}$	$\langle J_\mu\, J_\nu\rangle$	σ_∞
m^2L^2	ϕ^2	$\langle \mathcal{O}\, \mathcal{O}\rangle$	Δ
α_C	$\phi\, C_{abcd}C^{abcd}$	$\langle T_{\mu\nu}T_{\rho\delta}\, \mathcal{O}\rangle$	$\mathcal{C}_{TT\mathcal{O}}$
α_F	$\phi\, F_{ab}F^{ab}$	$\langle J_\mu J_\nu\, \mathcal{O}\rangle$	$\mathcal{C}_{JJ\mathcal{O}}$
α_ψ	$\phi\psi^2$	$\langle \mathcal{O}_0\mathcal{O}_0\mathcal{O}\rangle$	$\mathcal{C}_{\mathcal{O}_0\mathcal{O}_0\mathcal{O}}$

Table 4.1: The five dimensionless parameters which characterize the bulk gravity theory and the dual correlators in the boundary CFT which they control. There is also a non-vanishing $\langle J_\mu J_\nu T_{\rho\delta}\rangle$ CFT correlator in this model that does not have a corresponding Bulk coupling to tune it.

dimensions Δ and Δ_0 for the operators $\mathcal{O}$ and $\mathcal{O}_0$ respectively are determined by eq. (2.8) from m and m_0 respectively. The scaling dimension Δ is taken to be above the unitary bound for $d+1$ dimensional CFTs, $\Delta_{\min} = d/2-1$. We further note that in the range $d/2-1 \leq \Delta < d/2$, the theory will contain at least one other relevant scalar, which can be thought of as $\mathcal{O}^2$. In this regime, the CFT dual thus describes a *multicritical* point instead of a simple critical point.

The interaction terms in S_ψ and S_A are the simplest interactions that can spawn a corrections to the linear responses $\langle \mathcal{O}_0\mathcal{O}_0\rangle$ and $\langle J_x J_x\rangle$ due to the scalar expectation value discussed in chapter 3. The As described in table 4.1 the coupling constant α_F is related to the vacuum CFT correlator $\langle J_x J_x \mathcal{O}\rangle$, while α_ψ is related to the vacuum CFT correlator $\langle \mathcal{O}_0\mathcal{O}_0\mathcal{O}\rangle$. The coupling constant α_C is related to the vacuum CFT correlator $\langle T_{\mu\nu}T_{\rho\sigma}\mathcal{O}\rangle$, but for our purposes, we will be matching it to the magnitude of the scalar vacuum expectation $\langle \mathcal{O}\rangle$.

4.2 Propagators

As detailed in section 2.3.1, the operators we have been discussing in chapter 3 have dual fields in anti de-Sitter space, and we have a prescription to extract CFT observables from these dynamical bulk fields. A powerful tool is to find the propagators for these various fields in a spacetime dual to the pure CFT, namely empty AdS space. This means in a spacetime without a black hole providing temperature, or any sources for the matter fields.

4.2.1 Scalar bulk-bulk propagator

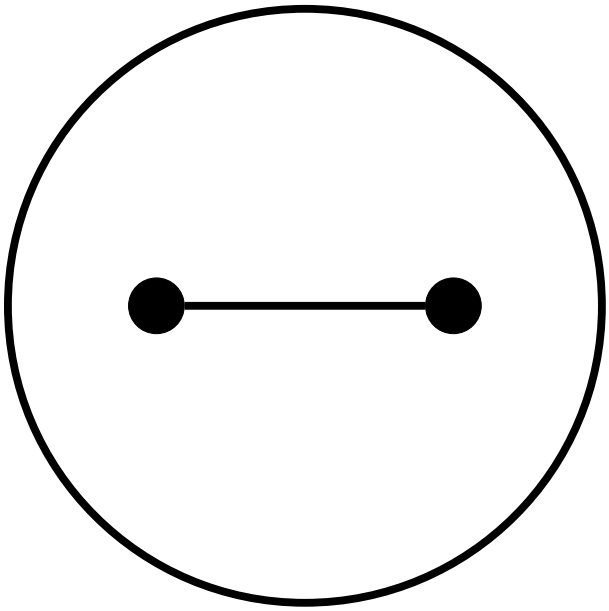

Figure 4.1: A Witten diagram depicting the scalar bulk-bulk propagator

The bulk-bulk scalar propagator is merely the general solution to the equations of motion for the scalar field. We are interested in the form of this propagator in momentum space so that we can see how to calculate n-point functions for the dual CFT. Scalar operators with a scaling dimension of Δ in a CFT will have a dual scalar field ϕ in AdS space with mass $m^2L^2 = \Delta(d-\Delta)$. The non-interacting action which governs the dynamics of such a field is given by S_ϕ in eq. (4.4) with $\alpha_C = 0$. Hence the equation of motion for the free scalar field ϕ is simply

$$0 = (\nabla^2 - m^2)\phi\,. \tag{4.7}$$

This equation of motion for ϕ is unsourced. In the Poincaré patch metric eq. (4.1) we have translation invariance in the boundary directions and therefore we will decompose the scalar field into its Fourier modes $\phi(x) = \int \frac{d^dk}{(2\pi)^d}\phi(z,k)e^{-ix\cdot k}$. The equations of motion

expanded in the Poincaré metric (4.1) gives

$$\begin{aligned} 0 =&(\nabla^2 - m^2)\phi \\ =&\frac{1}{\sqrt{-g}}\partial_z(\sqrt{-g}g^{zz}\partial_z\phi) + \frac{\Delta(d-\Delta)}{L^2}\phi - g^{ij}\partial_i\phi\partial_j\phi \\ =&\frac{z^2}{L^2}\left(\partial_z^2\phi - \frac{d-1}{z}\partial_z\phi\right) + \frac{\Delta(d-\Delta)}{L^2}\phi - \frac{z^2}{L^2}k^2\phi\,. \end{aligned} \tag{4.8}$$

This equation of motion is very similar to the modified Bessel equation, and the general solutions are

$$\phi = az^{d/2}K_{\Delta/2-d}(kz) + bz^{d/2}I_{\Delta/2-d}(kz) \tag{4.9}$$

where K and I are the modified Bessel functions. The general bulk-bulk Green's function depicted in figure 4.1 is given by

$$G(z,z';k) = \begin{cases} z'\,(z/z')^{d/2}K_{\Delta-d/2}(kz)I_{\Delta-d/2}(kz') & \text{if } z' > z \\ z'\,(z/z')^{d/2}K_{\Delta-d/2}(kz')I_{\Delta-d/2}(kz) & \text{if } z > z' \end{cases}. \tag{4.10}$$

The Green's function (4.10) is such that $(\nabla^2 - m^2)G(z,z';k) = \delta(z-z')$ and that $\phi = \int dz' G(z,z';k)F(z')$ is the general solution to the equation $(\nabla^2 - m^2)\phi = F(z)$. The expression eq. (4.10) is the bulk-to-bulk propagator for a scalar field in AdS space.

4.2.2 Scalar bulk-boundary propagator

If we are to make assertions about the underlying CFT that is dual to this AdS space, we will want to know how information from the boundary propagates into the bulk. An important piece of the puzzle is that a sourced scalar field in AdS space will have a characteristic asymptotic behaviour near to the AdS boundary, specifically

$$\phi(z) \approx \phi_0 z^{d-\Delta}. \tag{4.11}$$

The bulk-boundary propagators give us a tool to transfer CFT data from the boundary to the bulk. Since the on shell action sometimes evaluates to infinity we introduce a near-boundary surface cutoff $z = \epsilon$ in order to keep track of the divergences, the most robust solution to the scalar equation of motion eq. (4.9) which have the appropriate asymptotic boundary conditions is

$$\phi(z,k) = \phi_0(k)\epsilon^{d-\Delta}\frac{z^{d/2}K_{\Delta-d/2}(kz)}{\epsilon^{d/2}K_{\Delta-d/2}(k\epsilon)}\,, \tag{4.12}$$

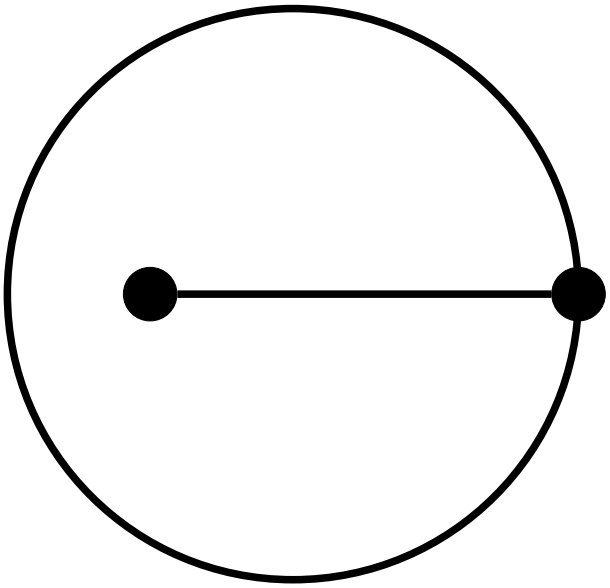

Figure 4.2: A Witten diagram depicting the scalar bulk-boundary propagator

where $\phi_0(k)$ represents the CFT source for the AdS scalar field. If we are not concerned with divergences, then the properly normalized bulk-boundary propagator for a scalar field in AdS can be written as

$$\phi(z,k) = \phi_0(k)\frac{z^{d/2}k^{\Delta-d/2}K_{\Delta-d/2}(kz)}{\Phi(d,\Delta)} \tag{4.13}$$

where Φ is defined as

$$\Phi(d,\Delta) \equiv 2^{\Delta-\frac{d}{2}-1}\Gamma\left(\Delta-\frac{d}{2}\right). \tag{4.14}$$

This propagator, depicted in figure 4.2, can be used to directly assess tree-level three-point functions, as we will see in section 4.3.

4.2.3 Scalar boundary-boundary propagator

The CFT two-point function $\langle\mathcal{O}\mathcal{O}\rangle$, depicted in figure 4.3, is directly accessible to a conformal field theory. From the AdS/CFT dictionary eq. (2.18) we have that

$$\langle\mathcal{O}(\boldsymbol{k})\mathcal{O}(-\boldsymbol{k})\rangle = -\frac{1}{2}\frac{\partial^2 S}{\partial\phi_0(\boldsymbol{k})\partial\phi_0(-\boldsymbol{k})} \tag{4.15}$$

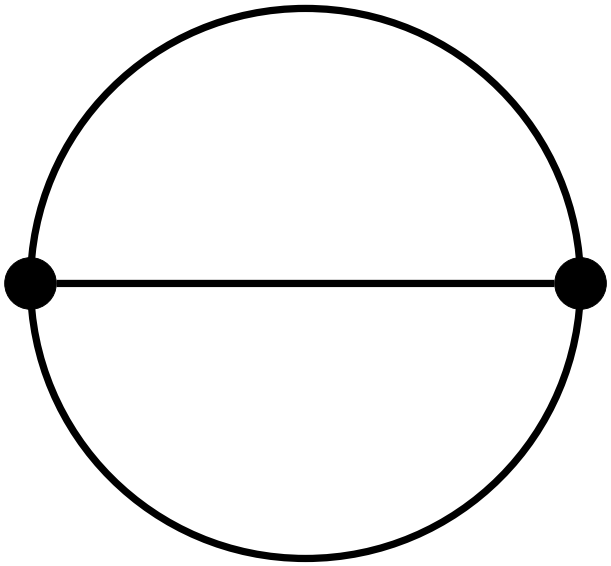

Figure 4.3: A Witten diagram depicting the scalar two-point function

The scalar field ψ will have a leading asymptotic behaviour

$$\phi(u) = \phi_0 z^{d-\Delta} + \phi_1 z^{\Delta} + O(z^d). \tag{4.16}$$

As seen in appendix A, the first term corresponds with the CFT source for the scalar field while the second term in eq. (4.16) corresponds with the expectation value $\langle \mathcal{O} \rangle$ of the scalar operator, the relationship between them is

$$\langle \mathcal{O} \rangle = \phi_1 \left(2\Delta - d\right) \left(\frac{L}{\ell_p}\right)^{d-1} \tag{4.17}$$

It is natural to expand the scalar field in momentum space

$$\phi(u, \boldsymbol{x}) = \int \frac{d^d k}{(2\pi)^d} e^{i\boldsymbol{k}\cdot\boldsymbol{x}} \phi(u, \boldsymbol{k}). \tag{4.18}$$

The retarded Green's function for the scalar field ψ is defined as

$$S = \int \frac{d^d k}{(2\pi)^d} \frac{1}{2} \phi_0(-k) G^R_{\mathcal{O}\mathcal{O}}(k) \phi_0(k) \Big|_{u\to 0} \tag{4.19}$$

After utilizing the equations of motion, adding renormalization counter terms (see appendix A), and integrating by parts, one arrives at

$$S_{\text{on shell}} = -\frac{L^{d+1}}{2\ell_p^{d-1}} \int \frac{d^d x}{z^d} \left(\frac{(d-\Delta)}{z} \phi^2 - \phi \partial_z \phi \right) \Big|_{z=\epsilon} \tag{4.20}$$

which after substituting (4.16), we see that the on shell action is now finite

$$S_{\text{on shell}} = \frac{L^{d+1}}{2\ell_p^{d-1}} \int d^d x (2\Delta - d)\phi_1 \phi_0 \,. \tag{4.21}$$

Using equation (2.18) we arrive at the scalar two-point function

$$\langle \mathcal{O}\mathcal{O} \rangle = G^R_{\mathcal{O}\mathcal{O}} = \frac{L^{d-1}}{\ell_p^{d-1}} (2\Delta - d) \frac{\phi_1}{\phi_0}. \tag{4.22}$$

If we substitute the expansion eq. (4.13) for the scalar field into eq. (4.22) we get

$$\langle \mathcal{O}(-k)\mathcal{O}(k) \rangle = (2\Delta - d) \frac{L^{d-1}}{\ell_p^{d-1}} \frac{\Gamma(d/2 - \Delta)}{\Gamma(\Delta - d/2)} k^{2\Delta - d} \tag{4.23}$$

which allows us to fix the normalization of the two-point function, from eq. (3.4)

$$\mathcal{C}_{\mathcal{O}\mathcal{O}} = (2\Delta - d) \frac{L^{d-1}}{\ell_p^{d-1}} \frac{\Gamma(d/2 - \Delta)}{\Gamma(\Delta - d/2)} \tag{4.24}$$

4.2.4 Gauge bulk-bulk propagator

Similar to the scalar bulk-bulk propagator, the gauge bulk-bulk propagator is the general solution to the equation of motion for A_μ. As above, we will work in momentum space. In order to calculate n-point functions involving the CFT vector current J_μ, it is useful to know the bulk gauge AdS propagator. The free on shell action for the Maxwell field is

$$S_{\text{Maxwell}} = -\frac{1}{4g_d^2} \int d^{d+1}x \sqrt{-g} F_{ab} F^{ab} \tag{4.25}$$

where $F_{ab} = \partial_a A_b - \partial_b A_a$ and the with equations of motion for A_a found by varying eq. (4.25) with respect to A_a

$$0 = \nabla_a F^{ab}. \tag{4.26}$$

Once again, we will be decomposing the field into momentum space

$$A_\mu(x) = \int \frac{d^d k}{(2\pi)^d} A_\mu(z, k) e^{-ix\cdot k}. \tag{4.27}$$

The equations of motion for the transverse component (say $k = k_y \hat{y}$) of the gauge field is

$$0 = A_x'' - \frac{d-3}{z} A_x' - k^2 A_x \,. \tag{4.28}$$

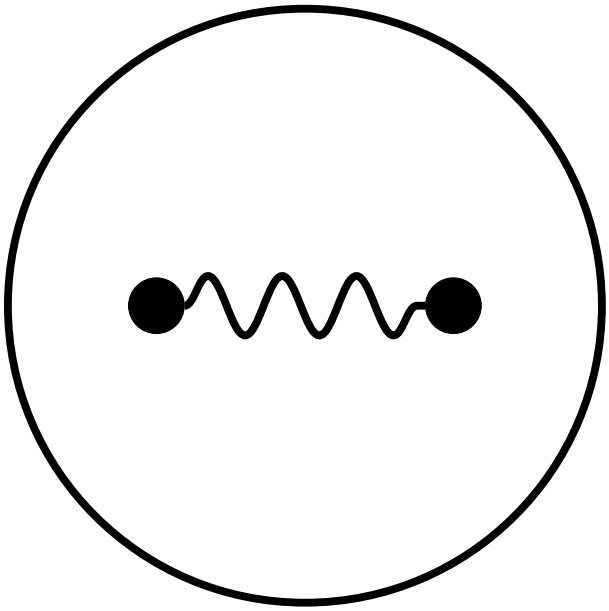

Figure 4.4: A Witten diagram depicting the gauge bulk-bulk propagator

The general solution to the transverse gauge equations of motion in momentum space are

$$A_x = a(k) z^{d/2-1} K_{d/2-1}(kz) + b(k) z^{d/2-1} I_{d/2-1}(kz), \tag{4.29}$$

where a and b are arbitrary functions of the momentum k. The gauge bulk-bulk propagator can then be found in the same manner as for the scalar field

$$G(z, z'; k) = \begin{cases} z' \, (z/z')^{d/2-1} K_{d/2-1}(kz) I_{d/2-1}(kz') & \text{if } z' > z \\ z' \, (z/z')^{d/2-1} K_{d/2-1}(kz') I_{d/2-1}(kz) & \text{if } z > z' \end{cases} . \tag{4.30}$$

The Green's function has the property that $(\partial_z^2 - \frac{d-3}{z}\partial_z - k^2) G(z, z'; k) = \delta(z - z')$. $G(z, z'; k)$ is the gauge bulk-bulk propagator.

4.2.5 Gauge bulk-boundary propagator

The bulk-boundary gauge propagator is an important tool for us to be able to do any kind of correlation function involving the vector current J_x in the boundary CFT using AdS/CFT. The asymptotic behaviour for the gauge field A_x is such that $A_x(z) \approx A_0$. *i.e.,* the source term can be read off as the value for the gauge field at the boundary. The

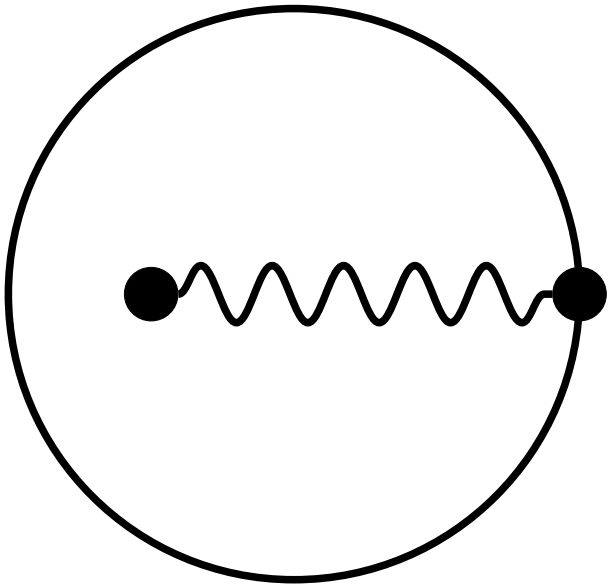

Figure 4.5: A Witten diagram depicting the gauge bulk-boundary propagator

bulk-boundary propagator then would have to be the appropriate limit for the bulk-bulk propagator. The general normalized form for the bulk-boundary propagator is therefore

$$A_x(z,k) = \frac{(z)^{d/2-1}K_{d/2-1}(kz)}{(\epsilon)^{d/2-1}K_{d/2-1}(k\epsilon)}A_0(k)\,, \tag{4.31}$$

where $\epsilon \to 0$ is a near-boundary UV cutoff used in evaluating the on shell action. If no renormalization is required for the on shell action, then the gauge bulk-boundary propagator can be simplified to

$$A_x(z,k) = \frac{(kz)^{d/2-1}K_{d/2-1}(kz)}{\Phi(d,d-1)}A_0(k) \tag{4.32}$$

where Φ was defined in eq. (4.14).

4.2.6 Gauge boundary-boundary propagator

The gauge boundary-boundary propagator is in essence the CFT two-point function $\langle J_x(-k)J_x(k)\rangle$. The propagator is found by inputting two bulk-boundary propagators into the on shell action

$$S_{\text{Maxwell}} = -\frac{1}{2g_d^2}\int \frac{d^dk}{(2\pi)^d}\sqrt{-g}g^{zz}g^{xx}A_x\partial_zA_x \tag{4.33}$$

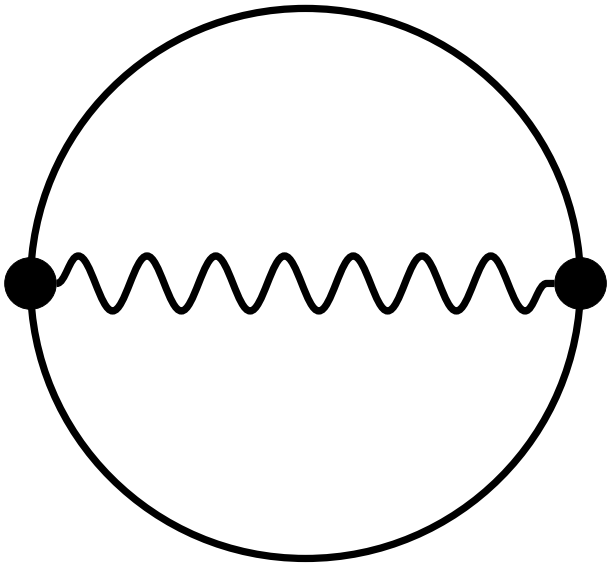

Figure 4.6: A Witten diagram depicting the conductivity

After using the equations of motion and integrating by parts, the on shell action reduces to a boundary term. After substituting eq. (4.31) into the action, we find

$$\begin{aligned} S_{\text{Maxwell}} &= -\frac{1}{2g_d^2}\int \frac{d^dk}{(2\pi)^k}\left(\frac{L}{z}\right)^{d-3} A_x(-k,z)\partial_z A_x(k,z)\Big|_{z\to\epsilon} \\ &= -\frac{L^{d-3}}{2g_d^2}\int \frac{d^dk}{(2\pi)^k} A_0(-k)\frac{K_{d/2-2}(k\epsilon)}{\epsilon^{d-3}K_{d/2-1}(k\epsilon)}A_0(k)\,. \end{aligned} \tag{4.34}$$

When taking the limit $\epsilon \to 0$, we take only the finite part of the expansion [32] and doing so yields

$$\langle J_x(-k)J_x(k)\rangle = -\frac{L^{d-3}}{g_d^2}(d-2)\frac{\Gamma(1-d/2)}{\Gamma(d/2-1)}\left(\frac{k}{2}\right)^{d-2}, \tag{4.35}$$

which allows us to fix $\mathcal{C}_{JJ}$ from eq. (3.7)

$$C_{JJ} \equiv \frac{L^{d-3}}{g_d^2}\sigma_\infty = \frac{L^{d-3}}{g_d^2}\frac{(d-2)}{2^{d-2}}\frac{\Gamma(1-d/2)}{\Gamma(d/2-1)}. \tag{4.36}$$

A keen observer will notice that the value for $\mathcal{C}_{JJ}$ has poles for even spacetime dimensions d [32]. The conductivity receives logarithmic corrections when evaluated for Euclidean frequencies. The latter require modulation by some additional length-scale. However,

note that for real-time frequencies a universal form is maintained. We will not delve into this very rich subject, but for these reasons we will not focus on the Euclidean frequency behaviour of the conductivity in even dimensions throughout this thesis.

4.3 Fixing CFT data with holography

In this section we will continue our endeavor to find the relationships between the bulk parameters and the CFT observables in table 4.1 by fixing the three-point function coefficients to the gravitational coupling constants.

4.3.1 $\mathcal{C}_{\mathcal{O}_0\mathcal{O}_0\mathcal{O}}$

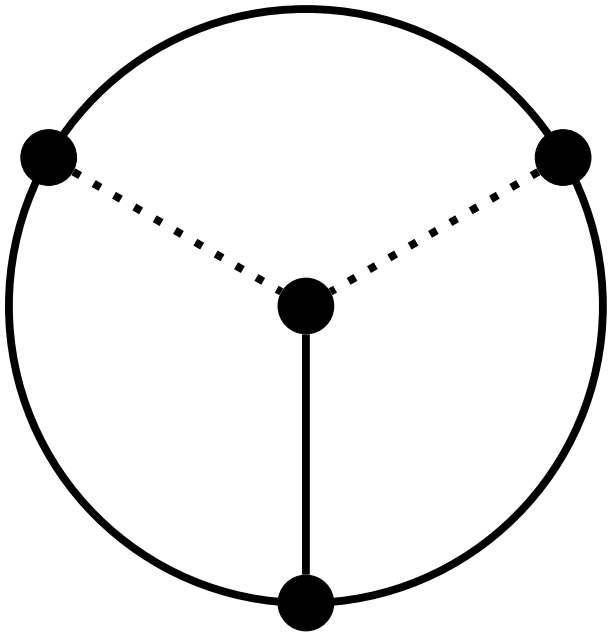

Figure 4.7: A Witten diagram depicting the $\langle \mathcal{O}_0\mathcal{O}_0\mathcal{O}\rangle$ three-point function

As we have seen in chapter 3, the presence of a relevant operator $\mathcal{O}$ can be felt in the scalar-scalar two-point function because of the non-vanishing three-point function $\langle \mathcal{O}_0\mathcal{O}_0\mathcal{O}\rangle$. Holographically, what this means is that the scalar transport will be modified by a scalar field if there is a $\phi\psi^2$ interaction term in the action. If we refer to the

action S_ψ in eq. (4.5) we see such a term being controlled by the coupling constant α_ψ. We can relate this bulk coupling constant with the CFT three-point coupling $\mathcal{C}_{\mathcal{O}_0\mathcal{O}_0\mathcal{O}}$ by following the AdS/CFT dictionary and evaluating the tree level action containing these three terms. The Witten diagram in figure 4.7 depicts this calculation. The three-point function can be found using

$$\langle \mathcal{O}_0(p_1)\mathcal{O}_0(p_2)\mathcal{O}(p_3)\rangle = -\frac{\delta^3 S}{\delta\psi_0(p_1)\delta\psi_0(p_2)\delta\phi_0(p_3)}\,. \tag{4.37}$$

The only term in the action that will contribute is $S = \frac{\alpha_\psi}{2\ell_p^{d-1}}\int d^{d+1}x\sqrt{-g}\phi\psi^2$. We can take this functional derivative by substituting for ϕ and ψ, the bulk-boundary propagators given by eq. (4.13)

$$\begin{aligned} S =& \frac{\alpha_\psi L^{d+1}}{2\ell_p^{d-1}}\int d^{d+1}x \int \frac{d^dp_1\, d^dp_2\, d^dp_3}{(2\pi)^{3d}} e^{i(p_1+p_2+p_3)\cdot x}\psi_0(p_1)\psi_0(p_2)\phi_0(p_3)\times \\ & \frac{z^{d/2-1}p_1^{\Delta_0-d/2}p_2^{\Delta_0-d/2}p_3^{\Delta-d/2}K_{\Delta_0-d/2}(p_1z)K_{\Delta_0-d/2}(p_2z)K_{\Delta-d/2}(p_3z)}{\Phi(d,\Delta_0)^2\Phi(d,\Delta)} \\ =& \frac{\alpha_\psi L^{d+1}\delta^d(p_1+p_2+p_3)}{2\ell_p^{d-1}\Phi(d,\Delta_0)^2\Phi(d,\Delta)} I(d/2-1,\Delta_0-d/2,\Delta_0-d/2,\Delta_0-d/2)\psi_0(p_1)\psi_0(p_2)\phi_0(p_3)\,. \end{aligned} \tag{4.38}$$

So as we can see the three-point function is given by

$$\langle \mathcal{O}_0(p_1)\mathcal{O}_0(p_2)\mathcal{O}(p_3)\rangle = -\frac{\alpha_\psi L^{d+1}\delta^d(p_1+p_2+p_3)}{\ell_p^{d-1}\Phi(d,\Delta_0)^2\Phi(d,\Delta)} I(d/2-1,\Delta_0-d/2,\Delta_0-d/2,\Delta_0-d/2) \tag{4.39}$$

and by comparing with eq. (3.11), we can relate the CFT coupling $\mathcal{C}_{\mathcal{O}_0\mathcal{O}_0\mathcal{O}}$ with the AdS constant α_ψ

$$\mathcal{C}_{\mathcal{O}_0\mathcal{O}_0\mathcal{O}} = -\frac{\alpha_\psi L^{d+1}}{\ell_p^{d-1}\Phi(d,\Delta_0)^2\Phi(d,\Delta)}. \tag{4.40}$$

4.3.2 $\mathcal{C}_{JJ\mathcal{O}}$

Relating the CFT coupling $\mathcal{C}_{JJ\mathcal{O}}$ to the bulk coupling α_F is done in a manner very similar to the previous section for relating $\mathcal{C}_{\mathcal{O}_0\mathcal{O}_0\mathcal{O}}$ to α_ψ. The main difference is that the term in the action has a more complex tensor structure and that we will be using the gauge bulk-boundary propagators rather than scalar propagators. The Witten diagram depicted

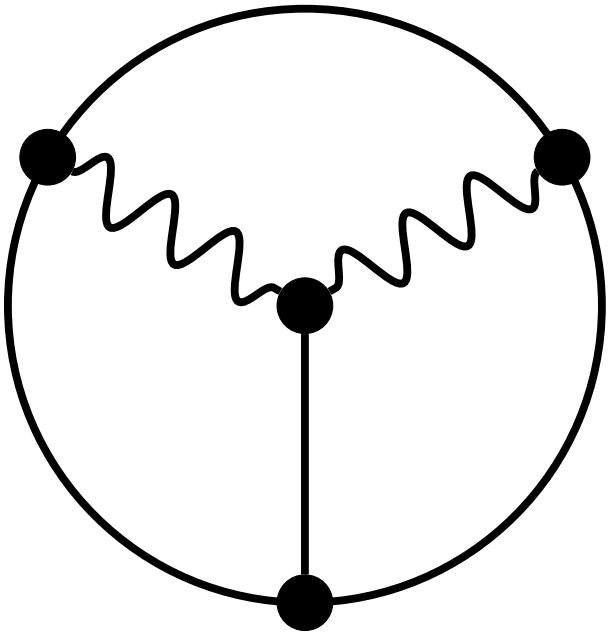

Figure 4.8: A Witten diagram depicting the $\langle J_x J_x \mathcal{O} \rangle$ three-point function

in figure 4.8 gives a pictorial description for the tree-level calculation of the $\langle J_x J_x \mathcal{O} \rangle$ three-point function. The only term in the action given in (4.6) that will contribute to the three-point function $\langle J_x(p_1) J_x(p_2) \mathcal{O}(p_3) \rangle$ is

$$S = -\frac{\alpha_F}{4g_d^2} \int d^{d+1}x \sqrt{-g} \phi F_{ab} F^{ab}. \tag{4.41}$$

The three-point function can be found from the on shell action via

$$\langle J_x(p_1) J_x(p_2) \mathcal{O}(p_3) \rangle = -\frac{\delta^3 S}{\delta A_{x0}(p_1) \delta A_{x0}(p_2) \delta \phi_0(p_3)} \,. \tag{4.42}$$

We won't get a triple Bessel integral quite as easily this time however, and so we will need to massage the action before reading off the appropriate relationship between $\mathcal{C}_{JJ\mathcal{O}}$ and α_F. First, we will expand the fields into their spectral forms and write F^2 in terms of its constituent gauge fields A_μ. Just as in the previous section, there will be a delta function that arises from doing the spacetime integrations

$$\begin{aligned} S = &- \frac{\alpha_F \delta^3(p_1 + p_2 + p_3)}{g_d^2} \times \\ &\int dz \sqrt{-g} g^{xx} g^{ab} \partial_a A_x(z, p_1) \partial_b A_x(z, p_2) \phi(z, p_3) \,. \end{aligned} \tag{4.43}$$

As we continue to derive the relationship between the constants, we will be suppressing the momentum-conservation delta function as well as the three source terms. A general strategy would be to remove all derivatives on the gauge fields. The first step in this process would be to integrate by parts on the ∂_a.

$$S = \frac{\alpha_F}{g_d^2}\int A_x(z,p_1)\partial_a(\sqrt{-g}g^{xx}g^{ab}\partial_b A_x(z,p_2)\phi(z,p_3)) \tag{4.44}$$

A marvelous simplification happens if we remove the scalar field ϕ from the derivative, the Maxwell equations of motion eq. (4.26) appear!

$$\begin{aligned} S =& \frac{\alpha_F}{g_d^2}\int A_x(z,p_1)\Big(\sqrt{-g}g^{xx}g^{ab}\partial_b A_x(z,p_2)\partial_a\phi(z,p_3) + \partial_a(\sqrt{-g}g^{xx}g^{ab}\partial_b A_x(z,p_2))\phi(z,p_3)\Big) \\ =& \frac{\alpha_F}{g_d^2}\int A_x(z,p_1)\Big(\sqrt{-g}g^{xx}g^{ab}\partial_b A_x(z,p_2)\partial_a\phi(z,p_3) + \sqrt{-g}\,\nabla_a(F^{ax}(z,p_2))\phi(z,p_3)\Big) \end{aligned} \tag{4.45}$$

We can do the same integration but with the roles of p_1 and p_2 reversed, and if we symmetrize over them we find the following boundary term

$$S = \frac{\alpha_F}{2g_d^2}\int \sqrt{-g}g^{xx}g^{ab}\partial_b(A_x(z,p_1)A_x(z,p_2))\partial_a\phi(z,p_3) \tag{4.46}$$

We can integrate by parts once more to completely remove derivatives from the gauge field

$$S = -\frac{\alpha_F}{2g_d^2}\int \partial_b(\sqrt{-g}g^{xx}g^{ab}\partial_a\phi(z,p_3))A_x(z,p_1)A_x(z,p_2). \tag{4.47}$$

By removing the g^{xx} term from the derivative we can recognize part of the equation of motion for the scalar field eq. (4.7)

$$\begin{aligned} S =& -\frac{\alpha_F}{2g_d^2}\int\left(\partial_b(\sqrt{-g}g^{ab}\partial_a\phi(z,p_3)) - \frac{2}{z}\sqrt{-g}g^{zz}g^{xx}\partial_z\phi(z,p_3)\right)A_x(z,p_1)A_x(z,p_2). \\ =& -\frac{\alpha_F}{2g_d^2}\int\left(\sqrt{-g}\,m^2\phi(z,p_3) - \frac{2}{z}\sqrt{-g}g^{zz}g^{xx}\partial_z\phi(z,p_3)\right)A_x(z,p_1)A_x(z,p_2) \\ =& \frac{\alpha_F}{2g_d^2}\int\left(\frac{L^{d+1}}{z^{d+1}}\frac{\Delta(d-\Delta)}{L^2}\phi(z,p_3) + \frac{2L^{d-3}}{z^{d-2}}\partial_z\phi(z,p_3)\right)A_x(z,p_1)A_x(z,p_2). \end{aligned} \tag{4.48}$$

The derivative for the bulk-boundary propagator eq. (4.13) is

$$\partial_z\phi(z,k) = \phi_0(k)\frac{k^{\Delta-d/2}z^{d/2-1}}{\Phi(d,\Delta)}\Big[\Delta K_{\Delta-d/2}(zk) - kzK_{\Delta-d/2+1},(kz)\Big] \tag{4.49}$$

Substituting this into the action

$$
\begin{aligned}
S =& \frac{\alpha_F L^{d-3}}{2g_d^2 \Phi(d,d-1)^2 \Phi(d,\Delta)} \times \\
\int \Big[& -2 z^{d/2} p_1^{d/2-1} p_2^{d/2-1} p_3^{\Delta-d/2+1} K_{d/2-1}(p_1 z) K_{d/2-1}(p_2 z) K_{\Delta-d/2+1}(p_3 z) \\
& (-\Delta(d-\Delta)+2\Delta) z^{d/2-1} p_1^{d/2-1} p_2^{d/2-1} p_3^{\Delta-d/2} K_{d/2-1}(p_1 z) K_{d/2-1}(p_2 z) K_{\Delta-d/2}(p_3 z) \Big] \\
=& -\frac{\alpha_F L^{d-3} \delta^p(p_1+p_2+p_3)}{g_d^2 \Phi(d,d-1)^2 \Phi(d,\Delta)} \Big[I(d/2, d/2-1, d/2-1, \Delta-d/2+1) \\
& + \frac{\Delta(d-\Delta-2)}{2} I(d/2-1, d/2-1, d/2-1, \Delta-d/2) \Big] A_{x0}(p_1) A_{x0}(p_2) \phi_0(p_3)
\end{aligned}
\tag{4.50}
$$

where we have explicitly reintroduced the delta function and the source terms in the last line. This gives us a three-point function

$$
\begin{aligned}
\langle J_x(p_1) J_x(p_2) \mathcal{O}(p_3) \rangle =& \frac{\alpha_z L^{d-3}}{g_d^2 \Phi(d,d-1)^2 \Phi(d,\Delta)} \Big[I(d/2, d/2-1, d/2-1, \Delta-d/2+1) \\
& + \frac{\Delta(d-\Delta-2)}{2} I(d/2-1, d/2-1, d/2-1, \Delta-d/2) \Big] .
\end{aligned}
\tag{4.51}
$$

By comparing this equation with eq.(3.16) we conclude that

$$
\mathcal{C}_{JJ\mathcal{O}} = \frac{\alpha_z L^{d-3}}{g_d^2 \Phi(d,d-1)^2 \Phi(d,\Delta)} .
\tag{4.52}
$$

Recall that Φ is defined in eq. (4.14).

This concludes our building-a-bridge journey. We are now free to make calculations and predictions using the full force of the AdS/CFT correspondence: calculating CFT observables using AdS dynamics.

Chapter 5

A holographic model

In this chapter, we will be exploring some simple theories of gravity that are solutions to the minimal bulk action introduced in section 4.1. The models we will be considering will consist of background gravitational solutions for the free bulk action (all α_i set to zero) in eq. (4.2), and treating the matter fields as small perturbations to the background geometry, *i.e.,* the bulk matter will negligibly affect the gravitational metric.

The first model that we consider is the planar AdS-Schwarzschild solution to the action Ee. (4.2), this spacetime is charge-less and has a black hole horizon and therefore has Hawking temperature. From the CFT perspective, the boundary to this spacetime represents a thermal quantum field theory that is conformal at zero temperatures.

We introduce more complex models in section 5.3.3 that include charge in the background spacetimes in two different ways. In one model we let the gauge field acquire a non-trivial background term proportional to the charge of the black hole. In this model, the $\alpha_F \phi F^2$ term provides a source for the scalar field and we allow $\alpha_C = 0$ since we no longer require to give the scalar field an engineered source. In another model, we give the background gravitational theory charge by introducing an additional gauge field and give it charge. We then calculate the conductivity for the original gauge field appearing in eq. (4.6), in this model we will once again require $\alpha_C \neq 0$ since the scalar field will not be sourced by the $\alpha_F \phi F^2$ term.

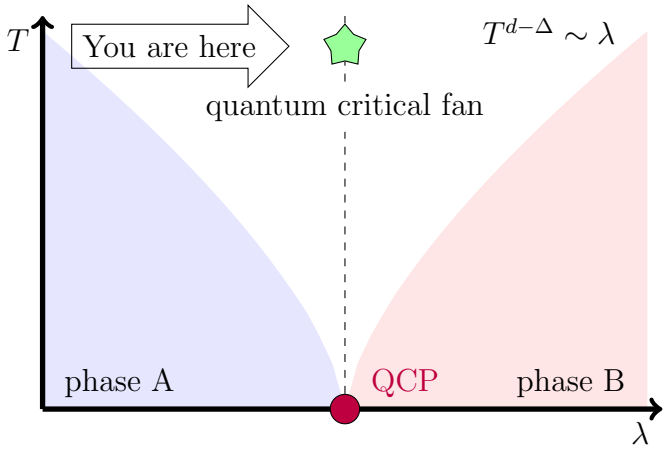

Figure 5.1: We are beginning to probe the finite temperature theory

5.1 The minimal model

Although, in the previous chapter we only considered relevant operators with $\Delta < d$, the following holographic analysis easily extends to irrelevant operators with $\Delta > d$ as well. However, certain technical issues arise for $\Delta \geq 2d$ — see further comments in footnote 2 and appendix D. If we look at the free (non-interacting) theory *i.e.,* $\alpha_\psi = \alpha_F = \alpha_C = 0$ in eq. (4.2) the corresponding boundary CFT is described as a thermal state with vanishing chemical potential. In particular, ϕ and A_a would both vanish in the bulk solution[1].

Now in principle, one would want to solve the full nonlinear equations of the full action eq. (4.2) to solve for a new black hole solution in which the scalar field has a nontrivial profile. However, the equations of motion for such a theory are very complex. We will instead treat the interacting matter as a perturbation to the background non-interacting geometry, in this manner we are able to systematically solve the equations of motion for the scalar ϕ and gauge A_μ fields to first order in the coupling strengths α_i. If one is interested in solving for these fields to second order α_i^2 then one would need to solve the

[1]The gauge field vanishes because we have assumed that the black hole is not charged, *i.e.,* the chemical potential vanishes in the boundary theory. If bulk scalar has a positive mass-squared, *i.e.,* $\Delta > d$, there are no hair theorems which ensure that ϕ vanishes, *e.g.,* [33]. However, with a negative mass-squared, *i.e.,* $\Delta < d$, stable black hole solutions can be found with nontrivial scalar hair, *e.g.,* [33–36]. However, from a holographic perspective, the latter solutions involve turning on the (dimensionful) coupling constant for the corresponding operator in the boundary theory *e.g.,* [35,36]. However, as explained below, we wish to focus on the critical theory in which this coupling vanishes and so we impose boundary conditions where the only black hole solutions have vanishing ϕ for the free theory.

Einstein-Maxwell equations while including back-reactions from the dynamic fields up to first order in α_i. For this thesis we focus primarily on a first-order perturbation about the free gravity theories.

We will move forward in two streams: firstly, we calculate the full-frequency response for the retarded scalar propagator and for the electrical conductivity and secondly, we make strides in understanding the high-frequency behaviour for these transport functions. All of these approaches are done in a weak-interacting perturbation about the background geometry which is blind to the effects of the interacting matter fields. Alternatively, since the bulk scalar is sourced by the interaction in eq. (4.4), one can think that we are working to leading order in a small α_C expansion. S_0 from eq. (4.3) is the background gravitational anti-de Sitter action, S_ϕ from eq. (4.4) is the action governing the relevant scalar that is sourced by the Weyl tensor. S_ψ from eq. (4.5) is the action for the scalar field ψ corresponding to a scalar operator $\mathcal{O}_0$, S_ψ includes a term that couples ψ to the field ϕ in a manner that will contribute to the $\langle \mathcal{O}_0 \mathcal{O}_0 \mathcal{O} \rangle$ correlation function. S_A from eq. (4.6) is the Maxwell term in the gravitational action, it contains the free Maxwell action with $F_{\mu\nu} = \partial_\mu A_\nu - \partial_\nu A_\mu$ as well as an interaction term between A_μ and ϕ. The massless gauge field A_μ corresponds to a conserved current J_μ in the boundary quantum theory and the interaction term contributes to the $\langle J_x J_x \mathcal{O} \rangle$ correlation function.

This holographic model is equipped to handle a conformal field theory in the presence of a relevant scalar operator $\mathcal{O}$ that deforms the CFT from the QCP. The bulk black hole solutions will naturally acquire a Hawking temperature, while the coupling between the scalar field ϕ and the Weyl tensor will source the scalar field equations, giving the scalar operator a non-zero expectation value $\langle \mathcal{O} \rangle_T \sim T^\Delta$ at finite temperatures. Even a scalar field dual to an operator at the QCP will acquire an expectation in this way even though the scalar field will have the asymptotic behaviour consistent with being dual to a critical operator. We would like to comment that the Weyl tensor is a natural choice of gravitational tensors to source the scalar field since the Weyl tensor is zero precisely when the the theory is conformal, *i.e.,* at zero temperatures the Weyl tensor vanishes, and similarly we can see that the Weyl tensor vanishes at the boundary of the spacetime.

We look at figure 5.1 to visualize which region of a characteristic QFT phase diagram we are probing with this holographic approach. We are currently probing the high temperature regime of a QCP. We investigate the holographic linear responses modified by a scalar deformation with this minimal model. That is to say a model which has all of the necessary ingredients to see the effects of a scalar operator in the conformal theory, but also a model that consistently presents a scalar operator that attains an expectation $\langle \mathcal{O} \rangle_T \sim T^\Delta$ which is tuned by the black hole temperature, even at the QCP.

A particular solution to the background metric S_0 eq. (4.3) that will be useful in demonstrating this calculation is the familiar planar AdS Schwarzschild black hole solution:

$$ds^2 = \frac{r^2}{L^2}(-f(r)dt^2 + \eta_{ij}dx^i dx^j) + \frac{L^2 dr^2}{r^2 f(r)}, \tag{5.1}$$

with $f(r) = 1 - r_0^d/r^d$. The black hole has an event horizon located at a radius $r = r_0$. If we take $r_0 \to 0$ we get the familiar Poincaré patch of AdS space. We introduce a change of variables in order to simplify future calculations. We define a dimensionless radial coordinate $u = r_0/r$, with which the metric becomes

$$ds^2 = \frac{r_0^2}{L^2 u^2}(-f(u)dt^2 + \eta_{ij}dx^i dx^j) + \frac{L^2 du^2}{u^2 f(u)}\,, \tag{5.2}$$

where $f(u) = 1 - u^d$. The black hole horizon is now conveniently located at $u = 1$ while $u \to 0$ is the AdS boundary. The black hole solution eq. (5.2) will have a conical singularity unless the Euclidean time $\tau = it$ is periodic. A quick way to see this is to take the near horizon limit $u \to 1$ and make the change of variables

$$(u-1) = \tfrac{f'(1)}{4L^2}\rho^2 \qquad ; \quad \tau = \tfrac{2L^2}{r_0 f'(1)}\theta. \tag{5.3}$$

For any choice of x^i, the section of the metric in these coordinates is

$$ds^2 = d\rho^2 + \rho^2 d\theta^2 \tag{5.4}$$

which is the familiar Euclidean metric in polar coordinates where $\theta = -\frac{r_0 f'(1)}{2L^2}\tau$ is periodic with period 2π. The Euclidean time τ is therefore periodic with a period of $-\frac{4\pi L^2}{f'(1)r_0}$, so the temperature for this spacetime is thus given by $T = -\frac{f'(1)r_0}{4\pi L^2}$. According to the usual AdS/CFT correspondence, this solution is dual to the CFT at finite temperature.

$$T = \frac{dr_0}{4\pi L^2} \tag{5.5}$$

The background gravitational solution that we have chosen is such that $A_\mu = 0$, hence the background has no chemical potential. We can see that the low-temperature limit approaches AdS space, this can be seen in coordinates where $z = \frac{L^2 u}{r_0} = \frac{L^2}{r}$, then the metric approaches

$$ds^2_{r_0<<L} \approx \frac{L^2}{z^2}\left(-dt^2 + dz^2 + \eta_{ij}dx^i dx^j\right)\,. \tag{5.6}$$

5.2 Background scalar field

We will be treating the coupling strength α_C defined in eq. (4.4) as a perturbation of the background solution, and hence the effect from a back reaction of ϕ on the metric, or, more generally, the observables will be negligible. The equations of motion derived from varying S_ϕ with respect to ϕ are

$$0 = (\nabla^2 - m^2)\phi + \alpha_C L^2 C_{abcd} C^{abcd}. \tag{5.7}$$

Because the black hole background eq. (5.2) is translation invariant in the boundary directions and because $C_{abcd}C^{abcd}$ depends only on u and since it is the only source for the scalar field ϕ in the equation of motion, the resulting scalar field ϕ will depend only on the coordinate u. Eq. (5.7) with the ansatz $\phi = \phi(u)$, is given by

$$\begin{aligned} 0 =& \phi''(u) + \left(\frac{f'(u)}{f(u)} - \frac{d-1}{u}\right)\phi'(u) + \frac{\Delta(d-\Delta)}{u^2 f(u)}\phi(u) \\ &+ \frac{d(d-1)^2(d-2)\alpha_C\, u^{2d-2}}{f(u)} \end{aligned} \tag{5.8}$$

The homogeneous part of eq. (5.8) has an exact solution given by

$$\begin{aligned} \phi(u) =& \phi_1\ {}_2\mathrm{F}_1\left(\frac{\Delta}{d}, \frac{\Delta}{d}\,;\, \frac{2\Delta}{d}\,;\, u^d\right) u^\Delta \\ &+ \phi_0\ {}_2\mathrm{F}_1\left(\frac{d-\Delta}{d}, \frac{d-\Delta}{d}\,;\, 2\frac{d-\Delta}{d}\,;\, u^d\right) u^{d-\Delta}, \end{aligned} \tag{5.9}$$

where ϕ_0 and ϕ_1 are integration constants and ${}_2\mathrm{F}_1(z_1, z_2\,;\, z_3\,;\, z_4)$ denotes the standard hypergeometric function. We can find the general solution to eq. (5.8) using Green's functions[2]

$$\begin{aligned} \phi(u) =& {}_2\mathrm{F}_1\left(\frac{\Delta}{d}, \frac{\Delta}{d}\,;\, \frac{2\Delta}{d}\,;\, u^d\right)\left(\phi_1 - \frac{d(d-1)^2(d-2)\alpha_C}{2\Delta - d} g_\Delta(u)\right) u^\Delta \\ &+ {}_2\mathrm{F}_1\left(\frac{d-\Delta}{d}, \frac{d-\Delta}{d}\,;\, 2\frac{d-\Delta}{d}\,;\, u^d\right)\left(\phi_0 + \frac{d(d-1)^2(d-2)\alpha_C}{2\Delta - d} h_\Delta(u)\right) u^{d-\Delta}\,, \end{aligned} \tag{5.10}$$

[2]This representation of the solution is only valid for $\Delta < 2d$. In particular, the integral defining $g_\Delta(u)$ in eq. (5.11) diverges for $\Delta \geq 2d$. Further, the two independent solutions presented in eq. (5.10) are actually identical for $\Delta = d/2$. Of course, the coefficients of $g_\Delta(u)$ and $h_\Delta(u)$ also diverge for this particular value of Δ. However, we note that the scalar field is still a smooth function of Δ at this special value and so where results are presented for $\Delta = d/2$ in actuality, we add a small positive number to the scaling dimension in order to carry out the calculation, for example $\Delta = d/2 + \epsilon$ where $\epsilon \sim 0.1^6$. Nevertheless, the special case $d = \Delta/2$ is treated in-depth in appendix D

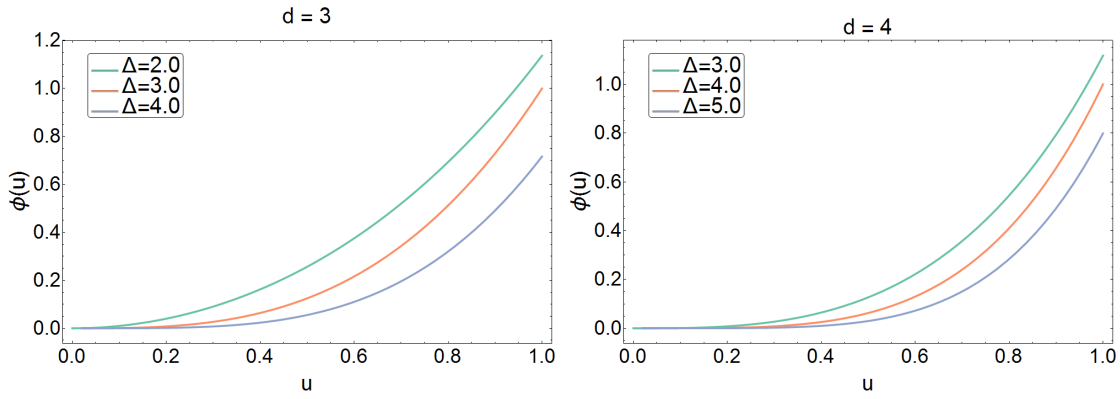

Figure 5.2: Scalar field profiles for the $d = 3$ (left) and $d = 4$ (right) scalar fields for several scaling dimensions in a critical theory ($\phi_0 = 0$) with $\phi_1 = 1$ for comparability between the curves.

where $g_\Delta(u)$ and $h_\Delta(u)$ are given by

$$\begin{aligned} g_\Delta(u) &= \int_0^u dy\, y^{2d-1-\Delta}\ {}_2\mathrm{F}_1\left(\frac{d-\Delta}{d}, \frac{d-\Delta}{d}; 2\frac{d-\Delta}{d}; y^d\right) , \\ h_\Delta(u) &= \int_0^u dy\, y^{d-1+\Delta}\ {}_2\mathrm{F}_1\left(\frac{\Delta}{d}, \frac{\Delta}{d}; \frac{2\Delta}{d}; y^d\right) . \end{aligned} \tag{5.11}$$

From the definitions given in eq. (5.11) we can see that $g_\Delta(0) = h_\Delta(0) = 0$, so the above solution has the expected characteristic asymptotic behaviour for a scalar field as $u \to 0$

$$\phi(u) = \phi_0 u^{d-\Delta}\left(1 + O(u^d)\right) + \phi_1 u^\Delta \left(1 + O(u^d)\right) \tag{5.12}$$

Note that we are using a dimensionless radial coordinate u, and both of the coefficients, ϕ_0 and ϕ_1 are dimensionless. Recall that the first term in eq. (5.12) is the non-normalizable mode which corresponds to a deformation in the boundary theory $\int d^d x \phi_0 \mathcal{O}(x)$. For the majority of this thesis we will be looking at when $\phi_0 = 0$, *i.e.,* when the boundary theory remains critical, but section 5.5 will go in-depth into the case where we deform the QFT away from the QCP with a finite ϕ_0.

The second term in eq. (5.12) corresponds to the normalizable mode which determines the expectation value $\langle \mathcal{O} \rangle$ of the scalar operator. The relationship between them is given by eq. (2.21), but with the manner in which ϕ_1 is defined in the u-coordinates, the one-point

function is

$$\langle \mathcal{O} \rangle = \phi_1 \left(2\Delta - d\right) \left(\frac{L}{\ell_p}\right)^{d-1} \left(\frac{4\pi T}{d}\right)^{\Delta} . \tag{5.13}$$

The Weyl tensor sources the scalar field in eq. (5.7), and so we find that the value of ϕ_1 is proportional to α_C. In practice, we require for the scalar field to be regular in the bulk, specifically near the black hole horizon, *i.e.*, $u \to 1$, the solution eq. (5.10) has a potential logarithmic divergence that is eliminated by setting

$$\phi_1 = \alpha_C \times \frac{d(d-1)^2(d-2)}{2\Delta - d} \left(g_\Delta(1) - \frac{\Gamma\left(2-\frac{2\Delta}{d}\right)\Gamma\left(\frac{\Delta}{d}\right)^2}{\Gamma\left(1-\frac{\Delta}{d}\right)^2\Gamma\left(\frac{2\Delta}{d}\right)} h_\Delta(1) \right) . \tag{5.14}$$

Note that $g_\Delta(1)$ and $h_\Delta(1)$ are both finite and can be determined by numerically evaluating the integrals in eq. (5.11). Figure 5.2 shows the numerically calculated scalar field profiles for $d = 3$ and $d = 4$ for various scaling dimensions. We can calculate the Taylor series expansion for the scalar profile to arbitrary orders. Here are the first few terms

$$\begin{aligned} \phi(u) = {} & \phi_0 u^{d-\Delta} + \phi_1 u^{\Delta} + \frac{(d-\Delta)}{2d} \phi_0 u^{2d-\Delta} + \frac{\Delta}{2d} \phi_1 u^{\Delta+d} \\ & - d(d-1)^2(d-2)\alpha_C u^{2d} \\ & + \frac{(d-\Delta)(2d-\Delta)^2}{4d^2(3d-2\Delta)} \phi_0 u^{3d-\Delta} + \frac{\Delta(d+\Delta)^2}{4d^2(d+2\Delta)} \phi_1 u^{2d+\Delta} + \cdots . \end{aligned} \tag{5.15}$$

We can speculate that the higher-order scaling terms correspond to composite operators. For example the u^{2d} term could be the result of some operator composing of two stress tensors $:TT:$ while the $u^{d+\Delta}$ could be the result of some stress-scalar composite operator. These operators are all irrelevant in the CFT.

5.3 Linear response

5.3.1 Scalar two-point function

One of the most easily accessible and useful quantities we can extract from the holographic model using the AdS/CFT correspondence is the scalar two-point function $\langle \mathcal{O}_0 \mathcal{O}_0 \rangle$. In this section we determine what effect the scalar deformation has on the scalar two-point function; we provide high-frequency asymptotic analytics as well as arbitrary full-frequency numerical analysis of $\langle \mathcal{O}_0 \mathcal{O}_0 \rangle$. From the AdS/CFT dictionary eq. (2.18) we know that

$$\langle \mathcal{O}_0(\boldsymbol{k}) \mathcal{O}_0(-\boldsymbol{k}) \rangle = -\frac{1}{2} \frac{\partial^2 S}{\partial \psi_0(\boldsymbol{k}) \partial \psi_0(-\boldsymbol{k})} . \tag{5.16}$$

The scalar field ψ, just like the scalar field ϕ, will also have the asymptotic behaviour

$$\psi(u) = \psi_0 u^{d-\Delta_0} + \psi_1 u^{\Delta_0} + O(u^d)\,. \tag{5.17}$$

It is natural to expand the scalar field in momentum space since the we have time and space translation symmetry in all directions except the radial u-direction

$$\psi(u,t,\boldsymbol{x}) = \int \frac{d^d q}{(2\pi)^d} e^{i\boldsymbol{q}\cdot\boldsymbol{x}} \psi(u,\boldsymbol{q}). \tag{5.18}$$

The retarded Green's function for the scalar field ψ is defined as

$$S = \int \frac{d^d k}{(2\pi)^d} \frac{1}{2} \psi_0(-k)\, G^R_{\mathcal{O}\mathcal{O}}(k)\, \psi_0(k) \Big|_{u\to 0} \tag{5.19}$$

where it can be shown that (see eq. (2.22) and appendix A)

$$G^R_{\mathcal{O}_0\mathcal{O}_0}(k) = \langle \mathcal{O}_0(-k)\mathcal{O}_0(k)\rangle = \frac{L^{d-1}}{\ell_p^{d-1}} (2\Delta_0 - d) \left(\frac{4\pi T}{d}\right)^{2\Delta_0 - d} \frac{\psi_1(k)}{\psi_0(k)}, \tag{5.20}$$

where we explicitly state that the asymptotic coefficients for the scalar field have k dependence, and is in essence what governs the full-frequency response for the scalar two-point function.

Thus all of the information for the scalar two-point function is encoded by the two parameters ψ_0 and ψ_1 for the scalar field ψ. Looking at our explicit model (4.2), we can find the equation of motion for the dynamic field $\psi(u)$ by varying (4.5) with respect to ψ, giving

$$(\nabla^2 - m_0^2)\psi + \alpha_\psi \phi \psi = 0\,, \tag{5.21}$$

which ψ be expanded in momentum space $\psi(u,t) = \int \frac{dt}{(2\pi)^d} e^{-i\omega t}\psi(u)$

$$\begin{aligned} 0 =& \psi'' + \left(\frac{f'}{f} - \frac{d-1}{u}\right)\psi' - \left(g^{tt}\omega^2 + m_0^2\right)\frac{\psi}{u^2 f} + \frac{\alpha_\psi \phi \psi}{u^2 f} \\ =& \psi'' + \left(\frac{f'}{f} - \frac{d-1}{u}\right)\psi' + \frac{d^2\omega^2\psi}{(4\pi T)^2 f^2} + \frac{\Delta_0(d-\Delta_0)}{u^2 f}\psi + \frac{\alpha_\psi \phi\psi}{u^2 f}\,. \end{aligned} \tag{5.22}$$

Note that the background scalar ϕ given in eq. (5.10) makes an appearance in the equations of motion for ψ. We also note that this equation is homogeneous, and as such it can be scaled arbitrarily. We can understand the freedom of rescaling physically from eq. (5.20)

since the observable quantity we are extracting from the scalar field depends only the quotient of two coefficients of ψ, so the overall scale has no affect on the correlation functions. The boundary conditions to eq. (5.22) are a little bit tricky, since the equation is divergent divergent near the black hole horizon. In order to regulate the divergence, we introduce another field $\psi(u) = f(u)^b \Psi(u)$ and enforce that $\Psi(u)$ be regular at the horizon. The equation of motion for this regularized scalar field is given by

$$\begin{aligned} 0 = \Psi'' &+ \left(\frac{(2b+1)f'}{f} - \frac{d-1}{u}\right)\Psi' \\ &+ \left(\frac{bf'}{f}\left(\frac{bf'}{f} - \frac{d-1}{u} + \frac{f''}{f'}\right) + \frac{d^2\omega^2}{(4\pi T)^2 f^2} + \frac{\Delta_0(d-\Delta_0)}{u^2 f}\Psi + \frac{\alpha_\psi \phi \Psi}{u^2 f}\right) \end{aligned} \tag{5.23}$$

We find that $b = -\frac{i\omega}{4\pi T}$ satisfies the in-falling boundary conditions and is one of the two conditions needed for $F(u)$ to be regular. If we write eq. (5.23) in a series expansion near the black hole horizon we can specify the second boundary condition for the value of $\Psi'(1)$ by requiring that the near-horizon behaviour of the scalar field Ψ is regular. Near the black hole horizon the divergent part of eq. (5.22) is

$$\begin{aligned} 0 = &\frac{1}{f^2}\left(b^2 f'^2 \Psi'' + \frac{d^2\omega}{(4\pi T)^2}\Psi''\right)_{u=1} \\ &+ \frac{1}{f}\left(bf''\Psi + (2b+1)f'\Psi' - (d-1)bf'\Psi + \Delta_0(d-\Delta_0)\Psi + \alpha_\psi\phi\Psi\right)_{u=1}. \end{aligned} \tag{5.24}$$

We can see the in-falling boundary condition $b = -\frac{i\omega}{4\pi T}$ realized in the second-order pole, while the boundary condition

$$\Psi'(1) = \frac{\Psi(1)}{d(2b+1)}\left(\Delta_0(d-\Delta_0) + \alpha_\psi\phi(1)\right) \tag{5.25}$$

is required to remove the first-order pole. As noted earlier, we can arbitrarily set $\Psi(1) = 1$ and get a well-defined boundary-value ordinary differential equation. Numerically, we can solve this equation of motion by *shooting* the solution from the horizon to the asymptotic boundary in order to determine the coefficients ψ_1 and ψ_0. We then determine the scalar-scalar two-point function by using eq. (5.20). Figure 5.3 shows an example two-point function numerical evaluation.

High-frequency scalar two-point function

As we discussed in section 3.2.3, we can analytically predict the asymptotic behaviour for the scalar two-point function in the presence of a relevant scalar deformation about the

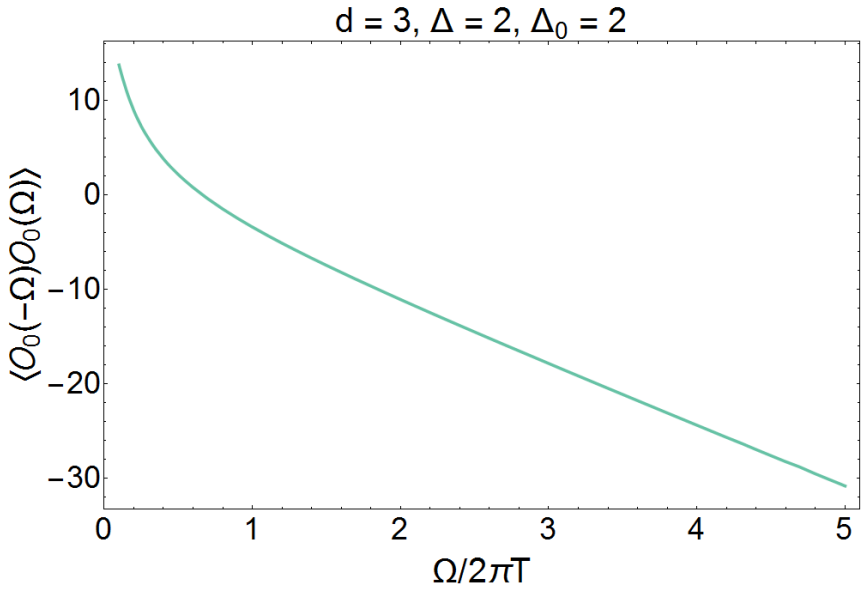

Figure 5.3: The scalar two-point function $\langle \mathcal{O}_0(-\Omega)\mathcal{O}_0(\Omega)\rangle$ evaluated for Euclidean frequencies with spacetime dimension $d = 3$ and with both scalar scaling dimensions fixed at $\Delta = \Delta_0 = 2$.

quantum critical point. Let us compare that analysis with this explicit model. Working in Euclidean frequencies, $\omega = i\Omega$ with $\Omega \gg T$, we will calculate the high-frequency behaviour of $\langle \mathcal{O}_0\mathcal{O}_0\rangle$ to first order in the interaction strength α_ψ for the interaction $\phi\psi^2$ in eq. (4.5). The coupling α_ψ corresponds to the CFT three-point coupling $\mathcal{C}_{\mathcal{O}_0\mathcal{O}_0\mathcal{O}}$, as mentioned in table 4.1. This interaction is responsible for controlling how the scalar two-point function is modified by a scalar deformation of the CFT as shown in eq. (3.29). In order to control the high-frequency behaviour, we introduce a rescaling of the radial variable $v = \frac{d\Omega}{4\pi T}u$. This variable is related to the pure AdS coordinate z that we used extensively in section 3.2 via $\Omega z = v$. We would then approach the pure AdS spacetime as $z \to 0$. At high-frequencies, eq. (5.22) becomes

$$\psi'' - \frac{d-1}{v}\psi' - \psi + \frac{\Delta_0(d-\Delta_0)}{v^2}\psi = -\frac{\alpha_\psi \phi\psi}{v^2}\,, \tag{5.26}$$

where we have made the high-frequency approximations $f \to 1$ and $f' \to 0$ because $u^d \ll 1$ in this limit. Of course our calculations will only be reliable up to the order $1/\Omega^d$. We make a field redefinition that will vastly simplify eq. (5.26) and produce a simple Green's function that we use to solve the first order perturbative equation. The field redefinition

is $\chi = v^{\Delta_0 - d}\psi$ which simplifies eq. (5.26) to

$$\chi'' + \frac{d+1-2\Delta_0}{v}\chi' - \chi = -\frac{\alpha_\psi \phi \chi}{v^2}\,. \tag{5.27}$$

In a perturbative approach, we expand the scalar field in a series given by powers of the coupling strength α_ψ

$$\psi = \psi^{(0)} + \alpha_\psi \psi^{(1)} + \alpha_\psi^2 \psi^{(2)} + \dots \tag{5.28}$$

we similarly decompose χ in the same manner. So, the equation of motion for the free part of the scalar field χ is

$$\chi''^{(0)} + \frac{d+1-2\Delta_0}{v}\chi'^{(0)} - \chi^{(0)} = 0\,, \tag{5.29}$$

which has homogeneous solutions

$$v^{\Delta_0 - d/2} K_{\Delta_0 - d/2}(v)\,, \quad v^{\Delta_0 - d/2} I_{\Delta_0 - d/2}(v), \tag{5.30}$$

or in terms of the scalar field ψ, these are the familiar solutions[3] for the free scalar field in pure AdS

$$\psi(v) = v^{d/2} K_{\Delta_0 - d/2}(v)\,, \quad \psi(v) = v^{d/2} I_{\Delta_0 - d/2}(v). \tag{5.31}$$

In our perturbative approach, the left hand side of eq. (5.27) will contribute at first order in α_ψ and, so we would like to know the Green's function for eq. (5.27) with boundary conditions $G(0,V) = G(v,\infty) = 0$. Such a Green's function can be determined from the homogeneous solutions

$$G(v,V) = \begin{cases} -V\,(v/V)^{\Delta_0 - d/2}\, I_{\Delta_0 - d/2}(v) K_{\Delta_0 - d/2}(V) & \text{if } V > v \\ -V\,(v/V)^{\Delta_0 - d/2}\, I_{\Delta_0 - d/2}(V) K_{\Delta_0 - d/2}(v) & \text{if } v > V \end{cases} \tag{5.32}$$

which has the property that $\left(\partial_v^2 + \frac{d+1-2\Delta_0}{v}\partial_v - 1\right) G(v,V) = \delta(v-V)$. In order for the free scalar field $\psi^{(0)}$ to be regular at the black hole horizon the solution to eq. (5.29) is simply the scalar *AdS* propagator eq. (4.13)

$$\psi^{(0)}(v) = \frac{v^{d/2} K_{\Delta_0 - d/2}(v)}{\Phi(d,\Delta_0)}. \tag{5.33}$$

[3] There are special values of d and Δ_0 where this solution must be modified with logarithmic corrections and the coefficients ψ_0 and ψ_1 no longer correspond to the coefficients of these Bessel functions. In appendix D we briefly discuss this phenomenon in the background scalar field ϕ. For the purposes of this thesis we will not go into detail to the special cases where this problem arises. In practice, if we wish to examine a point where this solution is not valid for a choice of Δ, but is valid for all Δ near to it, and the solution is well-behaved enough that we can take a small deviation $\Delta \sim \Delta + \epsilon$ for some small numerical ϵ, say $\sim 0.1^7$. The correct result is reproduced to high accuracy, *i.e.,* we can take the limit $\Delta \to \Delta_{\text{special}}$ in order to proceed.

Recall that the overall scale of the scalar field ψ and similarly χ is free to choose, so the constant $\Phi(d, \Delta_0)$, defined in eq. (4.14), conveniently sets $\psi^{(0)} \to v^{d-\Delta_0}$ as $v \to 0$. Now is a good time to define a new helper function for this calculation that is analogous to Φ for the other modified Bessel function I. We will define the corresponding limit for $x^{\Delta_0 - d/2} I_{\Delta_0 - d/2}(x)$ as well

$$\Theta(d, \Delta_0) \equiv x^{d/2-\Delta_0} I_{\Delta_0 - d/2}(x)\big|_{x\to 0} = \frac{1}{2^{\Delta_0 - d/2}\Gamma\left(\Delta_0 - \frac{d}{2} + 1\right)} \tag{5.34}$$

The quotient of these functions appear in the calculation of the retarded propagator, governed by eq. (5.20), the quotient is given by

$$\frac{\Theta(d, \Delta_0)}{\Phi(d, \Delta_0)} = \frac{1}{2^{2\Delta_0 - d - 2}(2\Delta_0 - d)\Gamma\left(\Delta_0 - \frac{d}{2}\right)^2} \,. \tag{5.35}$$

Before continuing, let us recall that the expression for the free scalar field in eq. (5.33) has for its asymptotic expansion

$$\psi^{(0)}(v) = v^{d-\Delta_0} + \frac{\ell_p^{d-1}\, \mathcal{C}_{\mathcal{O}_0\mathcal{O}_0}}{L^{d-1}(2\Delta_0 - d)}\, v^{\Delta_0} \,, \tag{5.36}$$

where $\mathcal{C}_{\mathcal{O}_0\mathcal{O}_0}$ is given in eq. (4.24) but replacing the operator $\mathcal{O}$ with $\mathcal{O}_0$. This confirms the two-point function $\langle \mathcal{O}_0 \mathcal{O}_0 \rangle$ for the free scalar field (defined in eq. (5.20))

$$\langle \mathcal{O}_0(-\Omega)\mathcal{O}_0(\Omega)\rangle = \Omega^{2\Delta_0 - d} \mathcal{C}_{\mathcal{O}_0\mathcal{O}_0} \,. \tag{5.37}$$

We can use the Green's function, to linear order in α_ψ, to construct high-frequency corrections to the linear response. The first order term in an expansion of eq. (5.27) in a perturbation of α_ψ is

$$\chi''^{(1)} + \frac{d + 1 - 2\Delta_0}{v}\chi'^{(1)} - \chi^{(1)} = -\frac{\phi\, \chi^{(0)}}{v^2} \,. \tag{5.38}$$

which we can now solve with the Green's function eq. (5.32)

$$\begin{aligned} \chi^{(1)} &= -\frac{1}{\Phi(d, \Delta_0)} \int_0^\infty dV\, G(v, V) \frac{\phi(V) V^{\Delta_0 - d/2} K_{\Delta_0 - d/2}(V)}{V^2} \\ &= \frac{1}{\Phi(d, \Delta_0)} v^{\Delta_0 - d/2} I_{\Delta_0 - d/2}(v) \int_0^\infty dV\, \frac{\phi(V) K_{\Delta_0 - d/2}(V)^2}{V} \end{aligned} \tag{5.39}$$

As mentioned earlier, this technique[4] is only reliable up to $1/\Omega^d$ corrections. Looking at eq. (5.12), we can safely substitute $\phi(V) = \phi_1 V^\Delta \left(\frac{4\pi T}{d\Omega}\right)^\Delta$ for a critical theory, to get the high frequency correction at first order in a perturbation of the interaction strength α_ψ at the desired sensitivity in the high-frequency expansion. Section 5.5 will explain how the scalar which deforms the boundary QFT away from the QCP is treated. Eq. (5.39) evaluates to

$$\chi^{(1)} = \frac{\alpha_\psi \phi_1}{\Phi(d,\Delta_0)} \left(\frac{4\pi T}{d\Omega}\right)^\Delta v^{\Delta_0 - d/2} I_{\Delta_0 - d/2}(v) \int_0^\infty dV V^{\Delta-1} K_{\Delta_0 - d/2}(V)^2 \tag{5.40}$$

The integral that appears in the above equation is denoted by $\Psi(d,\Delta,\Delta_0)$ and is given in eq. (3.15). This allows us to write

$$\psi^{(1)} = -\frac{\phi_1 v^{d/2} I_{\Delta_0 - d/2}(v) \Psi(d,\Delta,\Delta_0)}{\Phi(d,\Delta_0)} \left(\frac{4\pi T}{d\Omega}\right)^\Delta . \tag{5.41}$$

The important information that we want to extract from this expression is the coefficient to the v^{Δ_0} term (see eq.(5.20)). The coefficient $\psi_1^{(1)}$ is

$$\psi_1^{(1)} = -\phi_1 \Psi(d,\Delta,\Delta_0) \frac{\Theta(d,\Delta_0)}{\Phi(d,\Delta_0)} \left(\frac{4\pi T}{d\Omega}\right)^\Delta \tag{5.42}$$

So to first order in a perturbation of α_ψ we have that the scalar field expanded about $v = 0$ is

$$\begin{aligned}
\psi(v) =& v^{d-\Delta_0} + \frac{\ell_p^{d-1}}{L^{d-1}} \frac{\mathcal{C}_{\mathcal{O}_0\mathcal{O}_0}}{2\Delta_0 - d} v^{\Delta_0} - \frac{\alpha_\psi \phi_1 \Psi(d,\Delta,\Delta_0) v^{\Delta_0}}{2^{2\Delta_0 - d - 2}(2\Delta_0 - d)\Gamma(\Delta_0 - d/2)^2} \left(\frac{4\pi T}{d\Omega}\right)^\Delta \\
=& v^{d-\Delta_0} + \frac{\ell_p^{d-1}}{L^{d-1}} \frac{\mathcal{C}_{\mathcal{O}_0\mathcal{O}_0}}{2\Delta_0 - d} v^{\Delta_0} - \frac{\alpha_\psi \ell_p^{d-1} \langle \mathcal{O} \rangle \Psi(d,\Delta,\Delta_0) v^{\Delta_0}}{2^{2\Delta_0 - d - 2} L^{d-1}(2\Delta_0 - d)(2\Delta - d)\Gamma(\Delta_0 - d/2)^2 \Omega^\Delta}
\end{aligned} \tag{5.43}$$

where we used eq. (5.35) in the first line and we employ eq. (5.13) in order to write the expression in terms of the expectation value $\langle \mathcal{O} \rangle$. Eq. (5.20) gives us the scalar correlator

$$\langle \mathcal{O}_0(\Omega) \mathcal{O}_0(-\Omega) \rangle = \Omega^{2\Delta_0 - d} \left(\mathcal{C}_{\mathcal{O}_0\mathcal{O}_0} - \frac{\alpha_\psi \langle \mathcal{O} \rangle \Psi(d,\Delta,\Delta_0)}{2^{2\Delta_0 - d - 2}\Gamma(\Delta_0 - d/2)^2 (2\Delta - d)\Omega^\Delta} \right) . \tag{5.44}$$

[4]The technique mentioned being that we are assuming that $\Omega/T \gg 1$ and that we are explicitly ignoring factors of $(vT/\Omega)^d$

This expression for the two-point function of $\mathcal{O}_0$ in the presence of a deformation by a relevant operator $\mathcal{O}$ is generally valid for any d and all Δ that are not half-integers, but the function is well behaved within the unitary bound $\Delta > d/2 - 1$ and $\Delta_0 > d/2 - 1$ and so for the half-integer dimensions we assert that the two-point function can be found by interpolating from scaling dimensions that are near to Δ (see footnote 3). For completeness, we can expand eq. (5.44) so that we can express the two-point function entirely with the use of Gamma functions

$$\langle \mathcal{O}_0(\Omega)\mathcal{O}_0(-\Omega)\rangle = \Omega^{2\Delta_0-d}\left(\mathcal{C}_{\mathcal{O}_0\mathcal{O}_0} - \frac{\alpha_\psi\langle\mathcal{O}\rangle}{\Omega^\Delta}\frac{\sqrt{\pi}\Gamma\left(\frac{\Delta}{2}\right)\Gamma\left(\frac{\Delta+d-2\Delta_0}{2}\right)\Gamma\left(\frac{\Delta+2\Delta_0-d}{2}\right)}{2^{2\Delta_0-d}\Gamma(\Delta_0-\frac{d}{2})^2\Gamma\left(\frac{\Delta+1}{2}\right)(2\Delta-d)}\right). \tag{5.45}$$

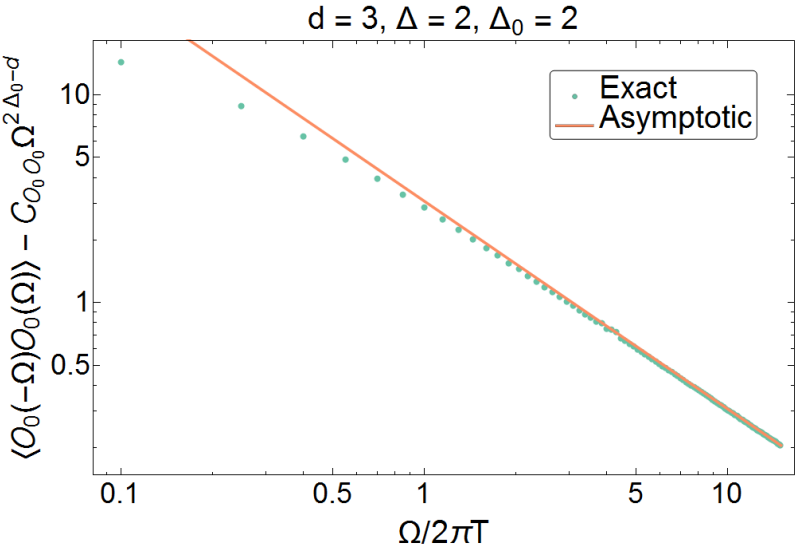

Figure 5.4: A log-log plot of the leading correction to the scalar two-point function from a relevant scalar deformation plotted against the holographic calculation with the leading contribution removed. Showing that the leading order estimates for the high-frequency behaviour are well respected.

If we substitute eq. (4.40) into eq. (5.45) we would reproduce eq. (3.29). So, perturbative conformal field theory is recovered in a limit of holography that can be used to accurately predict the high frequency thermal dynamics for some correlation functions. It also adds credibility to our holographic model that we are in fact probing the general CFT dynamics. In figure 5.4, we see a comparison between the numeric full-frequency response

$\langle \mathcal{O}_0(-\Omega)\mathcal{O}_0(\Omega)\rangle$ calculated from eq. (5.23) and the high-frequency asymptotic behaviour eq. (5.45) expected from the presence of a critical operator $\mathcal{O}$. The plots given showcase the precision of the calculation in the case where $d = 3$, $\Delta = 2$, $\Delta_0 = 2$. To close this section, let us numerically calculated high-frequency scalar two-point function with the predicted analytic expression. The high-frequency two-point function eq. (5.45) with $d = 3$, $\Delta = 2$, $\Delta_0 = 2$ is

$$\langle \mathcal{O}_0(\Omega)\mathcal{O}_0(-\Omega)\rangle = \Omega\left(-1 - \left(\frac{4\pi TL}{3\ell_p}\right)^2 \frac{\alpha_\psi \phi_1}{2\Omega^2}\right) \tag{5.46}$$

where ϕ_1 was found in equation eq. (5.14). The plots given in figure 5.4 are evaluated with $\frac{\alpha_\psi L^2}{\ell_p^2} = 1$ and $\phi_1 = 2.20703$ giving the expression for the expected high-frequency behaviour as

$$\langle \mathcal{O}_0(\Omega)\mathcal{O}_0(-\Omega)\rangle = \Omega(-1 - 19.3626\Omega^{-2}). \tag{5.47}$$

The power-law function that fits the high-frequency holographic calculation is found to be

$$\langle \mathcal{O}_0(\Omega)\mathcal{O}_0(-\Omega)\rangle = \Omega(-1 - 18.8143\Omega^{-1.97595}). \tag{5.48}$$

The coefficient for the power-law in the numerical fit has 2.8% error from the expected while the exponent has a 1.2% error. Our holographic model made some approximations. We consider only linear perturbations in α_C and high-frequency corrections stronger than $1/\Omega^d$, in addition to assuming that the holographic calculation for the scalar two-point function gives a power-law correction. Given that the fit is found by integrating the gauge equations of motion numerically from the black hole horizon to the AdS boundary, we find the magnitude of the errors to be acceptable.

5.3.2 Conductivity

We can do a similar treatment for calculating the conductivity for this holographic model and show that the large-frequency behaviour behaves exactly as predicted by the conformal field theory arguments of section 3. The conductivity is given by (for example [20])

$$\sigma = \frac{G^R_{JJ}}{i\omega} \tag{5.49}$$

where G^R_{JJ} is the retarded Green's function for the transverse gauge field A_x. The expression $1 + \alpha_F\, \phi(u)$ from eq. (4.6) occurs frequently, and we will simply denote this expression by

$X(u) = 1 + \alpha_F \phi(u)$. The retarded propagator is calculated by looking at the value of the on-shell action near the AdS boundary. The boundary action is given by

$$S = -\frac{1}{2g_d^2} \int d^d x \, \sqrt{-g} X g^{uu} g^{xx} A_x \partial_u A_x(u,x)\big|_{u\to 0} \tag{5.50}$$

which can be related to the retarded Green's function by [7]

$$S = \int \frac{d^d k}{(2\pi)^d} \, \frac{1}{2} A_x(-k) G^R_{JJ}(k) A_x(k)\Big|_{u\to 0} . \tag{5.51}$$

It is natural to expand the gauge field A_μ in momentum space since all directions other than u have translation invariance

$$A_\mu(u, \boldsymbol{x}) = \int \frac{d^d q}{(2\pi)^d} \, e^{i\boldsymbol{q}\cdot\boldsymbol{x}} \, A_\mu(u, \boldsymbol{q}) \, , \tag{5.52}$$

where, as usual $\boldsymbol{q}\cdot\boldsymbol{x} = -\omega t + \eta_{ij} q^i x^j$. Evaluating eq. (5.50) and using the definition of G^R_{JJ} eq. (5.51) we find

$$\begin{aligned} G^R_{JJ} &= -\frac{1}{g_d^2} \sqrt{-g} g^{uu} g^{xx} \frac{A_x(u,-k)\partial_u A_x(u,k)}{A_x(u,-k)A_x(u,k)}\Big|_{u\to 0} \\ &= -\frac{1}{g_d^2} \left(\frac{r_0}{L^2}\right)^{d-2} \left(\frac{L^{d-3} A'}{u^{d-3} A}\right)_{u\to 0} . \end{aligned} \tag{5.53}$$

Hence the conductivity can be calculated by observing the boundary behaviour of the maxwell gauge field A_x

$$\sigma(\omega) = -\frac{1}{i\omega g_d^2} \left(\frac{4\pi T}{d}\right)^{d-2} \left(\frac{L^{d-3} A'}{u^{d-3} A}\right)_{u\to 0} . \tag{5.54}$$

In addition, the membrane paradigm gives a unique perspective into the AdS/CFT correspondence. It allows us to realize the dissipative behaviour of the dual current in a thermal bath with the Maxwell field's interaction with the black hole horizon. For example, we can use holography to find the diffusion constant for Fick's law and the DC conductivity from Ohm's law (see section 2.5.2 and appendix B). The Diffusion constant is given in this model by

$$D = \frac{d}{4\pi T} X(1) \int_0^1 du \, \frac{u^{d-3}}{X(u)} . \tag{5.55}$$

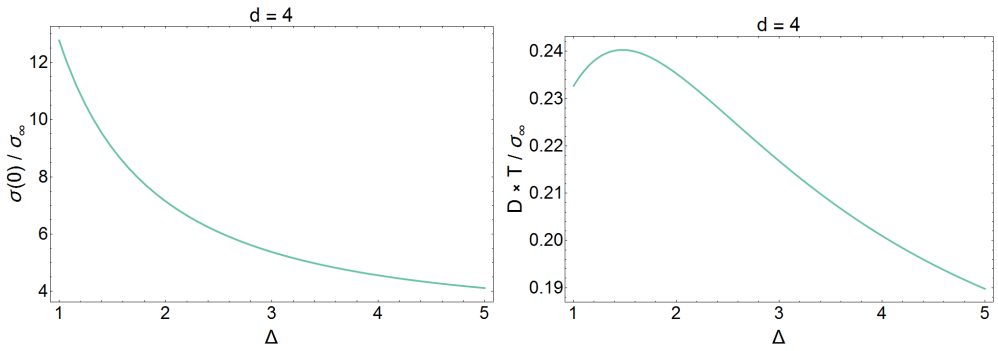

Figure 5.5: A plot of the DC conductivity (left) in $d = 4$ as a function of scaling dimension and a plot of the diffusion (right) in $d = 4$ as a function of scaling dimension.

The DC conductivity $\sigma(0)$ is found by applying Ohm's law on a stretched horizon [7, 37]

$$\sigma(0) = \left(\frac{4\pi LT}{d}\right)^{d-3} \frac{X(1)}{g_d^2}\,. \tag{5.56}$$

The DC conductivity is quite interesting since it is information that is found in deep IR and is usually outside of the scope of conformal perturbation theory, but which is reproduced in holographic calculations like those eqs. (5.55) and (5.56) Here the membrane paradigm gives us an interesting look at the behaviour of the Maxwell field all the way on the other farthest reaches of the bulk, near the black hole horizon.

The Maxwell gauge field can be obtained from the Maxwell equations of motion, which are derived by varying S_A with respect to A_μ yielding

$$\nabla_a \left[X F^{ab}\right] = 0\,. \tag{5.57}$$

We choose the standard radial gauge $A_u = 0$ and $\nabla^a A_a = 0$ and use the Fourier transformation eq. (5.52) of A to momentum space. We wish to solve for $A_x(u, \boldsymbol{q})$ in the background given by the black hole metric eq. (5.2) and sourced by the scalar profile given by eq. (5.10) in the critical regime $\phi_0 = 0$. Setting the spatial momentum to zero, *i.e.*, $\boldsymbol{q} = (\omega, 0, 0)$, we get an ordinary differential equation for the gauge field in this bulk spacetime

$$A_x''(u) + \left(\frac{X'(u)}{X(u)} + \frac{f'(u)}{f(u)} - \frac{d-3}{u}\right) A_x'(u) + \left(\frac{d\omega}{4\pi T}\right)^2 \frac{A_x(u)}{f(u)^2} = 0\,. \tag{5.58}$$

In order to determine the conductivity σ from eq. (5.54), we must determine the behaviour of the solutions of the equations of motion eq. (5.58) near the asymptotic boundary ($u \to 0$).

The scalar profile $\phi(u)$ appearing in eq. (5.58) is calculated via eq. (5.10), and the goal is to be able to numerically integrate a solution for A_x from the black hole horizon to the asymptotic boundary. Unfortunately, the momentum space gauge field has an logarithmic oscillatory divergence near the black hole horizon. In order to regulate this divergence, we will rescale the gauge field $A_x(u) = f(u)^b F(u)$ with $b = -\frac{i\omega}{4\pi T}$ which incorporates the infalling boundary condition for the gauge field [7]. This field redefinition gives us a field which is regular at the black hole horizon. The equation of motion for $F(u)$ is given by

$$F'' + \left(\frac{(1+2b)f'}{f} + \frac{X'}{X} - \frac{d-3}{u}\right) F' + \left(\frac{bf'}{f}\left(\frac{f''}{f'} + \frac{bf'}{f} + \frac{X'}{X} - \frac{d-3}{u}\right) - \frac{b^2 d^2}{f^2}\right) F = 0\,. \tag{5.59}$$

The gauge field is always defined only up to some overall constant factor, so we are free to set this constant. Likewise the redefined gauge field F is homogeneous and can also only be determined up to a constant. On the other hand, the derivative for the field F near the black hole horizon is set by requiring $F(u)$ to be regular. The only object in eq. (5.59) that is singular at the horizon is the blackening factor f. Organizing the poles into first and second order poles we see that near the black hole horizon equation eq. (5.59) becomes

$$\begin{aligned} 0 = &\frac{1}{f^2}\left(b^2 f'^2 - b^2 d^2\right) + \\ &\frac{1}{f}\left((1+2b)f'F' + \left(bf'' + bf'\frac{X'}{X} - bf'(d-3)\right)F\right) \end{aligned} \tag{5.60}$$

The second order pole is fixed by the in-falling boundary conditions, whereas we will need to impose boundary conditions on F near the black hole horizon to eliminate the first order pole. These boundary conditions are

$$F'(1) = -\frac{b}{1+2b}\left(2 + \frac{X'(1)}{X(1)}\right) F(1)\,. \tag{5.61}$$

In the following we take advantage of the freedom to scale $F(u)$ and we set $F(1) = 1$ for simplicity. For odd dimensions d, we can extract the conductivity from eq. (5.59) but logarithmic divergences appear for even dimensions. These divergences can be renormalized by introducing counterterms to the holographic action, but these terms violate the conformal invariance. The real-frequency conductivity is not affected by the logarithmic divergences, however and we can calculate this quantity without the need for counter-terms. For the Euclidean conductivities, we can extract universal behaviour for the conductivity but there will always be present a cutoff-dependent logarithm in the Euclidean frequency [38, 39]. In order to extract the conductivity from the gauge field profile, it is important to understand

how the gauge field behaves near the asymptotic boundary. So here we provide the near-boundary behaviour for the gauge field for the first few conformal dimensions that we can explore with this model

$$\begin{aligned} d=3; \quad & A_x(u) \to A_0 + A_1 u + O(u^2) \\ d=4; \quad & A_x(u) \to A_0 + A_2 u^2 + 8b^2 A_0 u^2 \log(\Lambda u) + O(u^3) \\ d=5; \quad & A_x(u) \to A_0 - \frac{b^2 d^2 A_0}{2} u^2 + A_3 u^3 + O(u^4)\,. \end{aligned} \tag{5.62}$$

Notice that the near-boundary behaviour can always be parameterized using two integration constants. This is due to the fact that the equation of motion governing the behaviour of the gauge field is a second order ordinary differential equation. The integration constants A_0 and A_{d-2} can be extracted numerically by regression on points sampled near the boundary of the numerical solution for eq. (5.59). By combining the expression for the conductivity eq. (5.54) with the introduction of the integration constants eq. (5.62), we can read the conductivity directly from the numeric solution

$$\begin{aligned} d=3; \quad & \sigma(\omega) = -\frac{4\pi T}{3i\omega g_4^2}\frac{A_1(\omega)}{A_0(\omega)} \\ d=4; \quad & \sigma(\omega) = -\frac{(\pi T)^2 L}{i\omega g_5^2}\left(\frac{2A_2(\omega)}{A_0(\omega)} - \frac{\omega^2}{2}\right) \\ d=5; \quad & \sigma(\omega) = -\frac{L^2}{i\omega g_6^2}\left(\frac{4\pi T}{5}\right)^2 \frac{A_3(\omega)}{A_0(\omega)}\,. \end{aligned} \tag{5.63}$$

If we look at the non-interacting limit $\alpha_C \to 0$, we find that the conductivity exactly matches with [39] for $d = 3$ and $d = 4$.

Figures 5.6 and 5.7 show the full-frequency conductivity for $d = 3, 4$ at various coupling strengths, and figure 5.8 showcases how the scaling dimension affects the conductivity. We observe from the figure the case of $\Delta = 1$ and $d = 4$ that the scalar deformation leads to a constant shift in the real part of the conductivity at high frequencies. This may seem odd because the curves do not reach the same asymptotic profile, but as can be seen from eq. (3.36), we expect a $\Delta = 1$ scalar expectation to cause a constant shift in the conductivity.

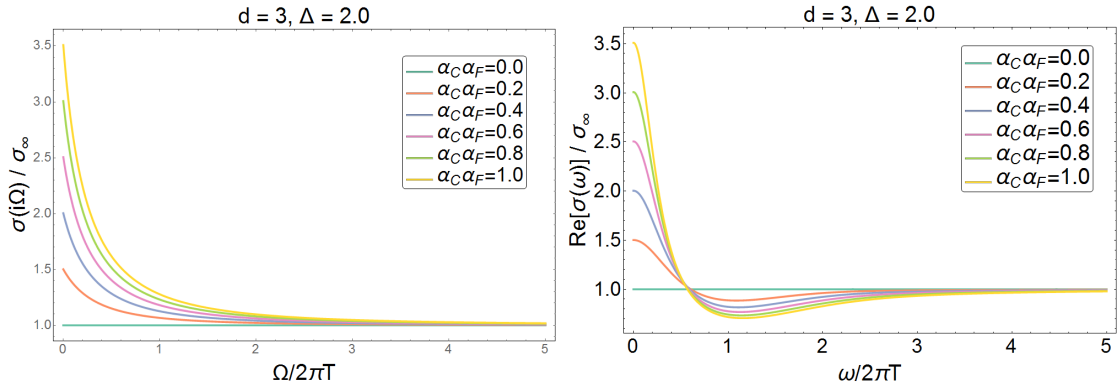

Figure 5.6: The Euclidean (left) and real (right) AC conductivity for $d = 3$ and $\Delta = 2$ for various choices of interaction strength

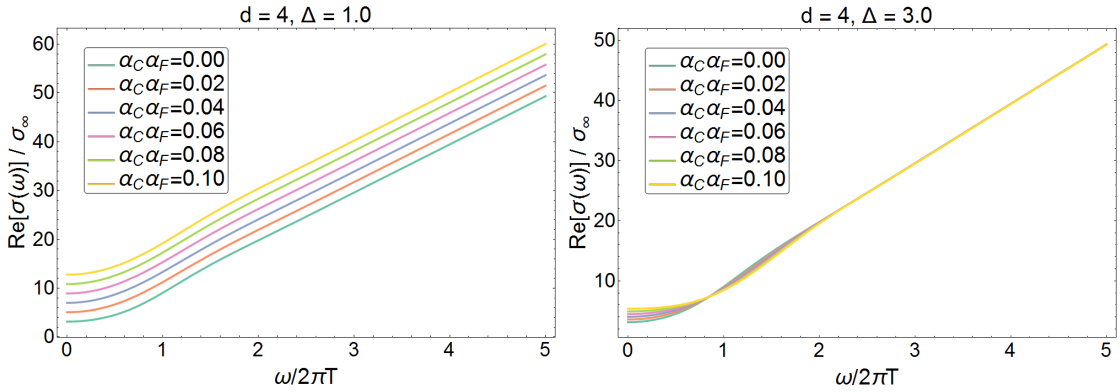

Figure 5.7: The real frequency AC conductivity for $d = 4$ for various choices of interaction strength. On the left is the AC conductivity in the presence of a relevant operator $\mathcal{O}$ with scaling dimension $\Delta = 1$, and on the right with scaling dimension $\Delta = 3$.

High-frequency AC conductivity

As explained in chapter 3 and demonstrated for scalar fields in section 5.3.1, we can compute the high-frequency asymptotics for the conductivity at frequencies much greater than the temperature. Working in Euclidean frequencies, this corresponds to evaluating $\sigma(\omega = i\Omega)$ with $\Omega \gg T$. In the following, we will calculate the high frequency asymptotics perturbatively in the dimensionless coupling α_F in the action eq. (4.6). Recall that this coupling controls the strength of the ϕF^2 interaction in eq. (4.6), which corresponds to the $\mathcal{C}_{JJ\mathcal{O}}$ coupling in the CFT (see table 4.1) and controls how the conductivity is affected

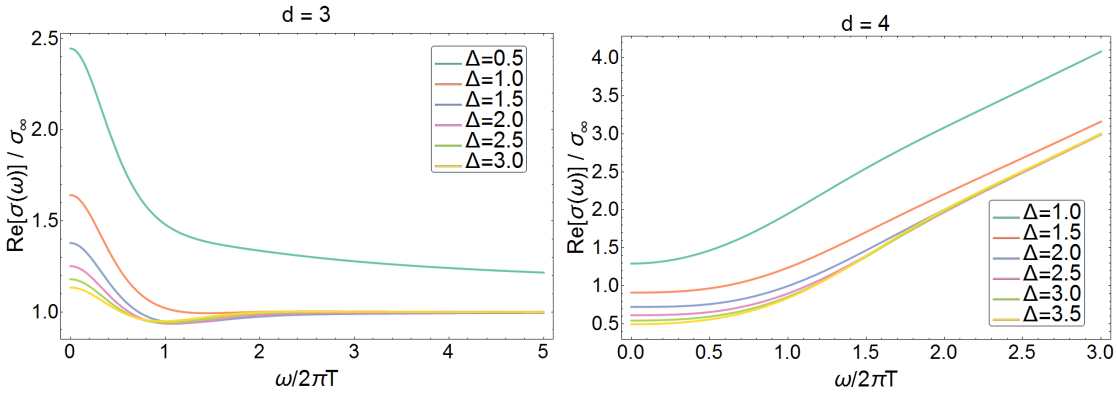

Figure 5.8: The real frequency AC conductivities for $d = 3$ (left) and $d = 4$ (right) for various choices of scaling dimension for the operator $\mathcal{O}$ that is deforming the theory.

by a scalar deformation, as seen in eq. (3.36). Much of this derivation is similar to the calculation for the scalar two-point function presented in section 5.3.1, but with the scaling dimension fixed at $\Delta_0 = d - 1$. In order to clean up the frequency dependence in what follows, we will rescale the radial variable $u = \frac{4\pi T v}{d\Omega}$. Then at large frequencies, eq. (5.58) gives

$$A_x'' - \frac{d-3}{v} A_x' - A_x = -\alpha_C \phi' A_x'. \tag{5.64}$$

In this equation, we have made the approximations $f' \to 0$, $f \to 1$. This allows us to calculate the high-frequency conductivity up to corrections of order $1/\Omega^d$. In our perturbative approach, we expand the gauge profile in a series controlled by the coupling strength α_F, *i.e.*,

$$A_x = A_x^{(0)} + \alpha_F A_x^{(1)} + \alpha_F^2 A_x^{(2)} + ... \tag{5.65}$$

We similarly expand the gauge equation of motion eq. (5.64), and at leading order, we have

$$\left(\partial_v^2 - \frac{d-3}{v}\partial_v - 1\right) A_x^{(0)} = 0\,. \tag{5.66}$$

It is useful to find the Green's function for eq. (5.66) since the perturbative gauge field $A_x^{(1)}$ will satisfy a non-homogeneous version of the same differential equation. The solutions to eq. (5.66) are

$$A_x(v) = v^{d/2-1} K_{d/2-1}(v), \quad A_x(v) = v^{d/2-1} I_{d/2-1}(v)\,. \tag{5.67}$$

The Green's function which we require vanishes at the horizon and at the AdS boundary, *i.e.*, , $G(0, V) = G(v, \infty) = 0$. We note that eq. (5.66) is the same equation as eq. (5.27)

with $\Delta_0 = d-1$. The Green's function is given by

$$G(v,V) = \begin{cases} -V(v/V)^{d/2-1} I_{d/2-1}(v) K_{d/2-1}(V) & \text{if } V > v \\ -V(v/V)^{d/2-1} I_{d/2-1}(V) K_{d/2-1}(v) & \text{if } v < V \end{cases} . \tag{5.68}$$

The Green's function $G(v,V)$ satisfies $\left(\partial_v^2 - \frac{d-3}{v}\partial_v - 1\right) G(v,V) = \delta(v-V)$. The solution to eq. (5.66) that is regular at the black hole horizon is simply

$$A_x^{(0)}(v) = \frac{v^{d/2-1} K_{d/2-1}(v)}{\Phi(d,d-1)}, \tag{5.69}$$

where Φ has been previously defined in eq. (4.14). The constant $\Phi(d,d-1)$ chosen is such that $A_x^{(0)}(0) = 1$. Useful for later, the derivative of the free gauge field propagator is

$$A_x'^{(0)}(v) = -\frac{v^{d/2-1} K_{d/2-2}(v)}{\Phi(d,d-1)} . \tag{5.70}$$

Continuing our first-order perturbative calculation for the conductivity, the term in eq. (5.64) which is linear in the small α_F expansion is

$$\left(\partial_v^2 - \frac{d-3}{v}\partial_v - 1\right) A_x^{(1)} = -\phi' A_x'^{(0)}. \tag{5.71}$$

From here, we can pause and note that the perturbative calculation for the conductivity and for the scalar two-point function differ from this point onwards. The fundamental difference being the tensorial structure differences between $F_{ab}F^{ab}$ and $\psi\psi$. Using the Green's function eq. (5.68), we can solve for $A_x^{(1)}$

$$\begin{aligned} A_x^{(1)}(v) &= -\int_0^\infty dV G(v,V)\phi'(V) A_x'^{(0)}(V) \\ &= \frac{v^{d/2-1} I_{d/2-1}(v)}{\Phi(d,d-1)} \int_0^\infty dV\, \phi'(V) K_{d/2-1}(V)\, V\, K_{d/2-2}(V) . \end{aligned} \tag{5.72}$$

We can now make use of the identity

$$2V^{d-2} K_{d/2-1}(V) K_{d/2-2}(V) = -\partial_V \left[V^{d-2} K_{d/2-1}(V)^2\right] \tag{5.73}$$

to help clean up the Bessel functions in eq. (5.72), leaving

$$A_x^{(1)}(v) = -\frac{v^{d/2-1} I_{d/2-1}(v)}{2\Phi(d,d-1)} \int_0^\infty dV \phi'(V)\, V^{3-d} \partial_V \left[V^{d-2} K_{d/2-1}(V)^2\right] . \tag{5.74}$$

We can now integrate by parts to remove the derivatives from the Bessel functions. Doing so we get an expression for $A_x^{(1)}$

$$A_x^{(1)}(v) = \frac{v^{d/2-1} I_{d/2-1}(v)}{2\Phi(d, d-1)} \int_0^\infty dV \ (\phi''(V)\, V - (d-3)\phi'(V)\,)\, K_{d/2-1}(V)^2 \,. \tag{5.75}$$

Just as with the scalar field prescription, this procedure is only reliable up to order $1/\Omega^d$ in the high frequency limit. Therefore we can safely make the substitution[5] $\phi(V) = \phi_1 \left(\frac{4\pi T}{\Omega}\right)^\Delta V^\Delta$ and get accurate results to first order in perturbation theory in the scalar deformation. Doing so yields

$$\begin{aligned} A_x^{(1)}(v) &= \frac{\phi_1 \Delta(\Delta - d + 2)}{2\Phi(d, d-1)} v^{d/2-1} I_{d/2-1}(v) \left(\frac{4\pi T}{d\Omega}\right)^\Delta \int_0^\infty dV\, V^{\Delta-1} K_{d/2-1}(V)^2 \\ &= \frac{\phi_1 \Delta(\Delta - d + 2)}{2\Phi(d, d-1)} v^{d/2-1} I_{d/2-1}(v) \left(\frac{4\pi T}{d\Omega}\right)^\Delta \Psi(d, \Delta, d-1)\,, \end{aligned} \tag{5.76}$$

where $\Psi(d, \Delta, d-1)$ was defined earlier in eq. (3.15). The conductivity eq. (5.54) then evaluates to

$$\begin{aligned} \sigma(\Omega) =& \frac{L^{d-3}}{g_d^2} \Omega^{d-3} \left(\sigma_\infty - \frac{\alpha_F \phi_1 \Delta(\Delta - d + 2)(d-2)\, \Theta(d, d-1) \Psi(d, \Delta, d-1)}{2\,\Phi(d, d-1)} \left(\frac{4\pi T}{d\Omega}\right)^\Delta \right) \\ =& \frac{L^{d-3}}{g_d^2} \Omega^{d-3} \left(\sigma_\infty - \frac{\alpha_F \ell_p^{d-1} \langle \mathcal{O} \rangle \Delta(\Delta - d + 2) \Psi(d, \Delta, d-1)}{L^{d-1}(2\Delta - d) 2^{d-3} \Gamma(d/2-1)^2 \Omega^\Delta} \right) \end{aligned} \tag{5.77}$$

We can expand $\Psi(d, \Delta, d-1)$ as well to get the full expression for the high-frequency conductivity in terms of gamma functions

$$\sigma(\Omega) = \frac{L^{d-3}}{g_d^2} \Omega^{d-3} \left(\sigma_\infty - \frac{\alpha_F \ell_p^{d-1} \langle \mathcal{O} \rangle}{L^{d-1} \Omega^\Delta} \frac{\Delta(\Delta - d + 2) \sqrt{\pi} \Gamma\left(\frac{\Delta}{2}\right) \Gamma\left(\frac{\Delta + d - 2}{2}\right) \Gamma\left(\frac{\Delta - d + 2}{2}\right)}{(2\Delta - d) 2^{d-1} \Gamma(d/2-1)^2 \Gamma\left(\frac{\Delta+1}{2}\right)} \right) . \tag{5.78}$$

Taking $d = 3$ we reproduce the conductivity given in [15].

$$\sigma(\Omega)_{d=3} = \frac{1}{g_4^2} \left(\sigma_\infty + \frac{\alpha_F \ell_p^2 \langle \mathcal{O} \rangle}{L^2 \Omega^\Delta} \frac{\Gamma(\Delta + 1)}{L^2 (2\Delta - 3) 2^\Delta} \right) . \tag{5.79}$$

[5] We will assume that the boundary theory is critical at this time. See section 5.5 for where we deform the theory by the relevant operator.

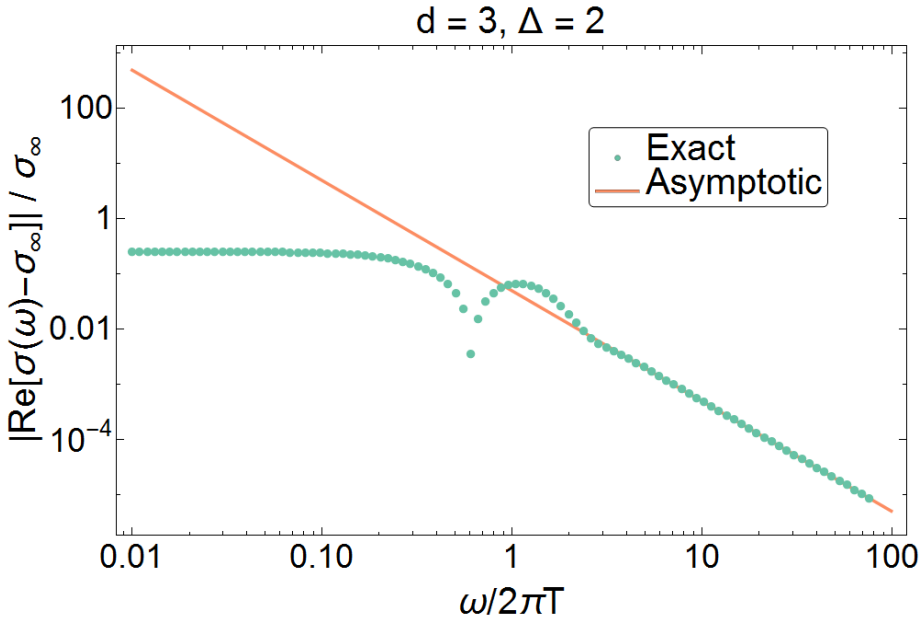

Figure 5.9: A comparison of the numerical calculation of σ with the asymptotic expansion eq. (5.77) with the leading contribution removed.

In section 5.4, we calculate the conductivity to higher orders in a T/Ω expansion for the $d = 3$ case, displaying the calculations done in [13]. Figure 5.9 shows how closely the exact full-frequency response matches the leading correction predicted from conformal perturbation theory and holography at high frequencies.

5.3.3 Reissner-Nordström models

We have seen the strength of the holographic and the conformal perturbation theory approach for how linear response functions behave when a scalar operator acquires an expectation value, we have also verified these predictions using a simple holographic model. In order to test the robustness of these claims, we will now do a similar treatment for slightly more complicated models and show that the conformal perturbation theory results of chapter 3 are indeed recovered in more complicated spacetimes. The action which sources the background metric is given by the free part (all interactions $\alpha_a = 0$ set to zero) of eq. (4.2)

$$S = \int d^{d+1}x\sqrt{-g}\left(\frac{1}{2\ell_p^{d-1}}(R+2\Lambda) - \frac{1}{4g_d^2}F_{ab}F^{ab}\right) \tag{5.80}$$

where $\Lambda = -\frac{d(d-1)}{2L^2}$, $R = R^{ab}{}_{ab}$ and $F_{ab} = \nabla_a A_b - \nabla_b A_a$. The Einstein-Maxwell equations of motion for the background geometry are determined by varying eq. (5.80) with respect to the metric (δg^{ab}) and the gauge field (δA_ν)

$$\begin{aligned} R_{\mu\nu} - \frac{1}{2}Rg_{\mu\nu} + \Lambda g_{\mu\nu} =& \frac{\ell_p^{d-1}}{g_d^2}\left(F_{\mu\rho}F_{\nu\sigma}g^{\alpha\beta} - \frac{1}{4}g_{\mu\nu}F_{ab}F^{ab}\right) \\ \nabla_\mu F^{\mu\nu} =& 0. \end{aligned} \tag{5.81}$$

A simple static uncharged solution to these equations is given in eq. (5.2). The next simplest modification that we can make is to give the black hole a charge. The static Reissner-Nordström solution is given by

$$\begin{aligned} ds^2 =& \frac{r_0^2}{u^2L^2}\left(-f(u)dt^2 + \delta^{ij}dx_i dx_j\right) + \frac{L^2du^2}{u^2f(u)} \\ A =& \sqrt{\frac{d-1}{d-2}}\frac{r_0 g_d \xi}{\ell_p^{\frac{d-1}{2}}L}(1-u^{d-2})dt \end{aligned} \tag{5.82}$$

where

$$f(u) = 1 - (1+\xi^2)u^d + \xi^2 u^{2(d-1)}. \tag{5.83}$$

The dimensionless radial coordinate u is rescaled in such a way that the "outer" black hole horizon is located at $u = 1$ and the asymptotic anti de-Sitter space boundary is located at $u \to 0$. The black hole horizon is extremal at precisely $\xi^2 = \frac{d}{d-2}$. Thus we will restrict our attention to $\xi^2 < \frac{d}{d-2}$. The temperature of this spacetime can be found by first changing variables to Euclidean time $t = i\tau$, and requiring the spacetime to be regular at the black hole horizon. The Euclidean metric

$$ds^2 = \frac{r_0^2}{u^2L^2}(f(u)d\tau^2 + \delta^{ij}dx_i dx_j) + \frac{L^2du^2}{u^2f(u)} \tag{5.84}$$

will have a conical singularity at the black hole horizon ($u \to 1$) unless the Euclidean time τ has the correct period. This calculation was carried out in Section 5.1, which shows that the temperature is given by $T = -\frac{f'(1)r_0}{4\pi L^2}$. In the Reissner-Nordström case, this becomes

$$T = \frac{(d-(d+2)\xi^2)r_0}{4\pi L^2}\,. \tag{5.85}$$

The model is designed to give the scalar operator $\mathcal{O}$ an expectation value $\langle\mathcal{O}\rangle \sim T^\Delta$. For the electrical conductivity to be modified by a scalar deformation we couple the maxwell

gauge field A_μ to the scalar field as in eq. (4.6) with $\alpha_F \neq 0$. Note that this coupling provides a source for the scalar field equations of motion because the gauge field is not trivial in the background gravitational solution. So it is not necessary to engineer an additional source for the scalar field, for this reason we fix $\alpha_C = 0$ in eq. (4.4). This is in contrast with the minimal model presented above which required an additional source to give the scalar operator a non-trivial expectation value. The full action for this model is given by eq. (4.2) with $\alpha_C = 0$ and $\alpha_\psi = 0$. Just as above, we are assuming that back reactions caused by the dynamical fields are negligible[6].

The equation of motion for ϕ is given by

$$(\nabla - m^2)\phi - \frac{\alpha_F \ell_p^2}{4g_d^2} F^2 = 0. \tag{5.86}$$

The background Maxwell gauge is given by eq. (5.82), so

$$F^2 = -\frac{2u^4 A_t'^2}{r_0^2}\,. \tag{5.87}$$

In the Schwarzschild-AdS ($\xi = 0$) solution to the Einstein-Maxwell equation, the exact homogeneous solution eq. (5.9) to the scalar equations of motion were found. But in general we will need to evaluate ϕ numerically since the added complexity for the blackening factor eq. (5.83) makes it difficult for us to find an exact solution. The conductivity is defined by eq. (2.23). The boundary action is given by

$$S = -\frac{1}{2g_d^2}\int d^d x\, \sqrt{-g} X g^{uu} g^x A_x \partial_u A_x(u,x)\big|_{u\to 0} \tag{5.88}$$

where the retarded Green's function is defined in eq. (5.51). By expanding A_x in momentum space (see eq. (5.52)), we see that the retarded propagator is given by eq. (5.53). In order to calculate the AC conductivity, we will solve the Einstein-Maxwell eqs. (5.81) in a linear perturbation about the background eq. (5.82). Assuming that the gauge field is frequency dependent and does not have a spatial momentum, *i.e.,* $\delta A_x = \int \frac{dt}{2\pi} e^{i\omega t}\delta A_x(u)$, the only perturbations that will have an effect on the conductivity are δA_x and δg_{xt} [40]. The linearized Einstein-Maxwell equations are found by substituting $A_x \to A_{x(0)} + \delta A_x$ and $g_{xt} \to \cancel{g_{xt(0)}} + \delta g_{xt}$ into eq. (5.81) where $A_{x(0)}$ and $g_{xt(0)}$ are the background solutions given

[6]This can be thought as a perturbative expansion in α_F, and that we are only working to linear order in α_F,*i.e.,* there is no back-reaction.

by eq. (5.82). A detailed derivation is given in appendix C with the result

$$\begin{aligned}0 =&\delta A_x'' + \left(\frac{X'}{X} + \frac{f'}{f} - \frac{d-3}{u}\right)\delta A_x' - \omega^2 \frac{g^{tt}}{g^{uu}}\delta A_x + \frac{2\ell_p^2}{g_d^2} g^{tt} A_t'^2 \delta A_x \\ =&\delta A_x'' + \left(\frac{X'}{X} + \frac{f'}{f} - \frac{d-3}{u}\right)\delta A_x' + \frac{\omega^2 L^4}{r_0^2 f(u)^2}\delta A_x \\ &- \frac{2(d-1)(d-2)u^2\xi^2}{g_d^2 f(u)}\delta A_x.\end{aligned} \tag{5.89}$$

This equation will have to be evaluated numerically. As before, there is a logarithmic-oscillatory singularity near the horizon As in section 5.3.2, we can redefine the gauge field as $\delta A_x(u) = f(u)^b F(u)$ in order to enforce in-falling boundary conditions. The field F must be regular at the black hole horizon, the gauge equations of motion for F are

$$\begin{aligned}0 =&F'' + \left(\frac{X'}{X} + \frac{(1+2b)f'}{f} - \frac{d-3}{u}\right)F' \\ &+ \left(\left(\frac{X'}{X} + \frac{bf'}{f} + \frac{f''}{f'} - \frac{d-3}{u}\right)\frac{bf'}{f} + \frac{\omega^2 L^4}{r_0^2 f^2} - \frac{2(d-1)(d-2)u^2\xi^2}{g_d^2 f}\right)F.\end{aligned} \tag{5.90}$$

Near the black hole horizon $u \to 1$, the (potentially) singular part of the above equation is

$$\begin{aligned}0 =&\frac{1}{f^2}\left(b^2 f'^2 + \frac{\omega^2 L^4}{r_0^2}\right)F \\ &+ \frac{1}{f}\left((1+2b)f'F' + bf'F\left(\frac{X'}{X} + \frac{f''}{f'} - \frac{d-3}{u}\right) - \frac{2(d-1)(d-2)\xi^2 F}{g_d^2}\right).\end{aligned} \tag{5.91}$$

Therefore, in order for the redefined gauge field F to be regular at the black hole horizon, we first require for $b = \pm\frac{i\omega L^2}{r_0 f'} = \pm\frac{i\omega}{4\pi T}$. This is enforced by the infalling boundary conditions on the gauge perturbation. Now the simple pole can be removed by appropriate boundary conditions on F and F'

$$\frac{F'(1)}{F(1)} = \frac{1}{(1+2b)f'(1)}\left(\left(\frac{2(d-1)(d-2)\xi^2}{g_d^2}\right) - bf'(1)\left(\frac{X'(1)}{X(1)} + \frac{f''(1)}{f'(1)} - d + 3\right)\right). \tag{5.92}$$

Since eq. (5.89) is linear, the scale of F is arbitrary and we set $F(1) = 1$. In figure 5.10, we see the plots of the conductivity calculated numerically for various values of the coupling constants. The scalar field ϕ in the charge-less case $\xi = 0$ has no sources, so the conductivity is not modified by the relevant scalar. This corresponds to the case where the scalar operator does not gain an expectation $\langle\mathcal{O}\rangle \neq 0$, so the $\xi = 0$ curve is simply the free

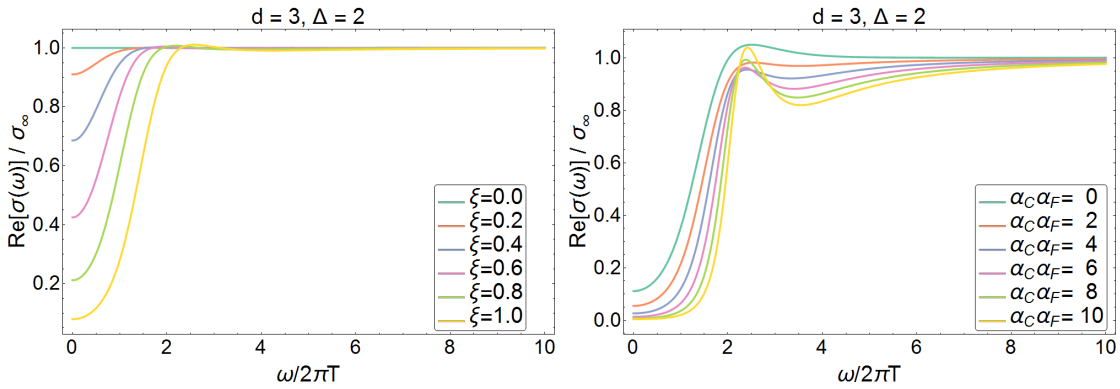

Figure 5.10: The numerical evaluation of the real part of the conductivity for $d = 3$ and $\Delta = 2$. On the left, we have $\alpha_C \alpha_F = 1$ plotted with various charge parameters ξ and on the right we have $\xi = 1$ plotted with various coupling strengths.

conductivity. This is seen by realizing that the scalar field equations are sourceless, so $X = 1$ and eq. (5.89) becomes the free gauge equation.

Figure 5.11 demonstrates agreement between the analytic prediction eq. (5.77) for high frequencies and the full numerical computation. An interesting feature for this model is that even without considering the scalar deformation, the corresponding QFT is already deformed from the CFT fixed point due to the presence of a finite charge in the gravity theory, and hence a chemical potential μ in the boundary theory. We generically expect contributions to the conductivity of the form

$$\sigma(\Omega) = \sigma_\infty \Omega^{d-3} \left(1 + a \frac{\lambda}{\Omega^{d-\Delta}} + b \frac{\langle \mathcal{O} \rangle}{\Omega^\Delta} + c \frac{\mu^2}{\Omega^2} + \cdots \right) \tag{5.93}$$

where the coefficient c is related to the four-point correlation function $\langle JJJJ \rangle$ in the CFT, which is non-vanishing in this holographic model due to graviton exchange in the bulk as depicted in figure 5.12.

We carefully choose $\Delta = 1.75 < 2$ to show in figure 5.11 because the scalar deformation will still be the leading correction to the conductivity in this model.

5.3.4 Decoupled gauge fields

In the previous section we considered a holographic model involving gravity coupled to a single Maxwell field. The latter is dual to a conserved current in the boundary theory and we examined modifications to the conductivity defined by the current when a

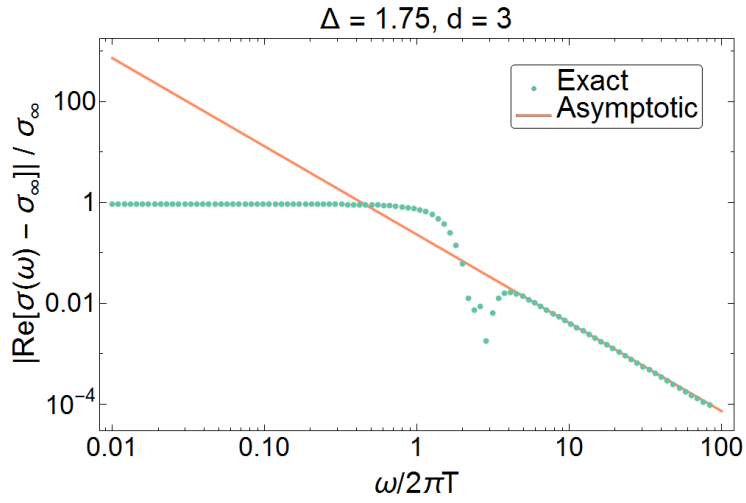

Figure 5.11: A log-log plot comparing the leading order analytic expression compared with the numerical calculation with the leading free part removed. Spacetime dimension is $d = 3$ while the relevant scalar dimension is $\Delta = 1.75$ and the charge parameter $\xi = 1$.

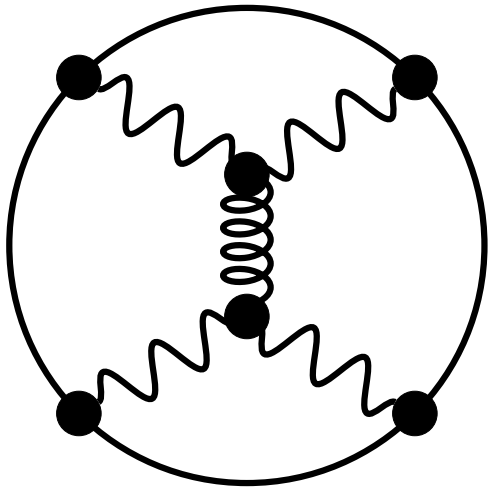

Figure 5.12: A representation of the graviton exchange in the $\langle JJJ \rangle$ calculation

chemical potential was introduced. In our model, these modifications emerged because of couplings between the current and a relevant operator, *i.e.,* the chemical potential induced an expectation value $\langle \mathcal{O} \rangle$.

We can instead have a bulk theory with two gauge fields, one is given a charge in the

background, while we evaluate the conductivity for the other charge-less gauge field. The two Maxwell fields will not interact with each other. The role for the former is to provide an enhanced geometry, and we observe how this geometry affects the conductivity of the latter.

Once again, in the we require an expectation value of the relevant scalar operator in the CFT. Since the interaction ϕF^2, where F denotes the unchanged gauge field, does not source the expectation value of the scalar operator $\langle \mathcal{O} \rangle$, we once again introduce an interaction between the scalar field and the Weyl curvature just as in section 4.1. Hence, the relevant scalar in this model will be sourced by the Weyl scalar $C_{abcd}C^{abcd}$ which vanishes at zero temperature and gives the appropriate scaling to the scalar expectation value $\langle \mathcal{O} \rangle_T \sim T^{\Delta}$. The full action for this model is given by

$$S_0 = \frac{1}{2\ell_p^{d-1}} \int d^{d+1}x\sqrt{-g}\left(R + \frac{d(d-1)}{L^2}\right) \tag{5.94}$$

$$S_\phi = -\frac{1}{2\ell_p^{d-1}} \int d^{d+1}x\sqrt{-g}\left[(\nabla_a\phi)^2 + m^2\phi^2 - 2\alpha_C L^2 \phi\, C_{abcd}C^{abcd}\right] \tag{5.95}$$

$$S_A = -\frac{1}{4g_d^2} \int d^{d+1}x\sqrt{-g}\left[\left(1 + \alpha_F\phi\right) F_{ab}F^{ab} + \tilde{F}_{ab}\tilde{F}^{ab}\right]. \tag{5.96}$$

which is similar to eq. (4.2) with no second scalar ψ and an additional background gauge field added, denoted $\tilde{A}$ and $\tilde{F}_{ab} = \partial_a\tilde{A}_b - \partial_b\tilde{A}_a$. The Maxwell field $\tilde{A}$ supports charge on the background black hole but this field does not source the scalar field ϕ. The background Reissner-Nordström solution is given by eq. (5.82) with $\tilde{A}$ replacing A. While the equation of motion for the scalar field is found in a perturbative expansion around this background solution. The scalar field must satisfy the equation of motion eq. (5.7). In this background eq. (5.82), the Weyl curvature scalar evaluates to

$$C_{abcd}C^{abcd} = \frac{(d-2)u^4 f''(u)^2}{dL^4}. \tag{5.97}$$

In the case where $\xi = 0$, the homogeneous part of equation eq. (5.7) has an exact solution given by eq. (5.9), but here in general the equation will need to be determined numerically.

We are interested in evaluating the conductivity for the probe gauge field with particular interest in how it is modified by the scalar deformation. In order to achieve this, we compute the dynamical scalar field ϕ and gauge field A_μ. The relevant part of the action is

$$S_{\text{int}} = -\frac{1}{4g_d^2} \int d^{d+1}x\sqrt{-g}(1 + a_F\phi)F^2. \tag{5.98}$$

The equation of motion for the gauge field A_x is given by varying S_{int} with respect to δA_x. Doing so gives

$$0 = \nabla_a (X F^{ab}) \,, \tag{5.99}$$

where $X = 1 + \alpha_F \phi$ and which when we use our particular solution and choice of coordinates for this model, the equation of motion for the perturbation δA_x of the gauge field is given by

$$\delta A_x'' + \left(\frac{X'}{X} + \frac{f'}{f} - \frac{d-3}{u} \right) \delta A_x' - \frac{\omega^2 L^4}{r_0^2 f^2} \delta A_x = 0 \tag{5.100}$$

This equation of motion is similar to eq. (5.58) except that the form for f is different, and the scalar field profile ϕ is also altered in this spacetime. The solution has a logarithmic-oscillatory singularity at the black hole horizon $u \to 1$. To avoid this issue, we follow the same prescription that we have used throughout this chapter. We define a regularized field $\delta A_x(u) = f(u)^b F(u)$ where F is regular. The equation of motion for F becomes

$$\begin{aligned} 0 =& F'' + \left(\frac{X'}{X} + \frac{(1+2b) f'}{f} - \frac{d-3}{u} \right) F' \\ &+ \left(\left(\frac{X'}{X} + \frac{b f'}{f} + \frac{f''}{f'} - \frac{d-3}{u} \right) \frac{b f'}{f} + \frac{\omega^2 L^4}{r_0^2 f^2} \right) F. \end{aligned} \tag{5.101}$$

Near the black hole horizon $u \to 1$, this equation's singular parts are

$$\begin{aligned} 0 =& \frac{1}{f^2} \left(b^2 f'^2 + \frac{\omega^2 L^4}{r_0^2} \right) F \\ &+ \frac{1}{f} \left((1+2b) f' F' + b f' F \left(\frac{X'}{X} + \frac{f''}{f'} - \frac{d-3}{u} \right) \right). \end{aligned} \tag{5.102}$$

In order for F to be regular, we will require once again to choose in-falling boundary conditions $b = -\frac{i\omega L^2}{r_0 f'} = -\frac{i\omega}{4\pi T}$. To remedy the simple pole at the horizon in the above equation we require the boundary condition

$$\frac{F'(1)}{F(1)} = -\frac{b}{1+2b} \left(\frac{X'(1)}{X(1)} + \frac{f''(1)}{f'(1)} - d + 3 \right) . \tag{5.103}$$

Figure 5.13 shows the conductivity found for various values of ξ and for various values of coupling strength $\alpha_C \alpha_F$, with $\xi = 0$ representing the charge-less solution Figure 5.14 shows that the predictions from chapter 3 and the perturbative holographic analysis done in section 5.3.2 agree with the exact calculation to a high degree of accuracy at high temperatures.

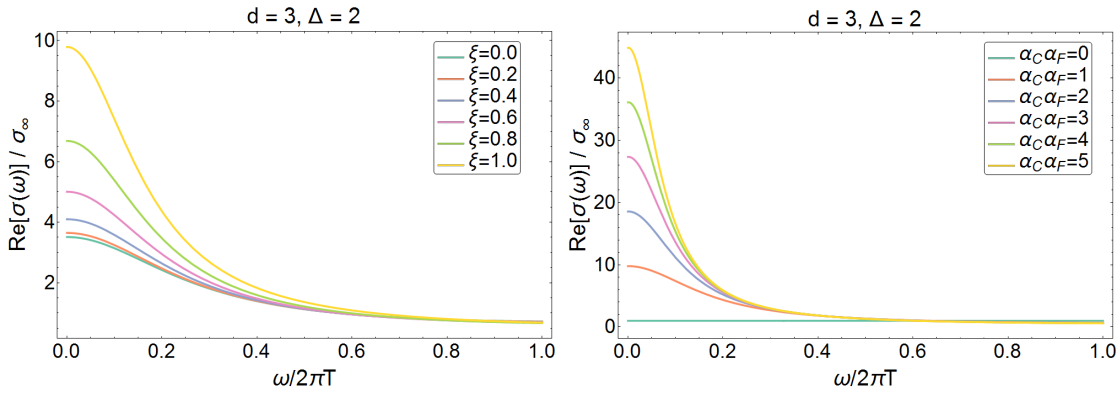

Figure 5.13: AC conductivity for the RN-Weyl model for various choices of the charge coefficient ξ with $\alpha_C \alpha_F = 1$. The evaluation of the real part of the conductivity is taken for $d = 3$, $\Delta = 2$.

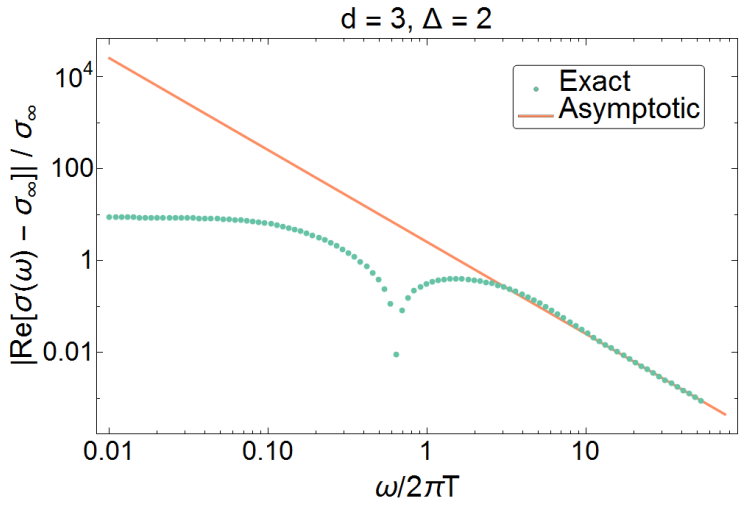

Figure 5.14: A log-log plot comparing the leading order analytic expression compared with the numerical calculation with the free contribution removed. Spacetime dimension is $d = 3$ while the relevant scalar dimension is $\Delta = 2$ and the charge parameter $\xi = 1$.

5.4 Conductivity in three dimensions

This section represents work done in [13], by myself and collaborators, where we were looking exclusively at the conductivity for CFTs with spacetime dimension $d = 3$. The work in this section mirrors many of the approaches for the general d case in the previous

sections, but we would like to focus on $d = 3$ for two main reasons.

Firstly, in performing the holographic high-frequency analysis, earlier in this chapter, we had to make a rather strong approximation $f \sim 1$, but in three dimensions we can simplify the equation of motion for the gauge field without resorting to this approximation, which allows us to make corrections for the conductivity in $d = 3$ to higher orders in the inverse frequency, $1/\Omega$.

Secondly, we will be comparing the $d = 3$ model with that presented in [15] in which the authors assumed that the scalar field profile behaved as a pure critical power-law $\tilde{\phi}(u) = \phi_1 u^{\Delta}$. The work in this thesis was originally inspired by a desire to find a suitable scalar field profile through dynamical means, rather than using an artificially produced scalar profile. We present the comparisons in this section.

In [15], a simple approach in the holographic model was to assume that the background AdS gravity solution was the same as in eq. (5.2) but that the scalar field, rather than being the result of some explicit matter content, was merely assumed to have the power-law behaviour indicative of a scalar operator at a QCP. The ansatz used was

$$\tilde{\phi}(u) = \phi_1 u^{\Delta} \,, \tag{5.104}$$

where we distinguish the power-law profile scalar field by $\tilde{\phi}$ from the scalar field ϕ introduced in section 5.2. From this ansatz, you can indeed derive results analogous to those found in section 5.3.2. But with some care, we can also unravel higher-order terms in the high frequency expansion for the conductivity. The scalar field $\tilde{\phi}$ introduced in [15] leaves something to be desired in setup (*e.g.,* what kind of matter would produce such a field), in power (*e.g.,* what can we extract using only a single coefficient) and in visualization (*e.g.,* how can we trust the full-frequency response if the scalar field is created with the sole purpose of capturing the high-frequency behaviour?). A self-contained model is also more aesthetically pleasing than an invented ad-hoc probe.

The work done in this section was inspired to circumvent these short-comings and it has provided a basis for this project as a whole. In the remainder of this section, we will refer to the model produced via the power-law scalar profile as the *power-law model* whereas the model that is described in section 4.1 will be referred to as the *Weyl-sourced model*. We use the same simple model introduced in section 5.3.2 and we find the full-frequency conductivity up to first order in a small α_F expansion[7].

[7] An exploration in finding the α_F^2 corrections to the conductivity can be found in appendix E.

Comparisons with power-law scalar profile

Before we get into all of the differences that are present between the power-law model and the Weyl-sourced model, let us look into the special case where they agree exactly. Namely, if the operator $\mathcal{O}$ is marginal. When the scaling dimension of $\mathcal{O}$ is d, then the critical solution to eq. (5.9) is simply a power-law, and the analysis of the power-law model and the Weyl-sourced model will be identical (see appendix D). Figure 5.15 compares the

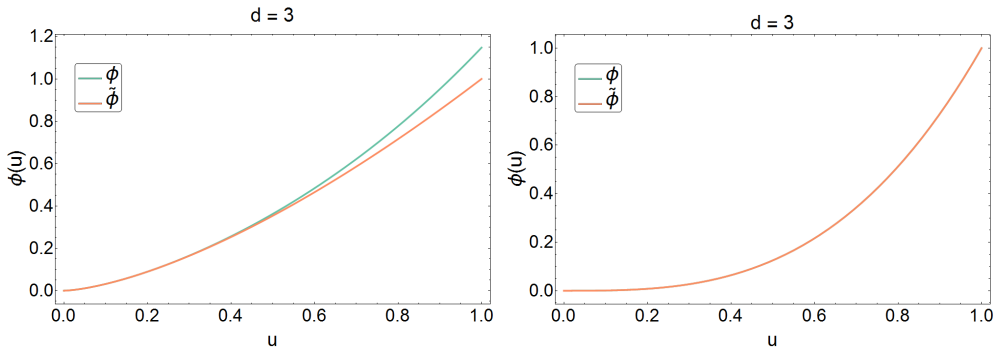

Figure 5.15: The scalar profile for the Weyl-sourced model compared with the power-law model. On the left the scaling dimension is $\Delta = 1.5$, akin to being near to the Wilson-Fisher $N = 2$ fixed point, and on the right the scaling dimension is $\Delta = 3$ representing a marginal operator. (Note that we only see one curve on the right, this is because the profiles are identical.)

scalar field profiles for the power-law model and the Weyl-sourced model. The profiles are fit such that the coefficient of normalizable mode ϕ_1 agrees in both cases. It seems that for relevant scalars that the Weyl-sourced scalar field has a larger amplitude deeper in the bulk than the power-law model while the opposite is true for irrelevant scalars. Of course the curves agree in the marginal case.

From section 2.5.2, the charge diffusion is given by

$$D = \frac{3}{4\pi T}(1 + \alpha_F\,, \phi(1)) \int_0^1 \frac{du}{1 + \alpha_F \phi(u)}\,, \tag{5.105}$$

and the DC conductivity is given by

$$\sigma(0) = \frac{1 + \alpha_F \phi(1)}{g_4^2}\,. \tag{5.106}$$

These quantities are compared for the two models in figure 5.16 where we can that the two curves intersect at precisely $\Delta = 3$. Analytically, the diffusion constant and the DC conductivity for the power-law model are given by

$$\begin{aligned} D &= \frac{3}{4\pi T}(1+\alpha_F\phi_1)\int_0^1 \frac{du}{1+\alpha_F\phi_1 u^\Delta} \\ &\approx \frac{3}{4\pi T}\left(1+\alpha_F\phi_1\frac{\Delta}{\Delta+1}\right) \\ \sigma(0) &= \frac{1+\alpha_F\phi_1}{g_4^2}. \end{aligned} \tag{5.107}$$

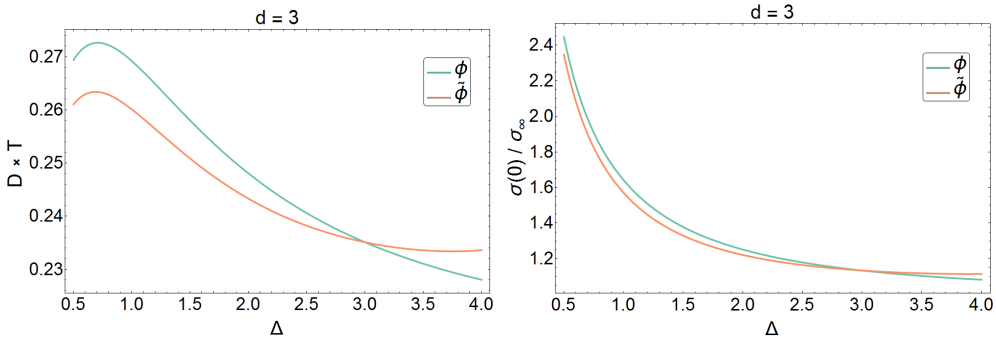

Figure 5.16: The diffusion and DC conductivity compared between the Weyl-sourced model and the power-law model as a functions of scaling dimension.

Clearly, the two models disagree at infra-red frequencies as the power-law model was only designed to measure ultra-violet properties. This highlights a point that was made earlier. That is, the power-law profile may have merit near the boundary of AdS, *i.e.*, in the ultra-violet, but as a probe to low-frequency dynamics it has questionable trustworthiness.

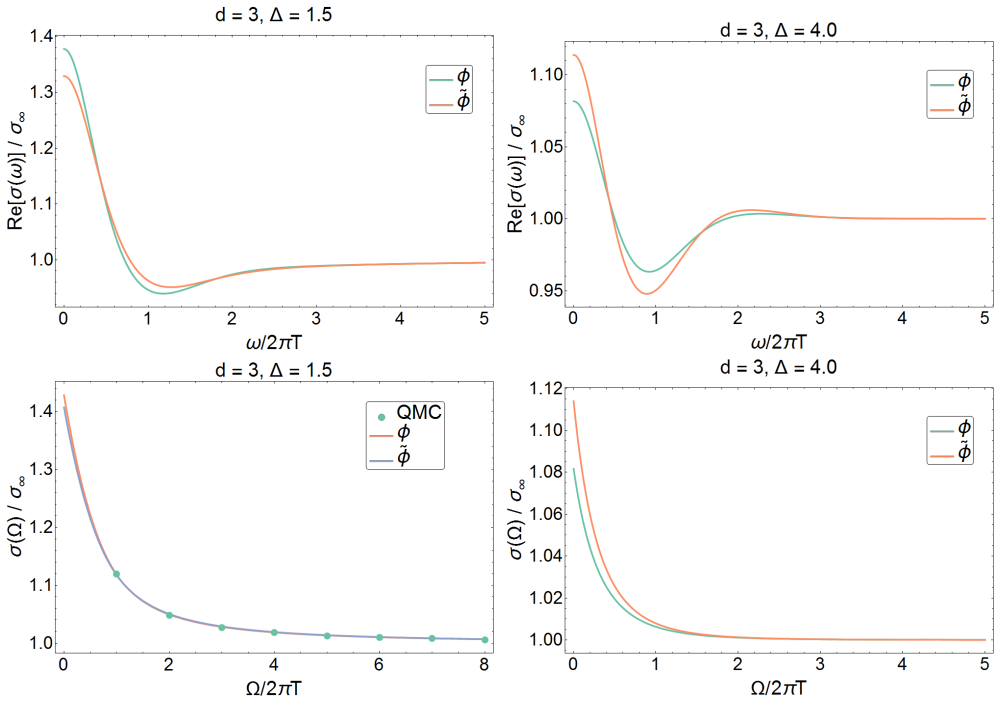

Figure 5.17: The AC conductivity for the Weyl-sourced and power-law models. On the top row, we have real-frequency conductivities for $\Delta = 1.5$ (left) and $\Delta = 4.0$ (right). On the bottom row we have the Euclidean frequency conductivities for $\Delta = 1.5$ (left) and for $\Delta = 4.0$ (right). On the bottom left plot we also include the quantum Monte Carlo data provided by [15] for Matsubara frequencies $\Omega = 2n\pi T$

Figure 5.17 shows the conductivity as calculated in the two models, as well as some Monte Carlo data[8] for the O(2) Wilson-Fisher CFT evaluated near the critical point ($\Delta \sim 1.5$) provided by [15]. The interaction strength that was input into the Euclidean frequency calculations for the conductivity were chosen ad-hoc so to fit the Monte Carlo data. As we can see both models are adequate to reproduce the numerical calculations.

In order to illustrate how the ad-hoc choice of using a power-law scalar field profile can lead to uncertain results we invent a new scalar field profile $\hat{\phi} = \phi_1 u^{\Delta}(1 + 2u^6 - 3u^{12})$. Such a scalar field profile does in fact have the correct asymptotic behaviour to describe a scalar field corresponding to a thermally deformed CFT, but deep in the bulk, this profile

[8]Monte Carlo simulations are able to calculate the conductivity for Euclidean Matsubara frequencies that arise in finite temperature quantum field theory. These frequencies are discrete multiples of $2\pi T$.

disagrees more strongly. For example, by design, the scalar profile $\hat{\phi}$ vanishes at the black hole horizon.

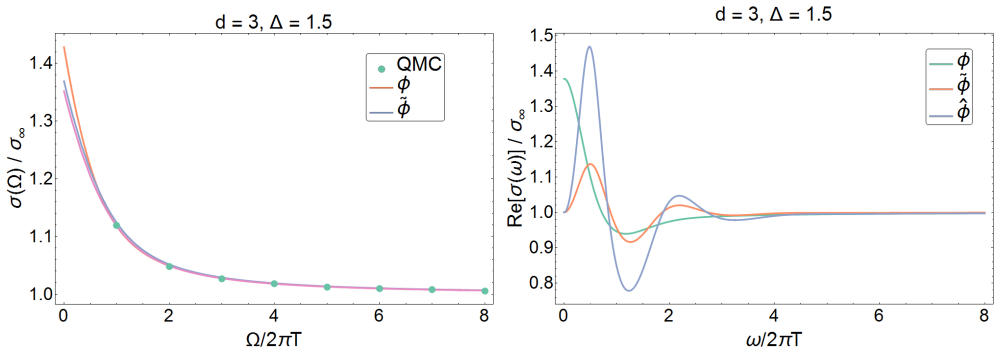

Figure 5.18: The invented scalar field profile $\hat{\phi}(u)$ seems to be a fine choice to reproduce the Monte Carlo results, but when we attempt to probe small real-time frequencies the theories disagree completely.

Figure 5.18 shows that we can reproduce the Monte Carlo data in the Euclidean frequency accurately with $\hat{\phi}$ but that the low-frequency dynamics of the real conductivity are very different from our other models. This fact emphasizes that we need a self-consistent mechanism in order to produce these scalar fields. Otherwise the infra-red physics produced by the holographic model will not likely be representative of any CFT you wish to probe.

High-frequency conductivity

As mentioned in section 5.3.2, when we make the approximation $f \to 1$ in the high-frequency perturbative analysis, the analysis only remains reliable up to the order $1/\Omega^d$. It turns out that in $d = 3$. there is an additional simplification that allows for us to do perturbative analysis without sacrificing any accuracy at this stage of the calculation. What follows, closely resembles the analysis in section 5.3.2 except we explicitly use $d = 3$ and make a change of variables which absorbs the role of the blackening factor f into the variable and we are able to neatly perform the high-frequency analytics [13].

We now compute the conductivity at frequencies much greater than the temperature. Working in Euclidean frequencies, this corresponds to evaluating $\sigma(\omega = i\Omega)$ with $\Omega \gg T$. We will calculate the high frequency asymptotics perturbatively in the dimensionless coupling α_F. Recall that this coupling controls the strength of the ϕF^2 interaction in eq. (5.96),

which determines how the scalar operator in the boundary modifies the conductivity. In this calculation, it is convenient to first change coordinates from u to z, where $dz/du = 1/f(u)$. The boundary, $u = 0$, corresponds to $z = 0$, however, the horizon $u = 1$ is stretched to $z = \infty$. With this coordinate choice, the equation determining the gauge field profile eq. (5.58) becomes

$$\left[\partial_z^2 - w^2\right] A_y = -\frac{\alpha_F \partial_z \phi}{1 + \alpha_F \phi}\, \partial_z A_y \,, \tag{5.108}$$

where we have introduced the rescaled (dimensionless) Euclidean frequency

$$w = \frac{3\Omega}{4\pi T} \,. \tag{5.109}$$

Now in our perturbative approach, we expand the gauge profile as $A_y = A_y^{(0)} + \alpha_F A_y^{(1)} + \alpha_F^2 A_y^{(2)} + \cdots$. Similarly, expanding the gauge equation eq. (5.108), the zeroth order component satisfies $\left[\partial_z^2 - w^2\right] A_y^{(0)} = 0$, and the solution (which is regular or "in-falling" at the horizon) is

$$A_y^{(0)} = e^{-wz} \,. \tag{5.110}$$

We can see the the zero'th order term in the expansion of eq. (5.63) is

$$\sigma = \frac{1}{g_4^2} + O(w^{-\Delta}). \tag{5.111}$$

We denote the asymptotic conductivity as $\sigma_\infty = \frac{1}{g_4^2}$. Next, to first order in α_F, eq. (5.108) yields

$$\left[\partial_z^2 - w^2\right] A_y^{(1)} = w e^{-wz}\, \partial_z \phi \,. \tag{5.112}$$

This equation can be solved with the use of the following Green's function

$$G(z, \tilde{z}) = -\frac{1}{w}\Big(\sinh(wz) e^{-w\tilde{z}}\, \theta(\tilde{z} - z) + \tilde{z} \leftrightarrow z \Big) \,, \tag{5.113}$$

where $[\partial_z^2 - w^2] G(z, \tilde{z}) = \delta(z - \tilde{z})$ and $G(z, \tilde{z})$ vanishes at $z \to 0$ and at $z \to \infty$. The solution to eq. (5.112) is then given by

$$\begin{aligned} A_y^{(1)} &= \int_0^\infty d\tilde{z}\; G(z, \tilde{z})\, w\, e^{-w\tilde{z}}\, \partial_{\tilde{z}} \phi \\ &= -\sinh(wz) \int_0^\infty d\tilde{z} e^{-2w\tilde{z}} \partial_{\tilde{z}} \phi \end{aligned} \tag{5.114}$$

To calculate the conductivity, we must evaluate $\sigma(i\omega)$ from eq. (5.63)

$$\frac{\sigma(iw)}{\sigma_\infty} = -\frac{1}{wg_4^2}\partial_z A_y\big|_{z=0} = 1 + \alpha_F \int_0^\infty dz\, e^{-2wz}\partial_z\phi + O(\alpha_F^2)\,. \tag{5.115}$$

Substituting the power series for $\phi(z) = \sum_\ell c_\ell\, z^{\alpha_\ell}$ into eq. (5.115) yields

$$\frac{\sigma(iw)}{\sigma_\infty} = 1 + \alpha_F \sum_\ell \frac{\Gamma(\alpha_\ell+1)}{(2w)^{\alpha_\ell}}\, c_\ell + O(\alpha_F^2)\,. \tag{5.116}$$

The first few terms in the near boundary expansion (*i.e.,* $u \to 0$) of the scalar field profile, assuming no scalar deformation, of the Weyl-sourced model eq. (5.15) are

$$\phi(u) = \phi_1 u^\Delta + \frac{\phi_1\Delta}{6}u^{\Delta+3} + \frac{12\alpha_C}{(\Delta-6)(3+\Delta)}u^6 + O(u^{\Delta+6})\,. \tag{5.117}$$

Given this result,[9] we obtain the first few terms for the conductivity at $w \gg 1$:

$$\frac{\sigma(iw)}{\sigma_\infty} = 1 + \frac{\phi_1\alpha_F\Gamma(\Delta+1)}{(2w)^\Delta} - \frac{\phi_1\alpha_F\Delta}{12}\frac{\Gamma(\Delta+4)}{(2w)^{\Delta+3}} + \frac{12\alpha_C\alpha_F\Gamma(7)}{(\Delta-6)(\Delta+3)(2w)^6} + O\left(\frac{1}{w^{\Delta+6}}\right). \tag{5.118}$$

Recall that $\phi_1 \propto \alpha_C$ as seen in eq. (5.14), we see explicitly here that in this expansion, the normalized conductivity is only a function of the two model parameters, Δ and $\alpha_C\alpha_F$, as well as the frequency $w = 3\Omega/(4\pi T)$.

One can easily extend the above analysis to second order in the coupling α_F — see appendix E. Here we note that at order 2, the leading correction to the high-frequency expansion eq. (5.118) is proportional to $(\phi_1\alpha_F)^2/w^{2\Delta}$ and therefore the leading $1/w^\Delta$ term above remains unchanged. In addition to higher orders in the perturbation theory in α_F, the background geometry will also pick up corrections at order α_F from the various ways that the scalar field couples to geometry *e.g.,* by $\sqrt{-g}m^2\phi^2$ or by $\sqrt{-g}\phi C^2$. However, the leading term above remains unchanged. That is, we can systematically verify that this method extracts the $1/\omega^\Delta$ term exactly to all orders in back-reaction and perturbation, as was demonstrated in section 5.3.2.

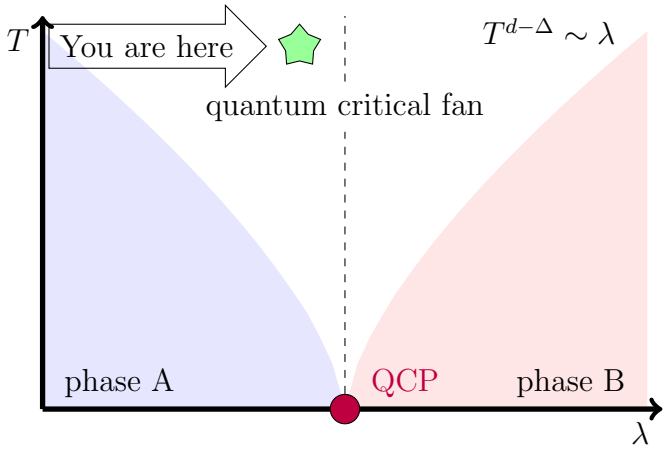

Figure 5.19: We are now probing the finite-temperature theory that is deformed by a scalar operator

5.5 Deforming away from criticality

Up to this point in the thesis, we have only been considering critical boundary theories, albeit at finite temperatures and sometimes with a finite chemical potential. This required the boundary behaviour of the scalar field to be tuned to $\phi(u) \sim u^{\Delta}$. Recall, that in general, the scalar field has an asymptotic expansion eq. (4.16)

$$\phi(u) = \phi_0 u^{d-\Delta} + \phi_1 u^{\Delta} + O(u^d). \tag{5.119}$$

In this section, we focus on high temperatures, then turning on a small coupling to $\mathcal{O}$, *i.e.,* allowing for $\phi_0 \neq 0$ should still leave the theory well within the regime of validity for the holographic model to describe the boundary CFT. We will restrict ourselves to small detuning with respect to temperature $T^{d-\Delta} \gg \lambda$. In terms of the phase diagram, we are in the situation depicted by figure 5.19. To compare with the corpus of the thesis, equation eq. (5.10) remains the general solution to the Weyl-sourced scalar field. In order to maintain regularity at the horizon, the normalizable mode needs to be modified from its value in the critical version

$$\phi_1 = \phi_1|_{\text{crit}} - \phi_0 \frac{\Gamma\left(2 - \frac{2\Delta}{d}\right) \Gamma\left(\frac{\Delta}{d}\right)^2}{\Gamma\left(1 - \frac{\Delta}{d}\right)^2 \Gamma\left(\frac{2\Delta}{d}\right)}. \tag{5.120}$$

Hence, the boundary theory responds linearly to the introduction of a small coupling ϕ_0.

[9] As well as using $u = z\left(1 - \frac{1}{4}z^3 + \frac{3}{28}z^6 + \cdots\right)$.

5.5.1 Scalar response to detuning

Given the new scalar profile, it is straightforward to evaluate the retarded scalar propagator and the dynamical conductivity. The full-frequency response for the scalar two-point function follows the same as in section 5.3.1, except that we have an additional free parameter to vary for the scalar field ϕ, namely ϕ_0. The remainder of the calculations including the boundary conditions remain unchanged.

High-frequency prediction

In this section we verify that this holographic model verifies the high-frequency prediction given in eq. (3.29). Recall the prescription for calculating the retarded scalar propagator in section 5.3.1. The first point where we actually probed the dynamics of the scalar field ϕ was quite late in the game. This occurred just after eq. (5.39) where we needed to know the power series profile for the scalar field. Let us resume this calculation, but instead let us focus on the source term in the scalar field profile, *i.e.*, $\phi(V) = \phi_0 V^{d-\Delta} \left(\frac{4\pi T}{d\Omega}\right)^{d-\Delta}$, and calculate the response of this deformation of the boundary theory. The expression for the first order (in α_F) term for the probe scalar field χ becomes

$$\chi^{(1)} = \frac{\alpha_\psi \phi_0}{\Phi(d,\Delta_0)} \left(\frac{4\pi T}{d\Omega}\right)^{d-\Delta} v^{\Delta_0 - d/2} I_{\Delta_0 - d/2}(v) \int_0^\infty dV\, V^{d-\Delta-1} K_{\Delta_0-d/2}(V)^2\,, \tag{5.121}$$

The integral that appears in the above equation is denoted by $\Psi(d, d-\Delta, \Delta_0)$ defined in eq. (3.15) which allows us to establish

$$\psi^{(1)} = -\frac{\alpha_\psi \phi_0 v^{d/2} I_{\Delta_0-d/2}(v) \Psi(d, d-\Delta, \Delta_0)}{\Phi(d,\Delta_0)} \left(\frac{4\pi T}{d\Omega}\right)^{d-\Delta}\,. \tag{5.122}$$

The important information that we want to extract from this expression is the coefficient to the v^{Δ_0} term (see eq. (5.20)). The coefficient $\psi_1^{(1)}$ is

$$\psi_1^{(1)} = -\alpha_\psi \phi_0 \Psi(d, d-\Delta, \Delta_0) \frac{\Theta(d,\Delta_0)}{\Phi(d,\Delta_0)} \left(\frac{4\pi T}{d\Omega}\right)^{d-\Delta} \tag{5.123}$$

So to first order in a perturbation of α_ψ we have that the probe scalar field expanded about $v = 0$ is

$$\begin{aligned} \psi(v) =& v^{d-\Delta_0} + \frac{\ell_p^{d-1}}{L^{d-1}} \frac{\mathcal{C}_{\mathcal{O}_0\mathcal{O}_0}}{2\Delta_0 - d} v^{\Delta_0} - \frac{\alpha_\psi \phi_0 \Psi(d, d-\Delta, \Delta_0) v^{\Delta_0}}{2^{2\Delta_0 - d - 2}(2\Delta_0 - d)\Gamma(\Delta_0 - d/2)^2} \left(\frac{4\pi T}{d\Omega}\right)^{d-\Delta} \\ & v^{d-\Delta_0} + \frac{\ell_p^{d-1}}{L^{d-1}} \frac{\mathcal{C}_{\mathcal{O}_0\mathcal{O}_0}}{2\Delta_0 - d} v^{\Delta_0} - \frac{\alpha_\psi \ell_p^{d-1} \lambda \Psi(d, d-\Delta, \Delta_0) v^{\Delta_0}}{2^{2\Delta_0 - d - 2} L^{d-1} (2\Delta_0 - d)\Gamma(\Delta_0 - d/2)^2 \Omega^{d-\Delta}} \end{aligned} \tag{5.124}$$

This expression for the scalar field, and recalling that the retarded propagator is given by eq. (5.20), we find that the correction to the scalar two-point function at order $\Omega^{d-\Delta}$ is given by

$$\langle \mathcal{O}_0(\Omega)\mathcal{O}_0(-\Omega)\rangle = \Omega^{2\Delta_0-d}\left(\mathcal{C}_{\mathcal{O}_0\mathcal{O}_0} - \frac{\alpha_\psi \lambda}{\Omega^{d-\Delta}}\frac{\Psi(d,d-\Delta,\Delta_0)}{2^{2\Delta_0-d-2}\Gamma(\Delta_0-d/2)^2}\right). \tag{5.125}$$

So we can give the high-frequency analytic predictions for the scalar two-point function up to corrections of $1/\Omega^d$. The full high-frequency prediction (combining eq. (5.44) and eq. (5.125)) is

$$\begin{aligned}\langle \mathcal{O}_0(\Omega)\mathcal{O}_0(-\Omega)\rangle = \Omega^{2\Delta_0-d}\Bigg(& \mathcal{C}_{\mathcal{O}_0\mathcal{O}_0} \\ & - \frac{\alpha_\psi \lambda}{\Omega^{d-\Delta}}\frac{\Psi(d,d-\Delta,\Delta_0)}{2^{2\Delta_0-d-2}\Gamma(\Delta_0-d/2)^2} \\ & - \frac{\alpha_\psi \langle\mathcal{O}\rangle}{\Omega^{\Delta}}\frac{\Psi(d,\Delta,\Delta_0)}{2^{2\Delta_0-d-2}\Gamma(\Delta_0-d/2)^2(2\Delta-d)}\Bigg).\end{aligned} \tag{5.126}$$

If we would combine the results from the conformal perturbation theory in eqs. (4.40) and eq. (3.29), we get the same thing as our interacting holographic model. Hence we have shown once again that the holographic model is probing the correct dynamics for the CFT observables. Figure 5.20 shows how the response of the conductivity is sensitive to variations of ϕ_0. We note the similarity of the plot for imaginary frequencies to the QMC results in [15, 41]

5.5.2 Conductivity response to detuning

Just as in the previous section, the scalar profile has changed its near-boundary behaviour. Given the new scalar profile, it is straightforward to evaluate the dynamical conductivity. The full-frequency response for the conductivity follows from the same calculation as in section 5.3.2, except that we have the additional free parameter ϕ_0. The remainder of the calculations including the boundary conditions remain unchanged. Figure 5.21 shows how the response of the conductivity is sensitive to variations of ϕ_0. We note the similarity of the plot for imaginary frequencies to the QMC results in [15, 41].

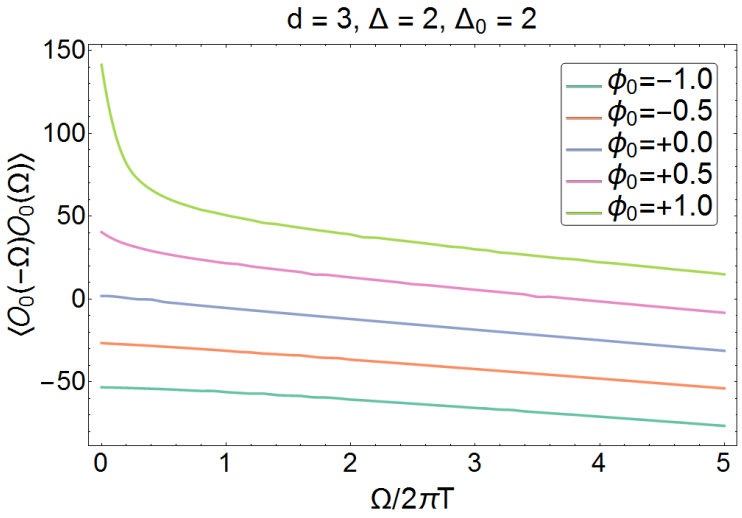

Figure 5.20: The scalar two-point function evaluated at Euclidean frequencies with $\Delta = 2$, $\Delta_0 = 2$, $\alpha_C \alpha_\psi = 1$ and $\phi_1 = 1$ for various strengths of the scalar deformation.

High-frequency predictions

Just as in the previous section, by the time our calculations for the high-frequency conductivity in section 5.3.2 required knowledge of the scalar field profile ϕ most of the work was already finished. Recalling eq. (5.75), but instead of using $\phi(u) \sim u^\Delta$, we will use the non-normalizable part of the scalar field. We insert $\phi(V) = \phi_0 V^{d-\Delta} \left(\frac{4\pi T}{d\Omega}\right)^{d-\Delta}$ into eq. (5.75) and calculate the response in the presence of the scalar deformation. The expression for the first order (in α_F) term for the gauge field A_y becomes

$$\begin{aligned} A_y^{(1)}(v) &= -\frac{\phi_0(d-\Delta)(2-\Delta)}{2\Phi(d,d-1)} v^{d/2-1} I_{d/2-1}(v) \left(\frac{4\pi T}{d\Omega}\right)^{d-\Delta} \int_0^\infty dV\, V^{d-\Delta-1} K_{d/2-1}(V)^2 \\ &= -\frac{\phi_0(d-\Delta)(2-\Delta)}{2\Phi(d,d-1)} v^{d/2-1} I_{d/2-1}(v) \left(\frac{4\pi T}{d\Omega}\right)^{d-\Delta} \Psi(d, d-\Delta, d-1)\,, \end{aligned} \tag{5.127}$$

The important information that we want to extract from this expression is the limit $\frac{A_y'}{u^{d-3}A_y}\Big|_{v\to 0}$ (see eq. (5.54)). So to first order in a perturbation of α_F we have that conductivity is given by

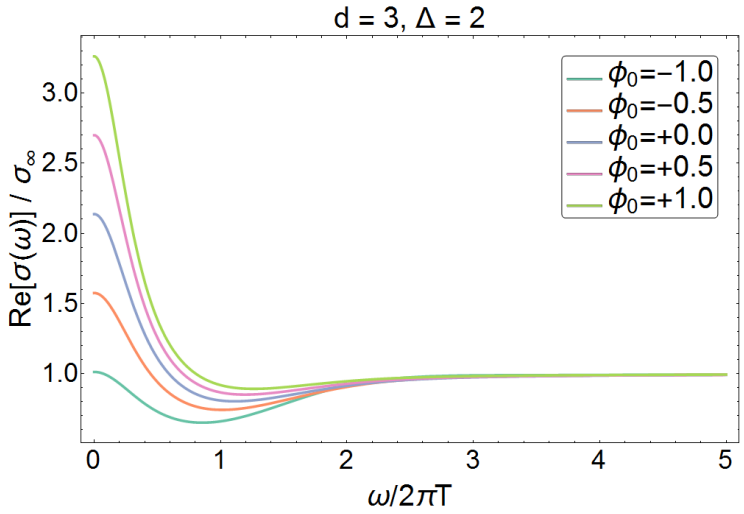

Figure 5.21: The AC conductivity for $\Delta = 2$, $\alpha_C \alpha_F = 1$ and $\phi_1 = 1$ for various strengths of the scalar deformation

$$\begin{aligned}\sigma(\Omega) = \frac{L^{d-3}}{g_d^2}\Omega^{d-3}\Bigg(\sigma_\infty - \\ -\frac{\alpha_F \phi_0 (d-\Delta)(2-\Delta)(d-2)\,\Theta(d,d-1)\Psi(d,d-\Delta,d-1)}{2\,\Phi(d,d-1)}\left(\frac{4\pi T}{d\Omega}\right)^{d-\Delta}\Bigg) \\ = \frac{L^{d-3}}{g_d^2}\Omega^{d-3}\left(\sigma_\infty - \frac{\alpha_F \ell_p^{d-1}\lambda}{L^{d-1}\Omega^{d-\Delta}}\,\frac{\alpha_F \ell_p^{d-1}\lambda (d-\Delta)(2-\Delta)\Psi(d,d-\Delta,d-1)}{2^{d-3}\Gamma(d/2-1)^2}\right).\end{aligned} \tag{5.128}$$

So we can give the high-frequency analytic results for the conductivity up to the Ω^{-d} correction. The full high-frequency prediction (combining eq. (5.77) and eq. (5.129)) up to

Ω^{-d} is

$$= \frac{L^{d-3}}{g_d^2}\Omega^{d-3}\Bigg(\quad \sigma_\infty \\ - \frac{\alpha_F \ell_p^{d-1}\lambda}{L^{d-1}\Omega^{d-\Delta}} \frac{(d-\Delta)(2-\Delta)\Psi(d,d-\Delta,d-1)}{2^{d-3}\Gamma(d/2-1)^2} \\ - \frac{\alpha_F \ell_p^{d-1}\langle\mathcal{O}\rangle}{L^{d-1}\Omega^{\Delta}} \frac{\Delta(\Delta-d+2)\Psi(d,\Delta,d-1)}{(2\Delta-d)2^{d-3}\Gamma(d/2-1)^2}\Bigg) . \tag{5.129}$$

Once again, if we combine the results for high-frequencies coming from conformal perturbation theory eq. (4.52) and eq. (3.36) we get the same results as above from our interacting holographic model.

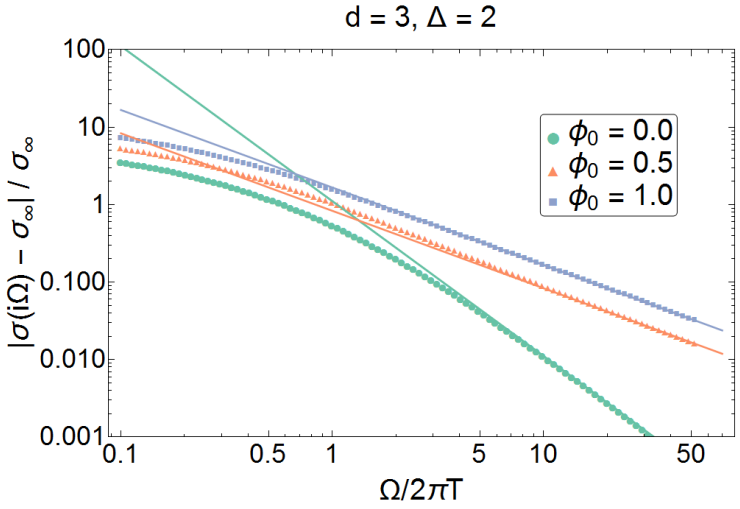

Figure 5.22: A log-log plot of the correction to the Euclidean conductivity prior to and after a scalar deformation. The coupling constant is fixed at $\alpha_C\alpha_F = 1$ and the renormalizable mode is $\phi_1 = 1$ for this calculation.

Figure 5.22 demonstrates how detuning the scalar field completely changes the order to which there are corrections in the linear response. For the example depicted, a scalar operator at criticality corrects the conductivity at high frequencies at the order Ω^{-2}, but the scalar deformation corrects the conductivity at the order Ω^{-1}.

It is a good time to update our $d = 3$ analytic spectral series for the conductivity given in eq. (5.118). The series expansion for the scalar field in a deformed conformal field theory

is

$$\begin{aligned}\phi(u) =&\phi_0 u^{3-\Delta} + \phi_1 u^{\Delta} + \frac{\phi_0(3-\Delta)}{6}u^{6-\Delta} + \frac{\phi_1\Delta}{6}u^{\Delta+3} \\ &+ \frac{12\alpha_C}{(\Delta-6)(\Delta+3)}u^6 + O(u^{\Delta+6}) + O(u^{9-\Delta})\,.\end{aligned} \tag{5.130}$$

By virtue of eq. (5.116) and footnote 9 we get the $d = 3$ correction to the conductivity in a deformed system as

$$\begin{aligned}\left.\frac{\sigma(iw)}{\sigma_\infty}\right|_{d=3} =&1 + \frac{\phi_0\alpha_F\Gamma(4-\Delta)}{(2w)^{3-\Delta}} + \frac{\phi_1\alpha_F\Gamma(\Delta+1)}{(2w)^{\Delta}} - \frac{\phi_0\alpha_F(3-\Delta)\Gamma(7-\Delta)}{12(2w)^{6-\Delta}} \\ &- \frac{\phi_1\alpha_F\Delta\Gamma(\Delta+4)}{12(2w)^{\Delta+3}} + \frac{12\alpha_C\alpha_F\Gamma(7)}{(\Delta-6)(\Delta+3)(2w)^6} + O\left(\frac{1}{w^{\Delta+6}}\right)\,.\end{aligned} \tag{5.131}$$

5.6 Sum rules

One of the main applications of the high-frequency conductivity asymptotics is the emergence of sum rules for transport coefficients. Such conductivity sum rules in near-critical systems were shown recently in [14, 15, 41]. Our goal is to understand when the following equality holds:

$$\int_0^\infty d\omega Re\left(\sigma(\omega) - \frac{\sigma_\infty L^{d-3}}{g_d^2}(i\omega)^{d-3}\right) = 0\,. \tag{5.132}$$

The equation is trivially true at the critical point when the scalar field has no source $\phi_1 = \phi_0 = 0$. The asymptotic expansion of the conductivity eq. (5.129) allows us to understand precisely when eq. (5.132) holds. We require for the first subleading term in the asymptotic expansion of $\sigma(\omega)$ to decay faster than ω^{-1} as $\omega \to \infty$. If this happens to be the case, then we can evaluate the integral via contour integration along the upper half-plane using the analyticity of $\sigma(\omega)$ to verify that there are no poles or branch cuts in this region. From [41] we can conclude that the sum rule is valid when

$$d - 2 < \Delta < 2 \tag{5.133}$$

generally. The left inequality is held whenever the scalar field has a source $\phi_1 \neq 0$ while the right inequality is enforced only when we have tuned away from criticality $\phi_0 \neq 0$. As can be discerned from eq. (5.133), the only dimension which supports the conductivity sum rules in a theory away from criticality is when $d = 3$, otherwise for critical theories sum rules are supported by every dimension. If we look at figure 5.8 we can qualitatively

inspect the cases for when the sum rules fail. In $d = 3$ we observe that for the $\Delta \leq 1$ curves there is an enhancement at small frequencies and the curves don't seem to reach the free conductivity $\sigma_\infty = 1$. In $d = 4$ we see that the curve corresponding to $\Delta = 1$ shifted by a constant from the free conductivity, therefore the integral eq. (5.132) has a finite integrand and thus diverges to infinity.

The analogue of eq. (5.132) for the scalar 2-point function $\langle \mathcal{O}_0 \mathcal{O}_0 \rangle$ is

$$\int_0^\infty d\omega \mathrm{Im} \left(\frac{\langle \mathcal{O}_0(\omega) \mathcal{O}_0(-\omega) \rangle}{\omega} - \mathcal{C}_{\mathcal{O}_0 \mathcal{O}_0} \frac{(i\omega)^{2\Delta_0 - d - 2}}{\omega} \right) = 0. \tag{5.134}$$

From eq. (3.24), we conclude that eq. (5.134) holds as long as

$$2\Delta_0 - d < \Delta < 2d - 2\Delta_0, \tag{5.135}$$

where the upper bound on Δ is only needed if the theory is deformed $\phi_0 \neq 0$.

Chapter 6

Conclusion

In this thesis we determined the universal nature of high-frequency responses to scalar deformations in conformal field theories. We have demonstrated the power that holography has in determining these response functions, not only at the QCP, but at finite temperatures, chemical potentials and when the CFT is being deformed by a relevant scalar operator. Both holography and conformal perturbation theory techniques were able to determine the first two leading corrections to linear response functions, such as the scalar two-point function $\langle \mathcal{O}_0 \mathcal{O}_0 \rangle$ and the conductivity σ, caused by deforming a CFT by a relevant scalar operator. In addition, holography is able to model the qualitative full-frequency dynamics for a wide array of CFTs, making it a powerful tool in studying condensed matter systems. Holographic methods have demonstrated that, for certain large-N matrix theories, that these dynamics are correct even when the ground state is far from a CFT.

The results are directly testable in quantum Monte Carlo simulations [15] and in experiments in cold atomic gases [42], in graphene [43], in cuprates [44] and in heavy fermions [45] to name a few.

6.1 Future directions

A possible avenue that can wield holographic models is when a critical theory is deformed not by a spatially homogeneous coupling λ, but by a random inhomogeneous coupling $\lambda(x)$. We expect the randomness to modify the form for the asymptotic expansions of the response functions. This generalization would be relevant for the recent numerical simulations that yielded the dynamical conductivity across the disorder-tuned superconductor-insulator transition governed by Anderson theory of localization [46].

Another interesting subject is to observe the effects on linear response functions from the back-reaction of the bulk geometry from the new dynamic fields. The holographic model presented in chapter 5 was constructed as a perturbation about the amplitude of the bulk scalar, this is equivalent to a perturbative expansion of the dimensionless coupling α_C. In terms of the boundary theory, this approach is equivalent to requiring that the thermal expectation value of $\mathcal{O}$ is much smaller than the thermal energy density *i.e.,* $|\langle\mathcal{O}\rangle_T|/T^\Delta \ll \langle T_{00}\rangle_T/T^d$. In chapter 5 we only carried out our analysis to linear order in α_C, so the unmodified black hole geometry was sufficient. The next step in extending the perturbative construction would be to include contributions from the scalar action (4.4) in the gravitational equations of motion. The back-reaction of the scalar would produce $O(\alpha_C^2)$ perturbations in the black hole metric and, in turn, the linear response functions would be of the order $O(\alpha_C^2)$. Going beyond a first order perturbation also suggests the possibility of obtaining bounds on the holographic couplings α_C and α_F from the boundary theory, similar to the bounds found in [7, 47]. An initial exploration of higher-order perturbative effects on the conductivity is given for $d = 3$ in appendix E where we find the conductivity to the perturbative order $O(\alpha_C^2)$. In order to find the next perturbative term in the conductivity we are also required to consider a bulk perturbative expansion in α_C.

One could also extend the analysis of the conductivity to include the most general contribution of the $\langle JJT\rangle$ coupling, *i.e.,* holographically one would extend the gauge field action to include an interaction $C_{abcd}F^{ab}F^{cd}$. The new interaction coupling would modify the conductivity by introducing terms proportional to $1/\Omega^d$. This modification is likely to contribute meaningfully when the conformal dimension of $\mathcal{O}$ is near to d.

We barely scratched the surface on the types of models that we can engineer in order to probe a multitude of quantum field theories near quantum critical points. This thesis has demonstrated that even the simplest models are able to provide useful qualitative insight that can point us toward discovering new universal qualities of CFTs.

References

[1] S. Sachdev, *Quantum Phase Transitions*. Cambridge University Press, England, 2 ed., 2011.

[2] M. P. A. Fisher, G. Grinstein and S. M. Girvin, *Presence of quantum diffusion in two dimensions: Universal resistance at the superconductor-insulator transition*, *prl* **64** (Jan., 1990) 587.

[3] K. Damle and S. Sachdev, *Nonzero-temperature transport near quantum critical points*, *Phys. Rev. B* **56** (Oct., 1997) 8714–8733, [arXiv:cond-mat/9705206].

[4] D. T. Son and A. O. Starinets, *Viscosity, Black Holes, and Quantum Field Theory*, *Ann. Rev. Nucl. Part. Sci.* **57** (2007) 95–118, [0704.0240].

[5] R. Baier, P. Romatschke, D. T. Son, A. O. Starinets and M. A. Stephanov, *Relativistic viscous hydrodynamics, conformal invariance, and holography*, *JHEP* **04** (2008) 100, [0712.2451].

[6] C. P. Herzog, P. Kovtun, S. Sachdev and D. T. Son, *Quantum critical transport, duality, and M-theory*, *Phys.Rev.* **D75** (2007) 085020, [hep-th/0701036].

[7] R. C. Myers, S. Sachdev and A. Singh, *Holographic Quantum Critical Transport without Self-Duality*, *Phys. Rev.* **D83** (2011) 066017, [1010.0443].

[8] D. R. Gulotta, C. P. Herzog and M. Kaminski, *Sum Rules from an Extra Dimension*, *JHEP* **1101** (2011) 148, [1010.4806].

[9] W. Witczak-Krempa and S. Sachdev, *Dispersing quasinormal modes in (2+1)-dimensional conformal field theories*, *PRB* **87** (Apr., 2013) 155149, [1302.0847].

[10] W. Witczak-Krempa and S. Sachdev, *The quasi-normal modes of quantum criticality*, *Phys.Rev.* **B86** (2012) 235115, [1210.4166].

[11] K. Chen, L. Liu, Y. Deng, L. Pollet and N. Prokof'ev, *Universal Conductivity in a Two-Dimensional Superfluid-to-Insulator Quantum Critical System*, *Physical Review Letters* **112** (Jan., 2014) 030402, [1309.5635].

[12] W. Witczak-Krempa, *Quantum critical charge response from higher derivatives in holography*, *Phys. Rev. B* **89** (Apr., 2014) 161114, [1312.3334].

[13] R. C. Myers, T. Sierens and W. Witczak-Krempa, *A Holographic Model for Quantum Critical Responses*, *JHEP* **05** (2016) 073, [1602.05599].

[14] A. Lucas, T. Sierens and W. Witczak-Krempa, *Quantum critical response: from conformal perturbation theory to holography*, 1704.05461.

[15] E. Katz, S. Sachdev, E. S. Sorensen and W. Witczak-Krempa, *Conformal field theories at nonzero temperature: Operator product expansions, Monte Carlo, and holography*, *Phys. Rev.* **B90** (2014) 245109, [1409.3841].

[16] J. M. Maldacena, *The Large N limit of superconformal field theories and supergravity*, *Int. J. Theor. Phys.* **38** (1999) 1113–1133, [hep-th/9711200].

[17] E. Witten, *Anti-de Sitter space and holography*, *Adv. Theor. Math. Phys.* **2** (1998) 253–291, [hep-th/9802150].

[18] S. S. Gubser, I. R. Klebanov and A. M. Polyakov, *Gauge theory correlators from noncritical string theory*, *Phys. Lett.* **B428** (1998) 105–114, [hep-th/9802109].

[19] O. Aharony, S. S. Gubser, J. M. Maldacena, H. Ooguri and Y. Oz, *Large N field theories, string theory and gravity*, *Phys. Rept.* **323** (2000) 183–386, [hep-th/9905111].

[20] M. Ammon and J. Erdmenger, *Gauge/gravity duality*. Cambridge Univ. Pr., Cambridge, UK, 2015.

[21] J. M. Maldacena, *The Large N limit of superconformal field theories and supergravity*, *Adv.Theor.Math.Phys.* **2** (1998) 231–252, [hep-th/9711200].

[22] E. D'Hoker and D. Z. Freedman, *Supersymmetric gauge theories and the AdS / CFT correspondence*, in *Strings, Branes and Extra Dimensions: TASI 2001: Proceedings*, pp. 3–158, 2002. hep-th/0201253.

[23] J. L. Petersen, *Introduction to the Maldacena conjecture on AdS / CFT*, *Int. J. Mod. Phys.* **A14** (1999) 3597–3672, [hep-th/9902131].

[24] P. Di Francesco, P. Mathieu and D. Senechal, *Conformal Field Theory*. Graduate Texts in Contemporary Physics. Springer-Verlag, New York, 1997, 10.1007/978-1-4612-2256-9.

[25] J. McGreevy, *Holographic duality with a view toward many-body physics*, *Adv. High Energy Phys.* **2010** (2010) 723105, [0909.0518].

[26] H. Osborn and A. C. Petkou, *Implications of conformal invariance in field theories for general dimensions*, *Annals Phys.* **231** (1994) 311–362, [hep-th/9307010].

[27] P. Kovtun, D. T. Son and A. O. Starinets, *Holography and hydrodynamics: Diffusion on stretched horizons*, *JHEP* **10** (2003) 064, [hep-th/0309213].

[28] K. S. Thorne, R. H. Price and D. A. Macdonald, eds., *BLACK HOLES: THE MEMBRANE PARADIGM*. 1986.

[29] K. Skenderis, *Asymptotically Anti-de Sitter space-times and their sstress energy tensor*, *Int. J. Mod. Phys.* **A16** (2001) 740–749, [hep-th/0010138].

[30] A. Bzowski, P. McFadden and K. Skenderis, *Implications of conformal invariance in momentum space*, *JHEP* **03** (2014) 111, [1304.7760].

[31] E. Barnes, D. Vaman, C. Wu and P. Arnold, *Real-time finite-temperature correlators from AdS/CFT*, *Phys. Rev.* **D82** (2010) 025019, [1004.1179].

[32] D. Chowdhury, S. Raju, S. Sachdev, A. Singh and P. Strack, *Multipoint correlators of conformal field theories: implications for quantum critical transport*, *Phys. Rev.* **B87** (2013) 085138, [1210.5247].

[33] T. Torii, K. Maeda and M. Narita, *Scalar hair on the black hole in asymptotically anti-de Sitter space-time*, *Phys. Rev.* **D64** (2001) 044007.

[34] E. Winstanley, *On the existence of conformally coupled scalar field hair for black holes in (anti-)de Sitter space*, *Found. Phys.* **33** (2003) 111–143, [gr-qc/0205092].

[35] A. Buchel, S. Deakin, P. Kerner and J. T. Liu, *Thermodynamics of the N=2* strongly coupled plasma*, *Nucl. Phys.* **B784** (2007) 72–102, [hep-th/0701142].

[36] A. Buchel, L. Lehner, R. C. Myers and A. van Niekerk, *Quantum quenches of holographic plasmas*, *JHEP* **05** (2013) 067, [1302.2924].

[37] A. Ritz and J. Ward, *Weyl corrections to holographic conductivity*, *Phys. Rev.* **D79** (2009) 066003, [0811.4195].

[38] A. M. García-García and A. Romero-Bermúdez, *Conductivity and entanglement entropy of high dimensional holographic superconductors*, *JHEP* **09** (2015) 033, [1502.03616].

[39] G. T. Horowitz and M. M. Roberts, *Holographic Superconductors with Various Condensates*, *Phys. Rev.* **D78** (2008) 126008, [0810.1077].

[40] S. A. Hartnoll, *Lectures on holographic methods for condensed matter physics*, *Class. Quant. Grav.* **26** (2009) 224002, [0903.3246].

[41] A. Lucas, S. Gazit, D. Podolsky and W. Witczak-Krempa, *Dynamical response near quantum critical points*, 1608.02586.

[42] A. Tokuno and T. Giamarchi, *Spectroscopy for Cold Atom Gases in Periodically Phase-Modulated Optical Lattices*, *Phys. Rev. Lett.* **106** (May, 2011) 205301, [1101.2469].

[43] A. Lucas, *Conductivity of a strange metal: from holography to memory functions*, *JHEP* **03** (2015) 071, [1501.05656].

[44] J. C. Zhang, E. M. Levenson-Falk, B. J. Ramshaw, D. A. Bonn, R. Liang, W. N. Hardy et al., *Anomalous Thermal Diffusivity in Underdoped* $YBa_2Cu_3O_{6+x}$, 1610.05845.

[45] M. Punk, A. Allais and S. Sachdev, *A quantum dimer model for the pseudogap metal*, *Proc. Nat. Acad. Sci.* **112** (2015) 9552, [1501.00978].

[46] M. Swanson, Y. L. Loh, M. Randeria and N. Trivedi, *Dynamical Conductivity across the Disorder-Tuned Superconductor-Insulator Transition*, *Physical Review X* **4** (Apr., 2014) 021007, [1310.1073].

[47] M. Brigante, H. Liu, R. C. Myers, S. Shenker and S. Yaida, *The Viscosity Bound and Causality Violation*, *Phys. Rev. Lett.* **100** (2008) 191601, [0802.3318].

[48] H. Casini, D. A. Galante and R. C. Myers, *Comments on Jacobson's "Entanglement equilibrium and the Einstein equation"*, *JHEP* **03** (2016) 194, [1601.00528].

[49] R. Emparan, C. V. Johnson and R. C. Myers, *Surface terms as counterterms in the AdS / CFT correspondence*, *Phys. Rev.* **D60** (1999) 104001, [hep-th/9903238].

[50] K. Skenderis, *Lecture notes on holographic renormalization*, *Class. Quant. Grav.* **19** (2002) 5849–5876, [hep-th/0209067].

[51] V. Balasubramanian, P. Kraus, A. E. Lawrence and S. P. Trivedi, *Holographic probes of anti-de Sitter space-times*, *Phys. Rev.* **D59** (1999) 104021, [hep-th/9808017].

[52] P. Kovtun, *Lectures on hydrodynamic fluctuations in relativistic theories*, *Journal of Physics A Mathematical General* **45** (Nov., 2012) 3001, [1205.5040].

[53] N. Iqbal and H. Liu, *Universality of the hydrodynamic limit in AdS/CFT and the membrane paradigm*, *Phys. Rev.* **D79** (2009) 025023, [0809.3808].

[54] J. Mas, J. P. Shock and J. Tarrio, *A Note on conductivity and charge diffusion in holographic flavour systems*, *JHEP* **01** (2009) 025, [0811.1750].

[55] H. Casini, D. A. Galante and R. C. Myers, *Comments on Jacobson's "Entanglement equilibrium and the Einstein equation"*, 1601.00528.

[56] A. Bzowski, P. McFadden and K. Skenderis, *Implications of conformal invariance in momentum space*, *Journal of High Energy Physics* **3** (Mar., 2014) 111, [1304.7760].

Appendix A

Holographic renormalization of scalar field

In this appendix we will explicitly derive the correct manner to use holography to calculate the scalar one-point and two-point functions. This appendix combines ideas from [20, 25, 32, 36, 48–51]. Recall that the AdS/CFT dictionary (see eq. (2.18)) gives us a prescription for calculating CFT correlation functions using holography. The scalar one-point and two-point functions are no different, but they suffer from a subtle challenge. That is, the free field action diverges on the boundary. The prescription: to add local counterterms in order for the action to evaluate to a finite value. Let us see how this is done in practice. Let's begin with a scalar field in asymptotically AdS spacetime with the near-boundary limit

$$\phi(z) = \phi_0 z^{d-\Delta} + \phi_1 z^{\Delta} + O(z^d)\,. \tag{A.1}$$

The action governing the equations of motion for this massive scalar is

$$S_{\text{free}} = -\frac{1}{2\ell^{d-1}} \int d^{d+1}x\sqrt{-g}\left((\nabla_a\phi)^2 + m^2\phi^2\right) \tag{A.2}$$

which we can break up into a vanishing bulk term and a boundary term where we introduce a near-boundary cutoff ϵ in order to understand the divergences.

$$S_{\text{free}} = -\frac{1}{2\ell^{d-1}} \int d^{d+1}x\sqrt{-g}(-\nabla^2 + m^2)\phi + \frac{1}{2\ell^{d-1}} \int_{z=\epsilon} d^d y\sqrt{-\gamma}g^{zz}\phi\partial_z\phi \tag{A.3}$$

The bulk action evaluates to zero due to the equations of motion for ϕ but the boundary term has a UV divergence. To see this lets substitute the near-asymptotic behaviour (A.1)

into the action

$$S_{\text{free}} = \frac{L^{d-1}}{2\ell_p^{d-1}} \int d^d y \left((d-\Delta)\epsilon^{d-2\Delta}\phi_0^2 + d\phi_0\phi_1 + \epsilon^{2\Delta-d}\Delta\phi_1^2 \right). \tag{A.4}$$

As we can see, the first term appearing in (A.4) is divergent if $\Delta > d/2$ which will be our assumption. This divergence can be renormalized by adding a local holographic counter-term

$$S_{\text{ct}} = -\frac{1}{2L\ell_p^{d-1}} \int d^d y \sqrt{-\gamma}\,(d-\Delta)\phi(x,z)^2 \tag{A.5}$$

so that when we evaluate the renormalized action $S_{\text{ren}} = S_{\text{free}} + S_{\text{ct}}$ we find that the action is finite, and when we take the limit $\epsilon \to 0$ we get

$$S_{\text{ren}} = \frac{L^{d-1}}{2\ell_p^{d-1}} \int d^d y (2\Delta - d)\phi_0\phi_1\,. \tag{A.6}$$

Now, acquiring the scalar one-point and two-point functions simply requires taking the variational derivative of eq. (A.6) with respect to the source $\phi_0(k)$

$$\langle \mathcal{O}(k) \rangle = \left(\frac{L}{\ell_p}\right)^{d-1} (2\Delta - d)\phi_1(k), \tag{A.7a}$$

$$\langle \mathcal{O}(-k)\mathcal{O}(k) \rangle = \left(\frac{L}{\ell_p}\right)^{d-1} (2\Delta - d)\frac{\phi_1(k)}{\phi_0(k)}. \tag{A.7b}$$

Taking care to include the factor of 2 that originates from taking the variation with respect to ϕ^2. The form for the two-point function might seem a bit mysterious, but following [48] we can see it to be the case if we introduce a small dynamic variable ζ such that $\phi_0 \to \zeta\phi_0$ and $\phi_1 \to \zeta\phi_0$ where ϕ_1 and ϕ_0 are simply constants, *i.e.*, ϕ_0 and ϕ_1 are proportionality constants for the source ($\zeta\phi_0$) and the response ($\zeta\phi_1$) and ζ encodes the dynamic information for the source. Then by taking the variational derivative with respect to $\zeta\phi_0$ we get the desired result.

Appendix B

Maxwell diffusion in the membrane paradigm

Work in this appendix uses some methods and arguments from [4, 7, 27, 37, 52]. The membrane paradigm has been used by many authors [4, 7, 27, 37, 52–54] to probe gravitational dynamics near black holes. In the context of the AdS/CFT we can use the membrane paradigm prescription in order to probe infrared dynamics for the dual conformal field theory. In the context of this thesis, we will use the membrane paradigm in order to demonstrate that the AdS Maxwell field behaves as a dissipative fluid near the black hole horizon. We can calculate the diffusion constant using Fick's law the DC conductivity using Ohm's law for the dual theory[1]. Before we dive in, let us expand an AdS metric near a black hole horizon. We will be assuming that we have a diagonal metric where the black hole horizon lies on a surface of constant $z = z_h$. The black hole metric is then approximately

$$ds^2 = \frac{L^2}{z_h^2}\left(-\gamma_t(z-z_h)dt^2 + \frac{dz^2}{\gamma_z(z-z_h)} + \eta_{ij}dx^i dx^j\right) . \tag{B.1}$$

The Maxwell gauge equations of motion are given by[2]

$$0 = \nabla_a \left(X F^{a\mu}\right) . \tag{B.2}$$

[1] Care must be made when making claims such as these, as often holographic models are made by matching near-asymptotic behaviour of fields and as such the dual theories will need to have a strong duality to be able to make claims on infrared quantities.

[2] these are the equations of motion for a Maxwell field coupled to a scalar field as seen in chapter 5

The equations of motion (B.2) naturally defines a conserved current

$$j^\mu = \sqrt{-g} X F^{\mu z}\big|_{z_m} \tag{B.3}$$

such that $\partial_\mu j^\mu = 0$. We have defined a membrane radius z_m that is very close to the black hole horizon $z_m - z_h \ll z_h$. We will show in this appendix that the current j^μ obeys Fick's law

$$j^x = -D\partial_x j^t \tag{B.4}$$

near the black hole horizon. The time-component and transverse components for the conserved current j are related to the Maxwell field by

$$\begin{aligned} j^t =& \sqrt{-g} g^{tt} g^{zz} X F_{tz} \\ j^x =& \sqrt{-g} g^{xx} g^{zz} X F_{xz} \,. \end{aligned} \tag{B.5}$$

Since the equations of motion have no dependence on spatial directions, we will assume that the Maxwell field has a plane-wave solution $A_\mu = A_\mu(t,z)e^{iqx}$. In order to prove Fick's law, we need to relate F_{xz} to F_{xt} so that we can use the solution for the time-component of the Maxwell field A_0 to find the diffusion constant. The in-falling wave boundary conditions ($A_\mu \sim (z-z_h)^{-\frac{i\omega}{\sqrt{\gamma_z \gamma_t}}} A_\mu^{\text{reg}}$) govern the ratio near the horizon

$$\frac{F_{zx}}{F_{tx}} = \frac{1}{\sqrt{\gamma_t \gamma_z}(z - z_h)}. \tag{B.6}$$

Before moving forward, it is useful to solve for the radial part of the time-component of the gauge field. The t-component equation of motion for the maxwell field in radial gauge $A_z = 0$, setting $\omega = q = 0$ is

$$0 = \partial_z \left(\sqrt{-g} X g^{zz} g^{tt} \partial_z A_t \right) \tag{B.7}$$

which we can surmise the general solution to A_t is

$$A_t = C(t) e^{iqx} \int_0^z \frac{dz g_{tt} g_{zz}}{\sqrt{-g} X} \,, \tag{B.8}$$

where $C(t)$ is an arbitrary function of time. We will now prove Fick's law, but first we will explain in what limit we are working in. We will be looking at spatial momenta that are much smaller than the Hawking temperature of the black hole, and also the time-dependent frequency is much smaller than the spatial momentum $\omega/q \sim q/T \ll 1$. The foliated membrane must be close enough to the horizon

$$\frac{z_m - z_h}{z_h} \ll \frac{q^2}{T^2}, \tag{B.9}$$

but it is also convenient for the black hole membrane to not be exponentially close to the black hole horizon

$$\log \frac{z_h}{z_m - z_h} \ll \frac{T^2}{q^2}, \tag{B.10}$$

both of these limits are simultaneously attainable. The reason why we do not want the membrane to be too close to the black hole horizon is because we want $|\partial_t A_x| \ll |\partial_x A_t|$ to simplify the derivation. The z component to the Maxwell equation of motion near the black hole horizon gives

$$iq(z - z_h)\gamma_t F_{zx} + \partial_t F_{tz} = 0 \tag{B.11}$$

thus, if we assume that the Maxwell gauge has a characteristic timescale $\partial_t \sim i\omega$ then

$$\partial_z A_x = \frac{\omega}{q}\frac{g_{xx}}{g_{tt}}\partial_z A_t. \tag{B.12}$$

We can use the solution for A_t eq. (B.8) to solve for A_x on the membrane near the black hole horizon. Doing so yields

$$A_x = \frac{C(t)\omega e^{iqx}}{q}\int \frac{dz g_{xx} g_{zz}}{\sqrt{-g}X} \sim \frac{\omega}{q}\log\left(\frac{z_h}{z_m - z_h}\right). \tag{B.13}$$

So we have that

$$\frac{|\partial_t A_x|}{|\partial_x A_t|} \sim \frac{\omega^2}{q^2}\log\left(\frac{z_h}{z_m - z_h}\right) \ll 1 \tag{B.14}$$

where the limit is due to eq. (B.10). We are now ready to prove Fick's law. Let us look first at j^x. We have due to eqs. (B.6) and (B.14)

$$j^x = iq\sqrt{-g}g^{xx}g^{xx}X\sqrt{\frac{\gamma_z}{\gamma_t}}A_t. \tag{B.15}$$

Similarly, $\partial_x j^t$ is given by

$$\partial_x j^t = iq\sqrt{-g}g^{xx}g^{xx}X\frac{\gamma_z}{\gamma_t}\partial_z A_t, \tag{B.16}$$

where we have made the simplification $g^{tt}g^{zz} = -g^{xx}g^{xx}\gamma_z/\gamma_t$. So Fick's law $j^x = -D\partial_x j^t$ is observed on the membrane with dispersion constant

$$D = \sqrt{-g^{xx}g^{xx}g_{tt}g_{zz}}\frac{A_t}{\partial_z A_t} \tag{B.17}$$

which we can evaluate using eq. (B.8)

$$D = -\sqrt{-g}\sqrt{-g^{xx}g^{xx}g^{tt}g^{zz}}X\Big|_{z=z_m}\int_0^{z_m}\frac{dz g_{tt}g_{zz}}{\sqrt{-g}X}. \tag{B.18}$$

We can also use Ohm's law $j^x = \sigma E^x$ to get the DC conductivity

$$\sigma_0 = \frac{1}{g_d^2}\sqrt{-g}\sqrt{-g^{xx}g^{xx}g^{tt}g^{zz}X}\Big|_{z=z_m}. \tag{B.19}$$

Appendix C

Reissner-Nordström supplementals

C.1 A detailed derivation for the linearized Einstein-Maxwell equation

In this appendix we will derive the linearized Einstein-Maxwell equations. The result is given in [40], and is derived in detail here.

C.1.1 Useful Riemannian geometry relations

In order to linearize the Einstein-Maxwell eqs. (5.81) it is useful to know how the Riemannian curvature tensors vary when perturbed. Here we provide a useful reference guide to these variations.

$$\delta g^{\mu\nu} = -g^{\rho\mu} g^{\sigma\nu} \delta g_{\rho\sigma} \tag{C.1}$$

$$\begin{aligned} \delta\Gamma^{\rho}_{\mu\nu} =& \frac{1}{2} g^{\rho\sigma} (\nabla_\nu \delta g_{\mu\sigma} + \nabla_\mu \delta g_{\sigma\nu} - \nabla_\sigma \delta g_{\mu\nu}) \\ =& \frac{1}{2} g^{\rho\sigma} (\partial_\nu \delta g_{\mu\sigma} + \partial_\mu \delta g_{\sigma\nu} - \partial_\sigma \delta g_{\mu\nu} - 2\Gamma^{\lambda}_{\mu\nu} \delta g_{\lambda\sigma}) \end{aligned} \tag{C.2}$$

$$\begin{aligned} \delta R_{\mu\nu} =& \ \nabla_\rho (\delta\Gamma^{\rho}_{\nu\mu}) - \nabla_\nu (\delta\Gamma^{\rho}_{\rho\mu}) \\ =& \ \partial_\rho (\delta\Gamma^{\rho}_{\nu\mu}) - \partial_\nu (\delta\Gamma^{\rho}_{\rho\mu}) + \Gamma^{\rho}_{\rho\alpha} \delta\Gamma^{\alpha}_{\mu\nu} \\ & - \Gamma^{\alpha}_{\mu\rho} \delta^{\rho}_{\alpha\nu} - \Gamma^{\rho}_{\alpha\nu} - \Gamma^{\alpha}_{\nu\mu} \delta\Gamma^{\rho}_{\rho\alpha} \end{aligned} \tag{C.3}$$

$$\begin{aligned}\delta R =& R_{\mu\nu}\delta g^{\mu\nu} + \nabla_\sigma(g^{\mu\nu}\delta\Gamma^\sigma_{\nu\mu} - g^{\mu\sigma}\delta\Gamma^\rho_{\rho\mu}) \\ =& - R_{\rho\sigma}g^{\rho\lambda}g^{\sigma\tau}\delta g_{\lambda\tau} \\ &+ g^{\lambda\tau}(\partial_\sigma\delta\Gamma^\sigma_{\lambda\tau} + \Gamma^\sigma_{\alpha\sigma}\delta\Gamma^\alpha_{\lambda\tau} - \Gamma^\alpha_{\sigma\lambda}\delta\Gamma^\sigma_{\alpha\tau} - \Gamma^\alpha_{\sigma\tau}\delta\Gamma^\sigma_{\lambda\alpha}) \\ &- g^{\lambda\sigma}(\partial_\sigma\delta\Gamma^\rho_{\rho\sigma} + \Gamma^\rho_{\sigma\alpha}\delta\Gamma^\alpha_{\rho\lambda} - \Gamma^\alpha_{\sigma\rho}\delta\Gamma^\rho_{\alpha\lambda} - \Gamma^\alpha_{\sigma\lambda}\delta\Gamma^\rho_{\rho\alpha})\end{aligned} \tag{C.4}$$

$$\delta(g_{\mu\nu}R) = Rg_{\mu\nu} + g_{\mu\nu}(R_{\lambda\tau}\delta g^{\lambda\tau} + \nabla_\sigma(g^{\lambda\tau}\delta\Gamma^\sigma_{\tau\lambda} - g^{\lambda\sigma}\delta\Gamma^\rho_{\rho\lambda})) \tag{C.5}$$

C.1.2 Some properties of the background solution

The background solution has some symmetries that we will be exploiting in order to derive the linear Einstein-Maxwell equations. The only Christoffel symbols that are non-trivial have as indices, a u component and any pair of coordinates. This property is because the metric components are diagonal and depend only on u.

$$\begin{aligned}\Gamma^{x_i}_{ux_i} =& -\frac{1}{u} \\ \Gamma^u_{x_ix_i} =& \frac{r_0^2 f(u)}{uL^4} \\ \Gamma^u_{tt} =& \frac{r_0^2 f(u)(uf'(u) - 2f(u))}{2uL^4} \\ \Gamma^u_{uu} =& -\frac{f'(u)}{2f(u)} - \frac{1}{u} \\ \Gamma^t_{ut} =& \frac{f'(u)}{2f(u)} - \frac{1}{u}\end{aligned} \tag{C.6}$$

As for the Ricci tensor, the property that will be exploited the most is the fact that the Ricci tensor is diagonal.

C.1.3 Linearized Einstein-Maxwell equations

In order to derive the linearized Einstein-Maxwell equations we will be perturbing the fields $A_x \to A_{x(0)} + \delta A_x$ and $g_{xt} \to \cancel{g_{xt(0)}} + \delta g_{xt}$ about the background solution eq. (5.82) and substituting them into eq. (5.81). We will be left with two coupled ordinary differential equations that will decouple nicely. In terms of the conductivity, the only term of interest is frequency dependent transverse perturbations of the gauge field $\delta A_x = \delta A_x(u)\int \frac{dt}{2\pi}e^{i\omega t}$. We begin by linearizing the x-component of the Maxwell equation $\nabla_\mu(XF^\mu{}_x)$. Firstly, we will find all of the terms that are linear in δA_x, *i.e.* we will calculate $\frac{\delta}{\delta A_x}\nabla_\mu(XF^\mu{}_x)$. Before

we begin, note that the only variations of the maxwell field F that will contribute are $\delta F_{(ux)}$ and $\delta F_{(tx)}$.

$$
\begin{aligned}
0 =&\delta\nabla_\mu(XF^\mu{}_x) && \text{(C.7)}\\
=&\delta\left(g^{\mu\nu}\left(\partial_\mu X F_{\nu x}+X\partial_\mu F_{\nu x}-X\Gamma^\sigma_{\mu x}F_{\nu\sigma}-\Gamma^\sigma_{\nu\mu}F_{\sigma x}\right)\right) && \text{(C.8)}\\
=&g^{uu}\partial_u X\delta F_{ux}+Xg^{uu}\partial_u\delta F_{ux}+Xg^{tt}\partial_t\delta F_{tx} && \text{(C.9)}\\
&-g^{\mu\nu}X\Gamma^\sigma_{\mu x}\delta F_{\nu\sigma}-Xg^{\mu\nu}\Gamma^u_{\nu\mu}\delta F_{ux}\\
=&g^{uu}X'\delta A'_x+Xg^{uu}\delta A''_x+Xg^{tt}(-\omega^2)\delta A_x && \text{(C.10)}\\
&-Xg^{uu}\Gamma^x_{ux}\delta A'_x+Xg^{xx}\Gamma^u_{xx}\delta A'_x-Xg^{\mu\nu}\Gamma^u_{\mu\nu}\delta A'_x\\
=&g^{uu}X\delta A''_x-\omega^2Xg^{tt}\delta A_x && \text{(C.11)}\\
&+\left(g^{uu}X'-Xg^{uu}\Gamma^x_{ux}+Xg^{xx}\Gamma^u_{xx}+\frac{1}{\sqrt{-g}}\partial_u(\sqrt{-g}g^{uu})\right)\delta A'_x\\
=&Xg^{uu}\delta A''_x+Xg^{uu}\left(\frac{X'}{X}+\frac{f'}{f}-\frac{d-3}{u}\right)\delta A'_x-\omega^2Xg^{tt}\delta A_x && \text{(C.12)}
\end{aligned}
$$

This equation is (not surprisingly) the same equation of motion for a gauge field perturbation in a non-charged background ($\xi = 0$) (5.58) except for the alteration of the blackening factor f. Let us now find the variation with respect to the metric perturbation $\frac{\delta}{\delta g_{xt}}\nabla_\mu(XF^\mu{}_x)$. Note that the only components of the Maxwell gauge field F which are non-trivial are $F_{ut} = A'_t$.

$$
\begin{aligned}
0 =&\delta g^{\mu\nu}\nabla_\mu(XF_{\nu x}) && \text{(C.13)}\\
=&\delta\left(g^{\mu\nu}\left(\cancel{\partial_\mu XF_{\nu x}}+\cancel{X\partial_\mu F_{\nu x}}-X\Gamma^\sigma_{\mu x}F_{\nu\sigma}-\cancel{X\Gamma^\sigma_{\nu\mu}F_{\sigma x}}\right)\right) && \text{(C.14)}\\
=&-\delta g^{\mu\nu}X\Gamma^\sigma_{\mu x}F_{\nu\sigma}-g^{\mu\nu}X\delta\Gamma^\sigma_{\mu x}F_{\nu\sigma} && \text{(C.15)}\\
=&-\delta g^{xt}X\Gamma^u_{xx}F_{tu}-Xg^{\mu\nu}F_{\nu\sigma}\left(\tfrac{1}{2}g^{\sigma\rho}(\partial_\mu\delta g_{\rho x}-\partial_\rho\delta g_{\mu x}-2\Gamma^\lambda_{\mu x}\delta g_{\lambda\rho})\right) && \text{(C.16)}\\
=&-Xg^{xx}g^{tt}\Gamma^u_{xx}A'_t\delta g_{xt} && \text{(C.17)}\\
&-\tfrac{1}{2}Xg^{uu}F_{ut}g^{tt}\delta g'_{tx}+\tfrac{1}{2}Xg^{tt}F_{tu}g^{uu}\delta g'_{tx}+Xg^{uu}F_{ut}g^{tt}\Gamma^x_{ux}\delta g_{xt}\\
=&-Xg^{xx}g^{tt}\Gamma^u_{xx}A'_t\delta g_{xt}-Xg^{uu}g^{tt}A'_t\delta g'_{tx}+Xg^{uu}g^{tt}\Gamma^x_{ux}A'_t\delta g_{xt} && \text{(C.18)}\\
=&Xg^{tt}A'_t(g^{uu}\Gamma^x_{ux}-g^{xx}\Gamma^u_{xx})\delta g_{xt}-Xg^{uu}g^{tt}A'_t\delta g'_{tx} && \text{(C.19)}\\
=&-Xg^{uu}g^{tt}A'_t(\tfrac{2}{u}\delta g_{xt}+\delta g'_{xt}) && \text{(C.20)}
\end{aligned}
$$

So the variation of the Maxwell equation gives us

$$
0=\delta A''_x+\left(\frac{X'}{X}+\frac{f'}{f}-\frac{d-3}{u}\right)\delta A'_x-\omega^2\frac{g^{tt}}{g^{uu}}\delta A_x-g^{tt}A'_t(\tfrac{2}{u}\delta g_{xt}+\delta g'_{xt}). \qquad \text{(C.21)}
$$

This is a coupled differential equation in δA_x and δg_{xt}, we need to find another coupled equation with these two variations. The (u, x) component of the Einstein equations gives a nice differential equation. Before we get into the derivation, we should discuss a few properties of the variation of the Christoffel symbols and how they relate to the variation of δg_{xt}. The variation of the Christoffel symbols are given by eq. (C.2), note that the variation of the Christoffel symbols are only non-trivial if they contain at least one t index and one x index, whereas conversely, the background Christoffel symbols do not mix the transverse direction x with time t. Also worth noting is that the variation of the Christoffel symbol $\delta\Gamma^t_{tx} = 0$ is trivial. The variation of the left hand side of the Einstein eqs. (5.81) with respect to δg_{xt} gives

$$\begin{aligned}
\delta G_{ux} =& \delta\left(R_{ux} - \frac{1}{2}Rg_{ux} + \Lambda g_{ux}\right) && \text{(C.22)}\\
=& \delta R_{ux} - \frac{1}{2}(\cancel{\delta R g_{ux}} + \cancel{R\delta g_{ux}}) + \cancel{\Lambda\delta g_{ux}} && \text{(C.23)}\\
=& \partial_\rho\delta\Gamma^\rho_{ux} - \cancel{\partial_x\delta\Gamma^\rho_{\rho u}} + \cancel{\Gamma^\rho_{\rho a}\delta\Gamma^u_{ux}} - \Gamma^\alpha_{u\rho}\delta\Gamma^\rho_{\alpha x} - \cancel{\Gamma^\rho_{\alpha x}\delta\Gamma^\alpha_{\rho u}} - \Gamma^x_{ux}\delta\Gamma^\rho_{\rho x} && \text{(C.24)}\\
=& \partial_t\delta\Gamma^t_{ux} - \cancel{\Gamma^t_{ut}\delta\Gamma^t_{tx}} - \cancel{\Gamma^x_{ux}\delta\Gamma^t_{tx}} && \text{(C.25)}\\
=& \partial_t\left(\frac{1}{2}g^{tt}(\delta g'_{xt} - 2\Gamma^x_{ux}\delta g_{xt})\right) && \text{(C.26)}\\
=& \partial_t\left(\frac{1}{2}g^{tt}\left(\delta g'_{xt} + \frac{2}{u}\delta g_{xt}\right)\right) . && \text{(C.27)}
\end{aligned}$$

We recognize this equation as having very similar dependence on A_t as the linearized Maxwell equation. The right hand side of the Einstein eqs. (5.81) do not depend on δg_{xt}, so let us take the variation with respect to δA_x

$$\begin{aligned}
\delta\left(\frac{\ell_p^{d-1}}{g_d^2}T_{ux}\right) =& \delta\left(\frac{\ell_p^{d-1}}{g_d^2}\left(F_{u\rho}F_{x\sigma}g^{\alpha\beta} - \frac{1}{4}\cancel{g_{ux}F_{ab}F^{ab}}\right)\right) && \text{(C.28)}\\
=& \frac{\ell_p^{d-1}}{g_d^2}g^{tt}F_{ut}\delta F_{xt} && \text{(C.29)}\\
=& -\partial_t\left(\frac{\ell_p^{d-1}}{g_d^2}g^{tt}A'_t\delta A_x\right) . && \text{(C.30)}
\end{aligned}$$

Putting both sides together, we have

$$0 = \left(\delta g'_{xt} + \frac{2}{u}\delta g_{xt}\right) + \left(\frac{2\ell_p^{d-1}}{g_d^2}A'_t\delta A_x\right) . \qquad \text{(C.31)}$$

Now we can substitute this equation into eq. (C.21) and we have the equation of motion for perturbations in the transverse Maxwell gauge

$$0 = \delta A_x'' + \left(\frac{X'}{X} + \frac{f'}{f} - \frac{d-3}{u} \right) \delta A_x' - \omega^2 \frac{g^{tt}}{g^{uu}} \delta A_x + \frac{2\ell_p^{d-1}}{g_d^2} g^{tt} A_t'^2 \delta A_x. \tag{C.32}$$

Appendix D

Special scalar dimensions in $d = 3$

In this appendix, we consider the scalar profile and conductivity for some special values of Δ in three dimensions $d = 3$. In particular, we show that the profile takes a simple power-law form when $\Delta = 3$, the marginal case. We also consider the solution for $\Delta = 6$, which sits on boundary of the values where eq. (5.10) is no longer valid, *i.e.,* $\Delta \geq 6$. We also comment on $\Delta = 3n$ for integer $n > 2$. Finally, we examine the case $\Delta = 3/2$ where eq. (5.10) also fails because the two independent solutions given there are in fact identical.

D.1 $\Delta = 3$

When the scaling dimension of the scalar operator is $\Delta = 3$, the bulk scalar field is massless. In this case, the scalar wave eq. (5.8) reduces to

$$u^4\,\partial_u\left(\frac{(1-u^3)\,\partial_u\phi(u)}{u^2}\right) + 12\alpha_C u^6 = 0\,. \tag{D.1}$$

The solution for the above has a simple closed form:

$$\phi(u) = -\frac{4\alpha_C}{3}\,(1-u^3) + c_1 + \frac{4\alpha_C - c_2}{3}\,\log(1-u^3)\,, \tag{D.2}$$

where c_1 and c_2 are integration constants. For $\phi(u)$ to have the desired critical boundary conditions, *i.e.,* $\phi \sim u^3$ near the asymptotic boundary $u \to 0$ and regularity at the horizon, we must choose $c_1 = \frac{4\alpha_C}{3}$ and $c_2 = 4\alpha_C$. With this choice, the solution reduces to

$$\phi(u) = \frac{4\alpha_C}{3}\,u^3 \tag{D.3}$$

which is the power law solution that was discussed in section 5.4 and in [15]. Substituting $\Delta = 3$ into the high frequency expansion of the conductivity eq. (5.116), we find

$$\frac{\sigma(iw)}{\sigma_\infty} = 1 + \frac{8\alpha_C\alpha_F}{(2w)^3} - \frac{720\alpha_C\alpha_F}{(2w)^6} + O\left(\frac{1}{w^9}\right) , \tag{D.4}$$

where w is defined in eq. (5.109). The first two terms of the series match the asymptotic expansion obtained using a WKB analysis in [12]. Here the two series of higher order terms have collapsed to a single series because the conformal weight of the scalar operator $\mathcal{O}$ matches that of the stress tensor. However, we should recall that we expect in a typical three-dimensional CFT the stress tensor will appear in the JJ OPE eq. (3.33) and so there would be additional contributions to the asymptotic expansion eq. (5.116), beginning at the order $1/w^3$.

D.2 $\Delta = 6$

The point where the scalar operator has scaling dimension $\Delta = 6$ is a special case because it sits on the border line of where the solution given in eq. (5.10) is no longer valid, *i.e.*, $\Delta \geq 6$. This situation is also distinguished by the fact that the source term in the bulk scalar eq. (5.7) and the normalizable mode have precisely the same asymptotic decay, *i.e.*, $u^\Delta = u^6$ — see comments below. We will see in the following that this leads to additional logarithmic factors appearing in the radial profile of the scalar.[1] Substituting $\Delta = 6$ into eq. (5.8) yields

$$u^4\,\partial_u\left(\frac{(1-u^3)\,\partial_u\phi(u)}{u^2}\right) - 18\,\phi(u) + 12\alpha_C u^6 = 0\,. \tag{D.5}$$

and we find the general solution to be

$$\begin{aligned}\phi(u) =& \frac{2-u^3}{u^3}\,c_1 + \frac{4+(2-u^3)\log(1-u^3)}{3u^3}\,c_2 \\ &- \frac{4\alpha_C}{3}\left[\frac{(2-u^3)(\log(1-u^3)-2\mathrm{Li}_2(u^3))}{u^3} + 6 - u^3\right. \\ &\left. - \frac{6\big(2u^3+(2-u^3)\log(1-u^3)\big)}{u^3}\,\log u\right],\end{aligned} \tag{D.6}$$

[1] We explicitly verified that if the power of the source term in eq. (5.7) is replaced by u^3, analogous logarithmic factors appear for $\Delta = 3$. Further, with the u^3 source term, the particular solution diverges for $\Delta > 3$ in analogy to the divergences discussed below for $\Delta > 6$.

where $\mathrm{Li}_2(z)$ is the dilogarithm. In the near-boundary limit $u \to 0$, the non-normalizable mode dominates with $\phi(u) \to \frac{2}{u^3}\left(c_1 + \frac{2}{3}\,c_2\right) + \cdots$. For this model to accurately represent a QCP, this term must vanish since it is the $u^{\Delta-d}$ mode. Thus we set $c_1 = -\frac{2}{3}c_2$ to eliminate the deformation. Further, there is a potential logarithmic divergence as we approach the black hole horizon, *i.e.*, $u \to 1$. In order to remove this singularity at the horizon, we must set $c_2 = 4\alpha_C$. With these choices, the solution reduces to

$$\phi(u) = -\frac{4\alpha_C}{3}\left[4 - u^3 - \frac{2(2-u^3)}{u^3}\,\mathrm{Li}_2(u^3) - \frac{6\big(2u^3 + (2-u^3)\log(1-u^3)\big)}{u^3}\,\log u\right]. \tag{D.7}$$

The leading two terms in the near-boundary expansion for $\phi(u)$ are given by

$$\phi(u \to 0) = -\frac{2\alpha_C}{27}\,u^6\,(18\,\log u + 1) + O(u^9 \log u)\,. \tag{D.8}$$

Surprisingly, we see that the leading asymptotic behaviour has a puzzling logarithmic enhancement with $u^6\,\log u$. However, given this scalar profile eq. (D.8), it is straightforward to determine the high frequency expansion of the conductivity following the analysis in chapter 5. To leading order, we find

$$\frac{\sigma(iw)}{\sigma_\infty} = 1 + \frac{16\alpha_C\alpha_F}{3}\,\frac{180\gamma_E - 451 + \log(2w)}{(2w)^6} + \cdots \tag{D.9}$$

where γ_E is Euler's constant. Hence there is a logarithmic enhancement in the expected $1/w^6$ contribution. However, we note again that for typical three-dimensional CFTs, this contribution would still be dominated by a $1/w^3$ term coming from the appearance of the stress tensor in the JJ OPE; our model does not contain such a contribution.

D.2.1 $\Delta = 3n$

The two previous cases $\Delta = 3, 6$ are part of a more general trend valid for $\Delta = d\,n = 3n$, with integer $n > 0$. With such a choice of scalar dimension, the equation of motion for the scalar admits a "simple" solution. For instance, for $\Delta = 9$ we find using the methods described above

$$\phi(u) = \frac{4\alpha_1}{3u^6}\Big[u^3\left(u^6 - 27u^3 + 36 + 54\left(u^3 - 2\right)\log u\right) \\ - 6\left(u^6 - 6u^3 + 6\right)\left(\mathrm{Li}_2\big(u^3\big) + 3\log u\,\log\left(1 - u^3\right)\right)\Big], \tag{D.10}$$

where $\mathrm{Li}_2(z)$ is the dilogarithm, which also appeared for the $\Delta = 6$ case. The small-u expansion reads:

$$\phi(u) = \frac{\alpha_1}{3}\, u^6 + \frac{\alpha_1}{225}\, u^9 \left(180 \log u + 43\right) + O(u^{12} \log u)\,. \tag{D.11}$$

This will lead to the first sub-leading term in the asymptotic conductivity to go as $(T/\Omega_n)^6$, irrespective of the fact that the scalar has $\Delta = 9$. This contribution comes from the particular solution of eq. (5.8) rather than the homogeneous solution, *i.e.,* it is driven by the source term in the scalar field equation. Analogous behaviour will also hold for $\Delta = 12, 15, \cdots$.

D.2.2 $\Delta > 6$

We now discuss the general scalar profile eq. (5.10) for general irrelevant scalar operators of large Δ. When the scalar field solution was introduced, we noted that if the boundary operator became too irrelevant, *i.e.,* for $\Delta \geq 6$, the profile given in eq. (5.10) was no longer valid. In particular, the function $g_\Delta(u)$ in eq. (5.11) diverges for these values of the conformal dimension. To better understand the physical significance of this divergence, we can introduce a UV cut-off surface at $u = \varepsilon \ll 1$. With this cut-off, $g_\Delta(u)$ becomes

$$g_\Delta(u) = \int_\varepsilon^u dy\, y^{5-\Delta}\, {}_2\mathrm{F}_1\left(1 - \frac{\Delta}{3}, 1 - \frac{\Delta}{3}\,; 2 - \frac{2\Delta}{3}\,; y^3\right)\,. \tag{D.12}$$

Now applying the usual boundary conditions, we would set $\phi_0 = 0$ and ϕ_1 would be fixed as in eq. (5.14). However, for that latter quantity, one finds

$$\phi_1 \simeq -\frac{12\alpha_C}{2\Delta - 3}\, g_\Delta(1) \simeq -\frac{12\alpha_C}{(\Delta - 6)(2\Delta - 3)} \left(\frac{3}{4\pi T\delta}\right)^{\Delta - 6}\,, \tag{D.13}$$

where we have written the dominant contribution in terms of δ, the physical short-distance cut-off in the boundary theory, using $\varepsilon = \frac{4\pi}{3} T\delta$. For example then, the expectation value $\langle \mathcal{O} \rangle_T$ in eq. (5.13) diverges in the limit that the cut-off is removed, *i.e.,* $\delta \to 0$. Therefore the holographic solution only really makes sense with a finite UV cut-off in this regime.

One might contrast the above treatment with the fact that eqs. (D.7) and (D.10) provide perfectly finite solutions for $\Delta = 6$ and 9, respectively. In fact, finite solutions can be generated for general $\Delta \geq 6$ by simply shifting the lower endpoint of the integral defining $g_\Delta(u)$ in eq. (5.11). Here, we would hold the endpoint fixed at some finite value of y, rather than tying it to the UV cut-off surface as in eq. (D.12), which amounts to

shifting ϕ_1 by a (divergent) constant. While this procedure yields a finite solution, it obscures the physical interpretation the holographic model by concealing the divergence in the expectation value $\langle\mathcal{O}\rangle_T$. We leave this point for ulterior study.

D.3 $\Delta = 3/2$

As noted previously, the scalar field solution eq. (5.10) breaks down at $\Delta = d/2 = 3/2$ because the two homogeneous solutions appearing there reduce to the same function, and thus are not independent, removing a degree of freedom for the solution. With $\Delta = 3/2$, the scalar wave eq. (5.8) is

$$u^4\partial_u\left(\frac{(1-u^3)\,\partial_u\phi(u)}{u^2}\right) + \frac{9}{4}\phi(u) + 12\alpha_C u^6 = 0\,. \tag{D.14}$$

The general solution of this equation can be written as

$$\begin{aligned}\phi(u) =& \tfrac{2}{\pi}\,u^{3/2}\,K(u^3)\,(\phi_1 - 8\alpha_C\,\tilde{g}_{3/2}(u)) \\ &+\ \tfrac{2}{3}\,u^{3/2}\,K(1-u^3)\,(\phi_0 + 8\alpha_C\,\tilde{h}_{3/2}(u))\end{aligned} \tag{D.15}$$

where $K(k^2) = F(\varphi = \frac{\pi}{2}, k)$ is the complete elliptical integral of the first kind. As our notation above suggests, there is a simple relationship between $K(u^3)$ and the hypergeometric function appearing in eq. (5.10) for $\Delta = 3/2$: $\frac{2}{\pi}K(u^3) = {}_2\mathrm{F}_1\big(\frac{1}{2},\frac{1}{2}\,;1\,;u^3\big)$. Further we can write $\frac{2}{3}K(1-u^3) \simeq \log u\ {}_2\mathrm{F}_1\big(\frac{1}{2},\frac{1}{2}\,;1\,;u^3\big) + \cdots$, were the ellipsis denotes terms polynomial in u^3. The functions $\tilde{g}_{3/2}(u)$ and $\tilde{h}_{3/2}(u)$ provide the particular solution of eq. (D.14) with

$$\tilde{g}_{3/2}(u) = \int_0^u dy\, y^{7/2}\,K(1-y^3) \quad \text{and} \quad \tilde{h}_{3/2}(u) = \tfrac{3}{\pi}\int_0^u dy\, y^{7/2}\,K(y^3)\,. \tag{D.16}$$

In order for the dual boundary theory to be conformal, we set $\phi_0 = 0$ which removes the logarithmic divergence as $u \to 0$ arising from $K(1-u^3)$. Approaching the black hole horizon with $u \to 1$, the functions $\tilde{g}_{3/2}(u)$, $\tilde{h}_{3/2}(u)$ and $K(1-u^3)$ are all finite, but $K(u^3)$ is logarithmically divergent. Therefore regularity at the horizon requires $\phi_1 = 8\alpha_C\,\tilde{g}_{3/2}(1)$.[2]

The result for $\langle\mathcal{O}\rangle_T$ given in eq. (5.13) is no longer valid in this special case, *e.g.*, substituting $\Delta = 3/2$ there yields a vanishing expectation value. Rather in this special

[2]Numerically, we find $\tilde{g}_{3/2}(1) = 0.4112$.

case, one has to revisit the holographic renormalization procedure to evaluate the scalar expectation value — see, *e.g.,* [55]:

$$\langle \mathcal{O} \rangle_T = -\frac{L^2}{2\ell_p^2} \left(\frac{r_0}{L^2}\right)^{3/2} \phi_1 \,. \tag{D.17}$$

Given the profile of the bulk scalar, the conductivity is calculated as described in section 5.3.2 and the results differ little from those for nearby values of Δ. Hence, *e.g.,* $\sigma(\omega)$ remains a smooth function of the conformal dimension in the vicinity of $\Delta = 3/2$. We can also use the above profile to evaluate the high-frequency expansion of the conductivity as in section 5.3.2. Here we need the Taylor expansion of $\phi(u)$ near the asymptotic boundary:

$$\phi(u) = \phi_1\, u^{3/2} + \frac{1}{4}\,\phi_1\, u^{9/2} - \frac{16}{27}\,\alpha_C\, u^6 + O(u^{15/2})\,. \tag{D.18}$$

We note that this expansion precisely matches that given in eq. (5.117) upon substituting $\Delta = 3/2$. Then from eq. (5.115), the first few terms in the expansion of the conductivity for $w \gg 1$ are

$$\frac{\sigma(iw)}{\sigma_\infty} = 1 + \frac{3\sqrt{\pi}}{4}\,\frac{\phi_1 \alpha_F}{(2w)^{3/2}} + \frac{945\sqrt{\pi}}{256}\,\frac{\phi_1 \alpha_F}{(2w)^{9/2}} - \frac{1280}{3}\,\frac{\alpha_C \alpha_F}{(2w)^6} + \cdots\,. \tag{D.19}$$

Again, the results here precisely matches the expansion in eq. (5.118) upon substituting $\Delta = 3/2$. Let us add that an interesting feature that appears at $\Delta = 3/2$ is that when we deform away from the critical point in the boundary theory by turning on ϕ_0, the leading term in this expansion is enhanced by a logarithmic factor similar to that in eq. (D.9). This extra logarithmic factor arises because with non-vanishing ϕ_0, the boundary expansion eq. (D.18) of the bulk scalar contains a new term proportional to $\phi_0\, u^{3/2} \log u$. As commented before, special care is required in evaluating the two- and three-point functions when $\Delta = 3/2$ [56].

Appendix E

$O(\alpha_F^2)$ corrections to conductivity

We saw in section 5.4 that to first order in α_F, the leading correction in the high frequency expansion of the conductivity appeared at order $1/w^{\Delta}$. In this appendix we extend the perturbative analysis presented in that section to order α_F^2 to see how the expansion will be modified at this order. We will continue to be working in the regime that there is no significant back reaction to the background geometry. Recall at the equation of motion for the gauge field is

$$\left[\partial_z^2 - w^2\right] A_x = -\frac{\alpha_F \partial_z \phi}{1+\alpha_F \phi}\, \partial_z A_x \,, \tag{E.1}$$

where we have previously changed variables from u to z via $dz/du = 1/f(u)$. We will decompose the gauge field perturbatively as in section 5.4, $A_x = A_x^{(0)} + \alpha_F A_x^{(1)} + \alpha_F^2 A_x^{(2)} + \cdots$. Recall that the zero'th order and first order in α_F equations of motion are

$$\begin{aligned} \left[\partial_z^2 - w^2\right] A_x^{(0)} &= \ \ 0 \\ \left[\partial_z^2 - w^2\right] A_x^{(1)} &= -\,\phi' A_x^{(0)\prime} \end{aligned} \tag{E.2}$$

and their solutions were detailed in section 5.4 given by eq. (5.110) and eq. (5.114).

$$A_x^{(0)} = e^{-wz}, \quad A_x^{(1)} = \int d\tilde{z} G(z,\tilde{z}) w e^{-w\tilde{z}} \phi'(\tilde{z}) \tag{E.3}$$

Recall that the Green's function for eq. (5.108) is given by eq. (5.113), and we can use this Green's function to iteratively solve for the perturbative gauge terms $A^{(i)}$. To second order in α_F the equation of motion is

$$\left[\partial_z - w^2\right] A_y^{(2)} = \partial_z A_y^{(0)}\, \phi\, \partial_z \phi - \partial_z A_y^{(1)}\, \partial_z \phi \,. \tag{E.4}$$

Using the Green's function in eq. (5.113), we then find

$$A_y^{(2)} = \int_0^\infty d\tilde{z}\, G(z,\tilde{z})\, \left(\partial_{\tilde{z}} A_y^{(0)}\, \phi\, \partial_{\tilde{z}}\phi - \partial_{\tilde{z}} A_y^{(1)}\, \partial_{\tilde{z}}\phi\right) \tag{E.5}$$

and taking the limit where we approach the asymptotic boundary, *i.e.*, $z \to 0$, the derivative of this expression yields

$$\partial_z A_y^{(2)}\big|_{z=0} = \int_0^\infty d\tilde{z}\, e^{-w\tilde{z}} \left(w e^{-w\tilde{z}}\, \phi\, \partial_{\tilde{z}}\phi + \partial_{\tilde{z}} A_y^{(1)}\, \partial_{\tilde{z}}\phi\right) , \tag{E.6}$$

We only wish to identify the leading correction for a high frequency expansion to eq. (5.77). For clarity, we will make the simplification of using only the critical theory power-law scalar profile: $\phi \sim \phi_1\, z^\Delta$. Note that we are using z^Δ rather than u^Δ here, but the two profiles are equivalent at this order in z — see footnote 9. We note *en passant* that our analysis thus applies to the simple ansatz of [15]. With this scalar profile, we find

$$\begin{aligned} \partial_z A_y^{(1)}\big|_{z=0} &= -\frac{\phi_1 w\, \Gamma(\Delta+1)}{(2w)^\Delta} \\ \partial_z A_y^{(2)}\big|_{z=0} &= \frac{\phi_1^2\, w\, (\,\Gamma(2\Delta+1) - \,\Gamma(\Delta+1)^2)}{2(2w)^{2\Delta}} \end{aligned} \tag{E.7}$$

Eq. (5.54) then yields

$$\frac{\sigma(iw)}{\sigma_\infty} = 1 + \frac{\phi_1\alpha_F\,\Gamma(\Delta+1)}{(2w)^\Delta} - \frac{(\phi_1\alpha_F)^2\,(\Gamma(2\Delta+1) - \Gamma(\Delta+1)^2)}{2(2w)^{2\Delta}} + O((\phi_1\alpha_F)^3)\,, \tag{E.8}$$

as the first three contributions in the α_F-expansion. Of course, the first two terms precisely match those found in eq. (5.77). We might note that the new $O(\alpha_F^2)$ correction implies that the existence of a new primary operator with conformal dimension 2Δ. $:\mathcal{O}^2:$ is a likely candidate [13].

Appendix F

Numerical results

This appendix forms a catalog for conductivity at various choices of spacetime dimension and scaling dimension.

F.1 $d = 3$

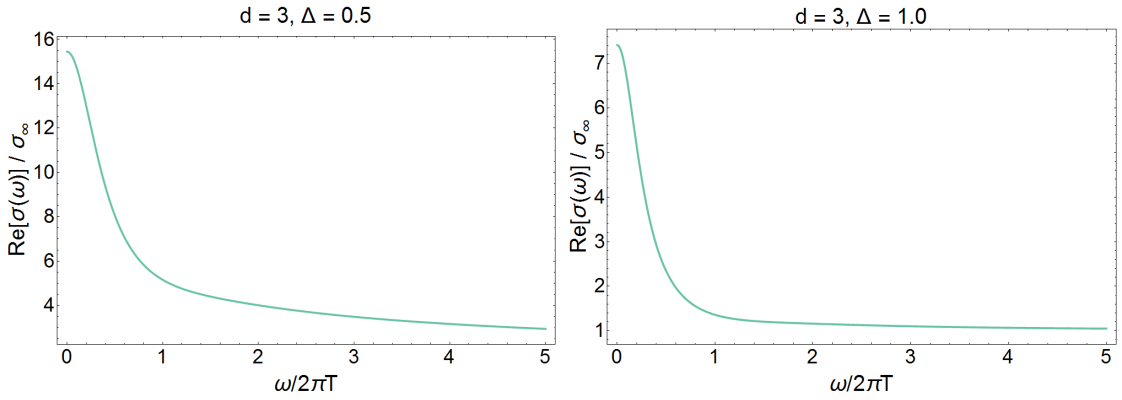

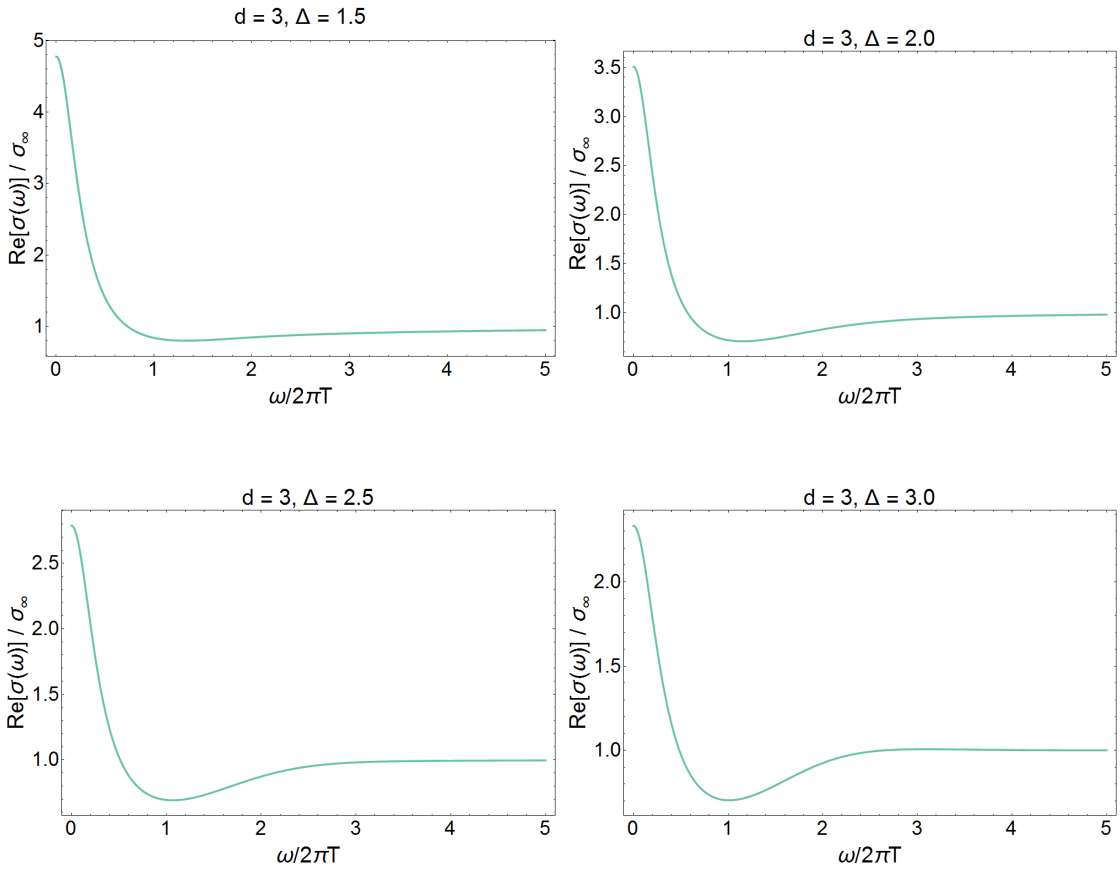

F.2 d=5

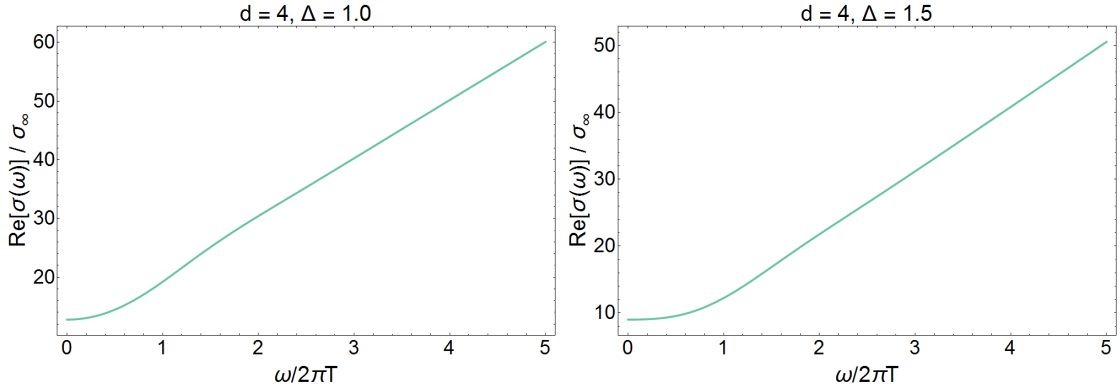

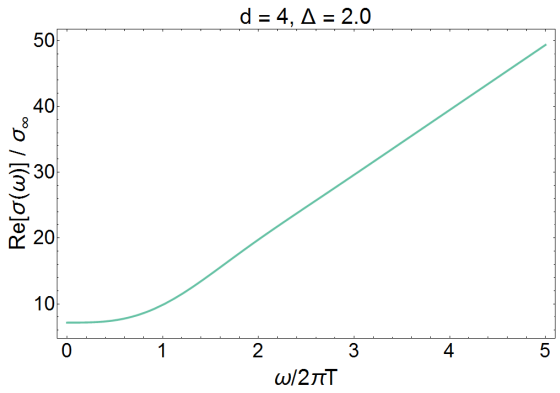
d = 4, Δ = 2.0
Re[σ(ω)] / σ∞
ω/2πT

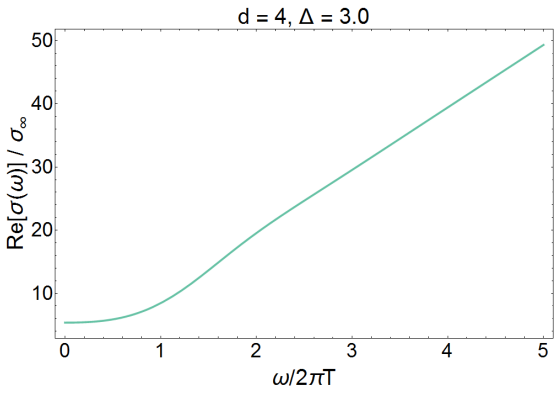
d = 4, Δ = 3.0
Re[σ(ω)] / σ∞
ω/2πT

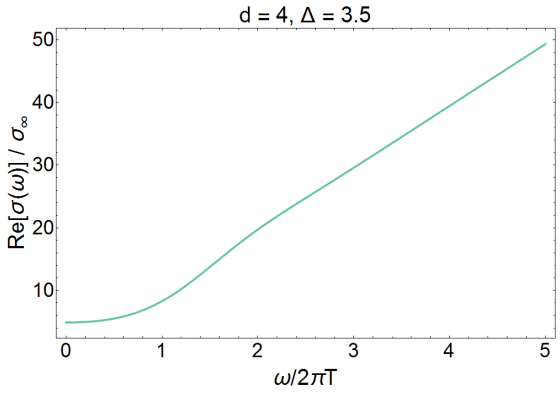
d = 4, Δ = 3.5
Re[σ(ω)] / σ∞
ω/2πT

F.3 d=4

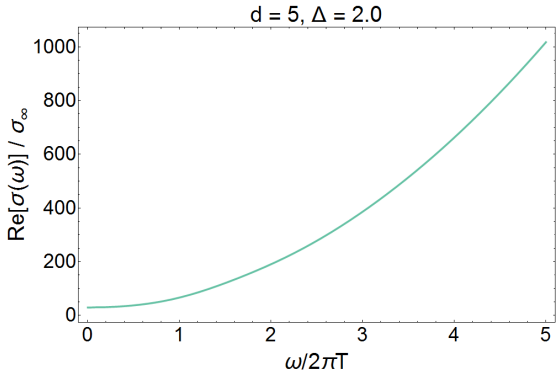
d = 5, Δ = 2.0
Re[σ(ω)] / σ∞
ω/2πT

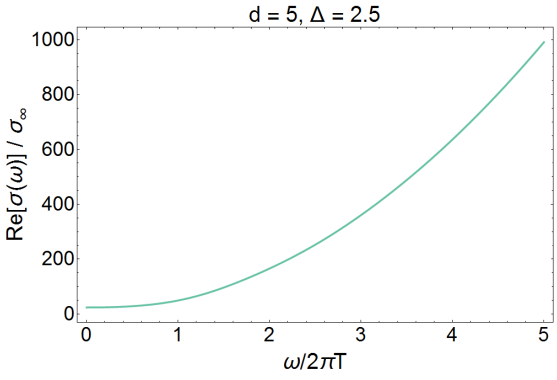
d = 5, Δ = 2.5
Re[σ(ω)] / σ∞
ω/2πT

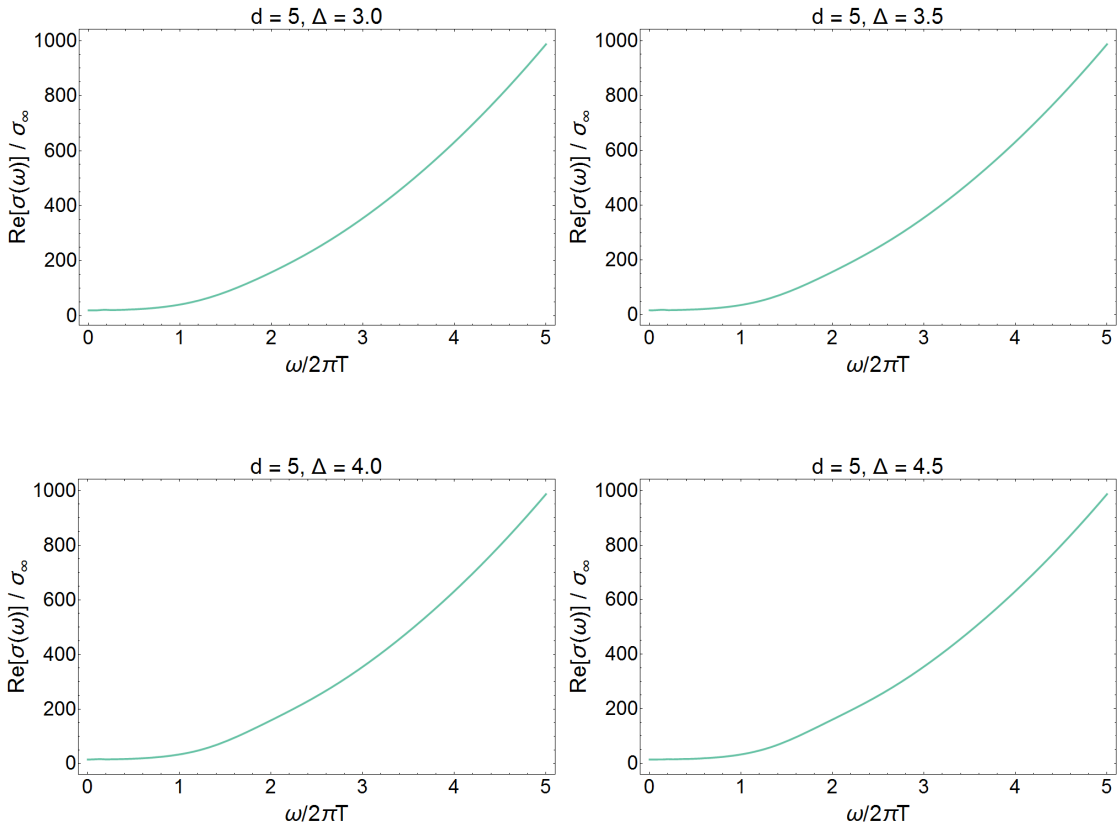
d = 5, Δ = 3.0
d = 5, Δ = 3.5
d = 5, Δ = 4.0
d = 5, Δ = 4.5
Re[σ(ω)] / σ∞
ω/2πT
0
200
400
600
800
1000
0
1
2
3
4
5